НАЦІОНАЛЬНА АКАДЕМІЯ НАУК УКРАЇНИ
ІНСТИТУТ ОРГАНІЧНОЇ ХІМІЇ НАН УКРАЇНИ
НАЦІОНАЛЬНИЙ ФАРМАЦЕВТИЧНИЙ УНІВЕРСИТЕТ

Рік заснування – 1966

ЖУРНАЛ ОРГАНІЧНОЇ ТА ФАРМАЦЕВТИЧНОЇ ХІМІЇ

JOURNAL OF ORGANIC AND PHARMACEUTICAL CHEMISTRY

2024 — том 22, випуск 4 (88)

Харків
НФаУ

У журналі розглянуто проблеми синтезу й аналізу органічних та елементоорганічних сполук, аналогів природних сполук і лікарських субстанцій, наведено результати фізико-хімічних досліджень у вищезазначених напрямах. Також з погляду (біо)органічної, фармацевтичної, аналітичної та фізичної хімії проаналізовано питання з різних аспектів рослинництва, ґрунтознавства й дослідження навколишнього середовища.

Для працівників науково-дослідних установ, вищих навчальних закладів та фахівців хімічного, фармацевтичного, біологічного, медичного і сільськогосподарського профілів.

«Журнал органічної та фармацевтичної хімії» внесено до затвердженого МОН України Переліку наукових фахових видань України (категорія «Б») для опублікування результатів дисертаційних робіт за спеціальністю 102 – Хімія та 226 – Фармація, промислова фармація (наказ МОН України від 28.12.2019 р. № 1643); індексовано в наукометричних базах даних: Chemical Abstracts (CAS), Index Copernicus; внесено до каталогів та пошукових систем: Directory of Open Access Journals (DOAJ), Bielefeld Academic Search Engine (BASE), Directory of Open Access scholarly Resources (ROAD), PKP Index, Ulrich's periodicals, Worldcat, НБУ ім. В. І. Вернадського і УРЖ «Джерело».

Затверджено до друку вченою радою Інституту органічної хімії НАН України, протокол № 23 від 17.12.2024 р.

Затверджено до друку вченою радою Національного фармацевтичного університету, протокол № 11 від 18.12.2024 р.

Адреса для листування: 61002, м. Харків, вул. Григорія Сковороди, 53, Національний фармацевтичний університет, редакція «Журналу органічної та фармацевтичної хімії». E-mail: publish@nuph.edu.ua, orgpharm-journal@nuph.edu.ua. Сайт: http://ophcj.nuph.edu.ua

Рішення Національної ради України з питань телебачення і радіомовлення № 1911 (протокол № 17 від 30.05.2024 р.) "Про заяви Національного фармацевтичного університету, м. Харків, щодо реєстрації суб'єкта у сфері друкованих медіа" (ідентифікатор медіа R30-05024)

Підписано до друку 21.12.2024 р. Формат 60 × 84 1/8.

Папір офсетний. Друк ризо. Умовн. друк. арк. 9,3. Обліков.-вид. арк. 10,76. Тираж 50 прим.

Редактори — О. Ю. Гурко, Л. І. Дубовик. Комп'ютерне верстання — О. М. Білинська

«Журнал органічної та фармацевтичної хімії». Том 22, випуск 4 (88), 2024

ISSN 2308-8303 (Print)

ISSN 2518-1548 (Online)

Journal of Organic and Pharmaceutical Chemistry

Advanced Research

OPEN ACCESS
Freely available online on
http://ophcj.nuph.edu.ua

UDC 546.27:54.05

A. M. Mishchenko[1], M. A. Nechayev[1,2], A. I. Subota[1,2], A. V. Kozytskiy[1], O. V. Svaliavyn[1,2], Yu. L. Lishchenko[1,3], A. M. Aleksandrova[2], Yu. V. Rassukana[2], D. O. Leha[1,4]

[1] Enamine Ltd, 78 Winston Churchill str., 02094 Kyiv, Ukraine
[2] Institute of Organic Chemistry of the National Academy of Sciences of Ukraine, 5 Akademik Kuhar str., 02094 Kyiv, Ukraine
[3] L. V. Pisarzhevskii Institute of Physical Chemistry of the National Academy of Sciences of Ukraine, 31 Nauky ave., 03028 Kyiv, Ukraine
[4] Taras Shevchenko National University of Kyiv, 60 Volodymyrska str., 01033 Kyiv, Ukraine

A New Convenient Method for Preparing Tetrabutylammonium *closo*-Dodecaborate

Abstract

A new synthetic procedure for preparing tetrabutylammonium *closo*-dodecaborate $(Bu_4N)_2B_{12}H_{12}$ by the solvent-free pyrolysis of tetrabutylammonium tetrahydroborate Bu_4NBH_4 has been developed. The procedure also provides isolation of pure tetrabutylammonium octahydrotriborate $Bu_4NB_3H_8$ as a by-product. The main advantages of the route proposed are convenience and utilization of readily available starting materials. The compounds prepared have been characterized by NMR and IR spectroscopy. Based on the DFT calculations of normal modes of the $[B_3H_8]^-$ and $[B_{12}H_{12}]^{2-}$ anions, the assignment of the main absorption bands in the IR spectra of the compounds synthesized has been performed.

Keywords: *closo*-dodecaborate; octahydrotriborate; pyrolysis; DFT calculations

А. М. Міщенко[1], М. А. Нечаєв[1,2], А. І. Субота[1,2], А. В. Козицький[1], О. В. Свалявін[1,2], Ю. Л. Ліщенко[1,3], А. М. Александрова[2], Ю. В. Рассукана[2], Д. О. Лега[1,4]

[1] ТОВ НВП «Єнамін», вул. Вінстона Черчилля, 78, м. Київ, 02094, Україна
[2] Інститут органічної хімії Національної академії наук України, вул. Академіка Кухаря, 5, м. Київ, 02094, Україна
[3] Інститут фізичної хімії ім. Л.В. Писаржевського Національної академії наук України, просп. Науки, 31, м. Київ, 03028, Україна
[4] Київський національний університет імені Тараса Шевченка, вул. Володимирська, 60, м. Київ, 01033, Україна

Новий зручний спосіб отримання тетрабутиламоній *клозо*-додекаборату

Анотація

Розроблено нову синтетичну процедуру отримання тетрабутиламоній *клозо*-додекаборату $(Bu_4N)_2B_{12}H_{12}$ шляхом піролізу тетрабутиламоній тетрагідроборату Bu_4NBH_4 без розчинника. Процедура також передбачає виділення чистого тетрабутиламоній октагідротриборату $Bu_4NB_3H_8$ як побічного продукту. Основними перевагами запропонованого підходу є його зручність і використання легкодоступних вихідних матеріалів. Одержані сполуки схарактеризовано методами ЯМР- та ІЧ-спектроскопії. На основі DFT-розрахунків нормальних коливань аніонів $[B_3H_8]^-$ та $[B_{12}H_{12}]^{2-}$ визначено структурні фрагменти, яким відповідають основні смуги поглинання в ІЧ-спектрах синтезованих сполук.

Ключові слова: *клозо*-додекаборат; октагідротриборат; піроліз; DFT-розрахунки

Citation: Mishchenko, A. M.; Nechayev, M. A.; Subota, A. I.; Kozytskiy, A. V.; Svaliavyn, O. V.; Lishchenko, Yu. L.; Aleksandrova, A. M.; Rassukana, Yu. V.; Leha, D. O. A new convenient method for preparing tetrabutylammonium *closo*-dodecaborate. *Journal of Organic and Pharmaceutical Chemistry* **2024**, *22* (4), 3–9.
https://doi.org/10.24959/ophcj.24.316264
Received: *15 October 2024*; **Revised:** *24 November 2024*; **Accepted:** *28 November 2024*

Funding: The work was supported by the National Research Foundation of Ukraine (grant No. 0123U104256).
Conflict of interests: The authors have no conflict of interests to declare.

■ Introduction

Highly symmetric icosahedral *closo*-dodecaborate anion $[B_{12}H_{12}]^{2-}$ fills one of the central places among numerous boron hydrides [1–3]. Compounds based on the *closo*-dodecaborate core are not only of great theoretical interest, but are also promising for the use in medicine as therapeutic agents in cancer treatment by neutron-capturing therapy [4, 5]. An inestimable advantage of these compounds is their low toxicity, which is due to the high chemical stability of the icosahedral B_{12} cluster. The development of an inexpensive method for preparing *closo*-dodecaborate salts from commercially available reagents is an important task on the way to the introduction of such drugs into medical practice.

Synthetic routes to *closo*-dodecaborate salts can be classified roughly into 3 groups according to the starting materials, which could be either boron hydride B_xH_y, octahydrotriborate $[B_3H_8]^-$ or tetrahydroborate $[BH_4]^-$. In early works, triethylammonium *closo*-dodecaborate $(Et_3NH)_2B_{12}H_{12}$ was prepared by the interaction of triethylamine borane Et_3NBH_3 with boron hydrides, such as B_5H_9 [6] or $B_{10}H_{14}$ [7]. In a similar manner sodium salt $Na_2B_{12}H_{12}$ was synthesized by the treatment of $NaBH_4$ with $B_{10}H_{14}$ in boiling diglyme [1, 8]. Despite this route being featured with high yields, it requires working with hazardous, flammable, and commercially unavailable boron hydrides.

The second group of synthetic routes is based on the disproportionation of octahydrotriborate anion $[B_3H_8]^-$ into $[B_{12}H_{12}]^{2-}$ and $[BH_4]^-$ in boiling diglyme. In turn, octahydrotriborate is preliminarily synthesized in the same reactor by the oxidation of $NaBH_4$ with iodine [9] or hydrocarbon halides [10]. The yields of *closo*-dodecaborate are generally higher in the latter case: for example, a tetrabutylammonium salt $(Bu_4N)_2B_{12}H_{12}$ was prepared in the yield of 84, 82, 81, and 80% *via* application of $PhCH_2Cl$, Ph_3CCl, $C_{10}H_7CH_2Cl$ and *n*BuBr, respectively [10]. However, this process is moisture sensitive, and diglyme should be thoroughly dried beforehand, increasing the complexity and total cost of the process.

Synthetic procedures, which include the pyrolysis of tetrahydroborate salts form another group of routes for preparing *closo*-dodecaborates. The formation of a magnesium salt $MgB_{12}H_{12}$ was achieved by the pyrolysis of an equimolar mixture of $Mg(BH_4)_2$ and tetraglyme at 200 °C for 8 h although the yield was not very high [11]. The preparation of sodium and potassium *closo*-dodecaborates in up to the yield of 95% was reported by reactions of the corresponding tetrahydroborates with trialkylamine boranes in high-boiling alkanes (dodecane, hexadecane) at 200–250 °C [1]. The temperature of the process can be lowered by replacing the cation with tetraalkylammonium. For example, a tetraethylammonium salt $(Et_4N)_2B_{12}H_{12}$ can be prepared by heating the suspension of Et_4NBH_4 in triethylamine borane at 185 °C, and it plays a dual role of a reagent and a heat-transfer liquid medium [1]. The main drawback of the method mentioned is the low purity of the product, which is contaminated with other polyhedral boron hydrides ($B_9H_9^{2-}$, $B_{10}H_{10}^{2-}$, $B_{11}H_{14}^-$) [12], and thus requires additional chromatographic purification. The high cost of triethylamine borane as a solvent is an additional obstacle for a large-scale application of this synthetic procedure.

The composition of the solid residue after the pyrolysis of tetraalkylammonium tetrahydroborate is known to depend strongly on the nature of the cation [1, 13]. Our study has revealed that a tetrabutylammonium cation favored the formation of *closo*-dodecaborate. Based on these findings, a convenient synthetic procedure for preparing $(Bu_4N)_2B_{12}H_{12}$ by the solvent-free pyrolysis of Bu_4NBH_4 was elaborated. The products were identified by ^1H and ^{11}B NMR spectroscopy. In some cases, the formation of *closo*-decaborate $[B_{10}H_{10}]^{2-}$ was detected. This fact deserves more attention in future studies since this anion is a valuable starting compound for the synthesis of carboranes. It is worth noting that ^1H NMR spectra of all solid products obtained show solely 4 resonances of Bu_4N^+ cation at 0.93 (t, J = 7.4 Hz, 3H), 1.30 (sx, J = 7.4 Hz, 2H), 1.57 (m, 2H) and 3.17 (m, 2H) ppm, therefore, only ^{11}B NMR spectra are discussed herein.

Assignment of the vibrations in IR spectra of the boranes is also a non-trivial task. In this paper, we report the assignment of the main absorption bands in the IR spectra of $(Bu_4N)_2B_{12}H_{12}$ and $Bu_4NB_3H_8$ based on DFT calculations of normal modes of the corresponding hydroborate anion.

■ Materials and methods

Starting materials and solvents were obtained from commercial sources and used as received. Tetrabutylammonium tetrahydroborate Bu_4NBH_4 was prepared according to the literature procedure [14] and its purity was determined by the iodometric titration method [15].

ISSN 2308-8303 (Print) / 2518-1548 (Online)

Nuclear magnetic resonance (NMR) spectra were measured on a Varian Unity Plus 400 spectrometer. ^{1}H chemical shifts were referenced to tetramethylsilane, and ^{11}B chemical shifts were referenced to $BF_3 \cdot Et_2O$. Infrared (IR) spectra were recorded on an IR5 spectrometer (Edinburgh Instruments) within the range of 4000–600 cm^{-1}.

The synthesis of $(Bu_4N)_2B_{12}H_{12}$ and $Bu_4NB_3H_8$

A 250 mL pear-shaped flask was charged with 30.00 g of Bu_4NBH_4 and connected to a diaphragm pump through a condenser (a 250 mL round-bottom flask equipped with a receiver adapter). After the pump was turned on, the reaction mixture was heated to 170 °C and kept at this temperature for 6 h. The solid residue left after the pyrolysis was transferred to a 100 mL beaker and stirred with 50 mL of boiling ethanol. After cooling to room temperature, the precipitate was filtered off, washed with a small amount of ethanol, and dried in air to give 4.10 g of $(Bu_4N)_2B_{12}H_{12}$ as a white solid.

^{1}H NMR (DMSO-d_6, 400 MHz), δ, ppm: 0.93 (3H, t, J = 7.4 Hz), 1.30 (2H, sx, J = 7.4 Hz), 1.57 (2H, m), 3.17 (2H, m). ^{11}B NMR (DMSO-d_6, 192,4 MHz), δ, ppm: –15.56 (12B, d, J = 126.4 Hz). IR (KBr), ν_{max}, cm^{-1}: 2960, 2936, 2873, 2464, 1470, 1381, 1153, 1053, 882, 740, 710.

The filtrate was evaporated to dryness under reduced pressure, and the residue was stirred with 25 mL of boiling ethyl acetate. After cooling to room temperature, the suspension was filtered, and the filtrate was evaporated to dryness under reduced pressure to give 2.44 g of $Bu_4NB_3H_8$ as a white solid.

^{1}H NMR (DMSO-d_6, 400 MHz), δ, ppm: 0.93 (3H, t, J = 7.4 Hz), 1.31 (2H, sx, J = 7.4 Hz), 1.57 (2H, m), 3.16 (2H, m). ^{11}B NMR (DMSO-d_6, 192,4 MHz), δ, ppm: –29.40 (3B, nonet, J = 33.1 Hz). IR (KBr), ν_{max}, cm^{-1}: 2962, 2935, 2875, 2437, 2386, 2117, 2066, 1569, 1470, 1382, 1299, 1137, 1009, 882, 778, 737, 711, 681, 647.

Computation details

The geometry optimization and normal coordinate analysis in the harmonic approximation of $[B_3H_8]^-$ and $[B_{12}H_{12}]^{2-}$ anions were carried out in a GAMESS (US) program package [16] (version 2023 R1) with the ωB97X-D functional [17] and the Karlsruhe triple zeta basis with one polarization function (TZVP) [18]. No symmetry restrictions were applied.

■ Results and discussion

Within the project concerned with the development of a convenient route for multi-gram scale production of *closo*-dicarbadodecaboranes, we were studying the pyrolysis of tetraalkylammonium tetrahydroborates in order to find optimal conditions for the conversion of $[BH_4]^-$ into *closo*-decaborate $[B_{10}H_{10}]^{2-}$. Previously, it was argued that the presence of butyl groups in tetraalkylammonium cation promotes the formation of $[B_{10}H_{10}]^{2-}$ [13]. However, in our preliminary experiments on the autoclave pyrolysis of Bu_4NBH_4 (in a pure state, as well as in a mixture with toluene) *closo*-dodecaborate $(Bu_4N)_2B_{12}H_{12}$ was always found to be the main solid product. One possible reason was that the increased pressure in the autoclave could be responsible for these results. To check this supposition, experiments on the pyrolysis of Bu_4NBH_4 in the vacuum were carried out. Pyrolysis products were studied by ^{1}H and ^{11}B NMR spectroscopy.

Firstly, the pyrolysis was performed in the vacuum of a water jet pump. Bu_4NBH_4 melts at ~130 °C and, upon further heating, begins to decompose at ~160 °C liberating tributylamine. The latter could be collected in the trap. During the remaining time (12 h), the temperature was maintained at 180 °C. The weight loss upon the pyrolysis was about 85–87%; *i.e.*, typically, 0.45–0.55 g of a solid residue were obtained from 5.00 g of Bu_4NBH_4). After the pyrolysis, the solid residue contained $(Bu_4N)_2B_{12}H_{12}$ and $(Bu_4N)_2B_{10}H_{10}$, which were identified by ^{11}B NMR (*see* positions of signals and coupling constants in the Experimental Part). In addition, it was found that a significant quantity of the starting material was transformed into polyborate, presumably due to the hydrolysis caused by water vapor.

To reduce the possible effect of water vapors, the pyrolysis was performed under the same conditions, but for a shorter period of time (3 h) until the evolution of gas ceased, and the residue in the reaction flask solidified. By this means, 1.87 g of a solid residue were obtained from 10.40 g of Bu_4NBH_4 (the weight loss was 8.53 g, 82.0%). To separate borate impurities, the residue was intensively mixed with 25 mL of dichloromethane, the mixture was filtered, and the filtrate was evaporated to dryness under reduced pressure to give 1.27 g of a white powder. Its ^{11}B NMR spectrum exhibits only the resonances of $[B_{12}H_{12}]^{2-}$ (–15.6 ppm) and $[B_{10}H_{10}]^{2-}$ anions (–0.9 and –28.8 ppm). Based on the relative intensities of these signals, it can be concluded that pyrolysis product is comprised of about 85% $(Bu_4N)_2B_{12}H_{12}$ and 15% $(Bu_4N)_2B_{10}H_{10}$ (mass percentages).

In another experiment, the pyrolysis of Bu_4NBH_4 was carried out under conditions, which excluded the presence of water vapor (the vacuum of a continuously working diaphragm pump). The temperature was maintained at a level just above the beginning of decomposition (160–170 °C). In typical experiments, about 12 g of an off-white solid were obtained by heating 45.00 g of Bu_4NBH_4 at 170 °C for 6 h (the weight loss was 70–75%). This solid contained 60% $(Bu_4N)_2B_{12}H_{12}$ and 40% $Bu_4NB_3H_8$ (mass percentages), as evidenced by ^{11}B NMR. Taking into account that the pyrolysis product contains a minor quantity of impurities, the efficient procedure for isolation of the main component was elaborated. The separation is based on different solubility of tetrabutylammonium hydroborates in organic solvents: $(Bu_4N)_2B_{12}H_{12}$ was insoluble in ethanol, while $Bu_4NB_3H_8$ is soluble in ethanol and ethyl acetate (*see* the Experimental Part for a detailed description).

The main advantages of the procedure proposed for the synthesis of $(Bu_4N)_2B_{12}H_{12}$ include the pyrolysis without adding any high-boiling solvent and purification of the products by simple recrystallization. Another advantage offered by the procedure proposed is that not only *closo*-dodecaborate, but also the octahydrotriborate byproduct $Bu_4NB_3H_8$ can be isolated, which is a more convenient route for preparing octahydrotriborate compared to other known methods based on reactions of $NaBH_4$ with iodine [19] or CuCl [20] in diglyme, with BH_3·THF [21], alkali metals tetrahydroborates with BH_3·THF [22] or BH_3·DMS [23] and reduction of BH_3·THF by sodium dispersed on silica gel [24].

The identity of the $(Bu_4N)_2B_{12}H_{12}$ and $Bu_4NB_3H_8$ prepared was additionally confirmed by IR (**Figure 1**) spectroscopy. In order to perform an accurate assignment of IR absorption bands associated with vibrations of the hydroborate anions, the normal coordinate analysis of $[B_{12}H_{12}]^{2-}$ (**Table 1**) and $[B_3H_8]^-$ (**Table 2**) was performed at ωB97X-D/TZVP level of theory. The bands associated with vibrations of the Bu_4N^+ cation were assigned according to [25].

The *closo*-dodecaborate anion (**Figure 2**, *a*) possesses an icosahedral symmetry with calculated BB and BH bonds of 1.78 and 1.21 Å, respectively. It has 3 × 24 – 6 = 66 vibrational modes, but only 3 groups of them are IR active (**Table 1**). The most intense bands in the IR spectrum of $(Bu_4N)_2B_{12}H_{12}$ are due to antisymmetric BH stretching (2464 cm^{-1}) and the BBH bending (1053 cm^{-1}) vibrations. The medium-intensity band in the low-frequency region with a maximum at 710 cm^{-1} is assigned to skeletal vibrations of the B_{12} cluster. Other absorption bands are attributed to vibrations of the Bu_4N^+ cation.

Table 1. Experimental IR absorption bands of $(Bu_4N)_2B_{12}H_{12}$ and calculated normal modes (ν_i) of $[B_{12}H_{12}]^{2-}$ anion

Band (cm^{-1}), intensity[a]	Assignment[b]	ν_i	Calculated frequency (cm^{-1})	Calculated intensity (km mol^{-1})
2960, m 2936, m 2873, m	*ν*(C–H)	-	-	-
2464, s	*ν*(B–H)	ν_{65} ν_{64} ν_{63}	2532.9 2532.6 2532.1	1200 1200 1202
1470, s 1381, m	*δ*(CH)	-	-	-
1153, w	*ρ*(CH_3)	-	-	-
1053, s	*δ*(BH)	ν_{54} ν_{53} ν_{52}	1083.0 1081.3 1079.9	44.8 45.2 44.8
882, m	*ν*(C–N)	-	-	-
740, m	*ρ*(CH_2)	-	-	-
710, m	τ	ν_{17} ν_{16}	721.0 717.9	7.2 7.2

Notes: [a] s – strong, m – medium, w – weak; [b] ν – stretching, δ – scissoring, ρ – rocking, τ – skeletal

The octahydrotriborate anion (**Figure 2**, *b*) has a structure of isosceles BBB triangle with BH_2 moieties at vertices. The base of the triangle is a conventional covalent B–B bond, and vertices at the legs are linked by bridging hydrogens. Due to the formation of bent B–H_b–B bonds, the legs are somewhat shorter (1.79 Å) than the base (1.83 Å). The calculated H_2B–B(H)H_2 stretching force constants (2.99 N cm^{-1}) are also larger than H_2(H)B–B(H)H_2 one (2.08 N cm^{-1}). The bent B–H_b–B bond is asymmetric: the interatomic distances (stretching force constants) for constituent B–H_b

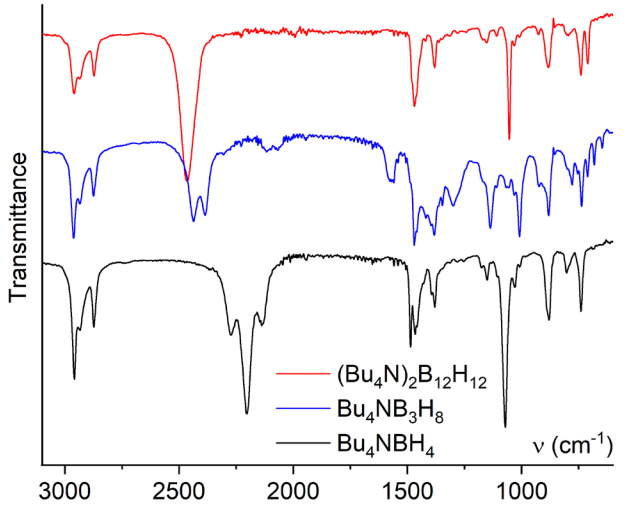

Figure 1. IR spectra of the tetrabutylammonium hydroborates prepared

ISSN 2308-8303 (Print) / 2518-1548 (Online)

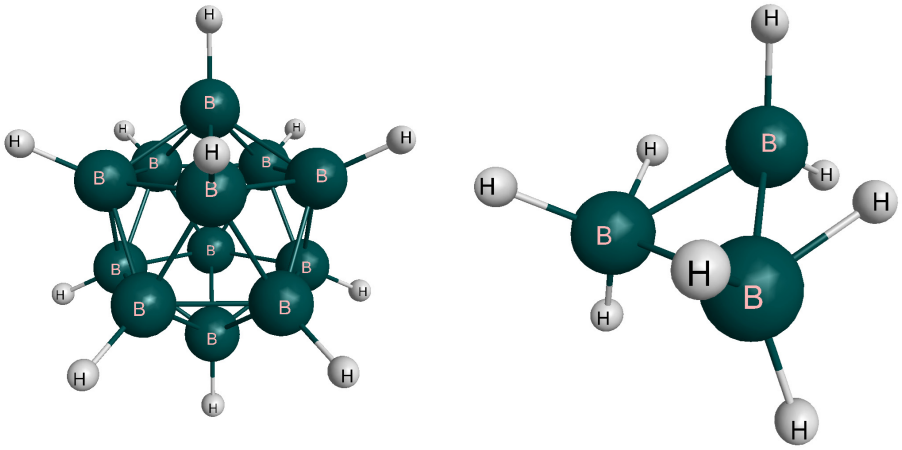

a *b*

Figure 2. Optimized structures of $[B_{12}H_{12}]^{2-}$ (*a*) and $[B_3H_8]^-$ (*b*)

Table 2. Experimental IR absorption bands of $Bu_4NB_3H_8$ and calculated normal modes (ν_i) of $[B_3H_8]^-$ anion

Band (cm^{-1}), intensity[a]	Assignment[b]	ν_i	Calculated frequency (cm^{-1})	Calculated intensity (km mol^{-1})
2962, s 2935, m 2875, m	ν(C–H)	-	-	-
2437, s	ν_{as}(B=H_2)	ν_{24}	2518.0	707
2386, s	ν_{as}({H}B=H_2) ν_s(B=H_2)	ν_{23} ν_{22}	2447.8 2445.1	175 409
2117, w	ν_s(B–H_b)	ν_{21}	2248.6	153
2066, w	ν_{as}(B–H_b)	ν_{20}	2204.2	42.3
1470, s 1382, s 1299, m	δ(CH)	-	-	-
1137, s	δ(BH_2)	ν_{15}	1162.3	61.7
1009, s	ω(BH_2)	ν_{12}	1042.5	85.8
882, s	ν(C–N)	-	-	-
778, m	ν(B–B)	ν_9 ν_8	823.8 812.8	8.0 11.0
737, s	ρ(CH_2)	-	-	-
711, m 681, m 647, w	τ	-	-	-

Notes: [a] s – strong, m – medium, w – weak; [b] *ν* – stretching, *δ* – scissoring, *ρ* – rocking, *ω* – wagging, *τ* – skeletal, *s* – symmetric, *as* – antisymmetric, *b* – bridging

parts are 1.26 Å (2.72 N cm^{-1}) and 1.48 Å (1.00 N cm^{-1}). For comparison, the length and force constant for the B–H bonds involving terminal hydrogen atoms are 1.21 Å and 3.36 N cm^{-1}, respectively. For the $[B_{12}H_{12}]^{2-}$ anion, the B–H force constant was calculated to be 3.46 N cm^{-1}. The computed values correspond to those previously reported in [26].

The IR spectrum of $Bu_4NB_3H_8$ is more complicated compared to $(Bu_4N)_2B_{12}H_{12}$ (**Figure 1**). The intense band in the 2330–2550 cm^{-1} range is split into 2 components. According to the calculations performed for $[B_3H_8]^-$, the higher frequency component (peaked at 2437 cm^{-1}) is attributed to the antisymmetric stretching of all three BH_2 moieties in the octahydrotriborate anion. The lower frequency component (peaked at 2386 cm^{-1}) is due to the symmetric counterpart of the previous vibration and antisymmetric BH_2 stretching in two BH_3 fragments. Two weak bands in the 2030–2150 cm^{-1} range are assigned to symmetric (higher frequency) and antisymmetric (lower frequency) B–H_b stretching involving bridging hydrogens. Strong, sharp bands at 1137 and 1009 cm^{-1} are assigned to scissoring and wagging deformations of the BH_2 moieties, respectively. In the low-frequency region two intense bands at 882 and 737 cm^{-1} are due to vibrations of the Bu_4N^+ cation (as can be seen from **Figure 2**, these bands are common for all tetrabutylammonium compounds studied), while other less intense bands are associated with BB stretching (band at 778 cm^{-1}) or other skeletal vibrations of the octahydrotriborate anion (bands below 720 cm^{-1}).

■ Conclusions

Tetrabutylammonium *closo*-dodecaborate $(Bu_4N)_2B_{12}H_{12}$ can be conveniently prepared by the thermal decomposition of Bu_4NBH_4 in the vacuum of a diaphragm pump. When the process is carried out at temperatures not exceeding 175 °C, both the final $(Bu_4N)_2B_{12}H_{12}$ and the intermediate $Bu_4NB_3H_8$ products can be isolated from pyrolysis residue by simple recrystallization. The procedure proposed is easy to handle and does not require any sophisticated equipment.

References

1. Sivaev, I. B.; Bregadze, V. I.; Sjoberg, S. Chemistry of *closo*-dodecaborate anion $[B_{12}H_{12}]^{2-}$: a review. *Collect. Czech. Chem. Commun.* **2002**, *67*, 679–727. https://doi.org/10.1135/cccc20020679.
2. Axtell, J. C.; Saleh, L. M. A.; Qian, E. A.; Wixtrom, A. I.; Spokoyny, A. M. Synthesis and applications of perfunctionalized boron clusters. *Inorg. Chem.* **2018**, *57* (5), 2333–2350. https://doi.org/10.1021/acs.inorgchem.7b02912.
3. Zhao, X.; Yang, Z.; Chen, H.; Wang, Z.; Zhou, X.; Zhang, H. Progress in three-dimensional aromatic-like closo-dodecaborate. *Coord. Chem. Rev.* **2021,** *444*, 214042. https://doi.org/10.1016/j.ccr.2021.214042.
4. Moss, R. L. Critical review, with an optimistic outlook, on Boron Neutron Capture Therapy (BNCT). *Appl. Radiat. Isot.* **2014,** *88*, 2–11. https://doi.org/10.1016/j.apradiso.2013.11.109.
5. Zhang, X.; Lin, Y.; Hosmane, N. S.; Zhu, Y. Nanostructured boron agents for boron neutron capture therapy: a review of recent patents. *Medical Review* **2023,** *3* (5), 425–443. https://doi.org/10.1515/mr-2023-0013.
6. Miller, H. C.; Miller, N. E.; Muetterties, E. L. Chemistry of Boranes. XX. Syntheses of Polyhedral Boranes. *Inorg. Chem.* **1964,** *3* (10), 1456–1463. https://doi.org/10.1021/ic50020a026.
7. Miller, H. C.; Muetterties, E. L.; Boone, J. L.; Garrett, P.; Hawthorne, M. F. Borane Anions. In *Inorg. Synth.*, 1967; pp 81–91. https://doi.org/10.1002/9780470132418.ch16.
8. Adams, R. M.; Siedle, A. R.; Grant, J. Convenient Preparation of the Dodecahydrododecaborate Ion. *Inorg. Chem.* **1964**, *3* (3), 461–461. https://doi.org/10.1021/ic50013a040.
9. Sharon, P.; Afri, M.; Mitlin, S.; Gottlieb, L.; Schmerling, B.; Grinstein, D.; Welner, S.; Frimer, A. A. Preparation and characterization of bis(guanidinium) and bis(aminotetrazolium)dodecahydroborate salts: Green high energy nitrogen and boron rich compounds. *Polyhedron* **2019,** *157*, 71–89. https://doi.org/10.1016/j.poly.2018.09.055.
10. Bykov, A. Y.; Mal'tseva, N. N.; Generalova, N. B.; Zhizhin, K. Y.; Kuznetsov, N. T. Reactions of sodium tetrahydroborate with alkyl and aryl halides: A new approach to the synthesis of $B_3H_8^-$ and $B_{12}H_{12}^{2-}$ anions. *Russ. J. Inorg. Chem.* **2013,** *58* (11), 1321–1323. https://doi.org/10.1134/S003602361311003X.
11. Tran, B. L.; Allen, T. N.; Bowden, M. E.; Autrey, T.; Jensen, C. M. Effects of Glymes on the Distribution of $Mg(B_{10}H_{10})$ and $Mg(B_{12}H_{12})$ from the Thermolysis of $Mg(BH_4)_2$. *Inorganics* **2021**, *9*, 41. https://doi.org/10.3390/inorganics9060041.
12. Mishchenko, A. M.; Lishchenko, Y. L.; Kozytskiy, A. V.; Konysheva, K. M.; Satska, Y. A.; Ryabukhin, S. V.; Volochnyuk, D. M.; Kolotilov, S. V.; Rassukana, Y. V. Preparation of *closo*-decaborate by pyrolysis of tetraethylammonium borohydride: revision and optimization for large-scale production. *ChemRxiv* **2024**. https://doi.org/10.26434/chemrxiv-2024-hrc1c.
13. Hill, W. E.; Johnson, F. A.; Hosmane, N. S. From sodium borohydride to 1,2-dicarba-*closo*-dodecaboranes. *Boron Chemistry–4*. Plenary and Session Lectures Presented at the Fourth International Meeting on Boron Chemistry, Salt Lake City and Snowbird, Utah, USA, July 9-13, 1979. P. 33–39.
14. Brändström, A.; Junggren, U.; Lamm, B. An improved method for the preparation of solutions of diborane. *Tetrahedron Lett.* **1972,** *13* (31), 3173–3176. https://doi.org/10.1016/S0040-4039(01)93995-4.
15. Lyttle, D. A.; Jensen, E. H.; Struck, W. A. Simple Volumetric Assay for Sodium Borohydride. *Anal. Chem.* **1952,** *24* (11), 1843–1844. https://doi.org/10.1021/ac60071a041.
16. Barca, G. M. J.; Bertoni, C.; Carrington, L.; Datta, D.; De Silva, N.; Deustua, J. E.; Fedorov, D. G.; Gour, J. R.; Gunina, A. O.; Guidez, E.; Harville, T.; Irle, S.; Ivanic, J.; Kowalski, K.; Leang, S. S.; Li, H.; Li, W.; Lutz, J. J.; Magoulas, I.; Mato, J.; Mironov, V.; Nakata, H.; Pham, B. Q.; Piecuch, P.; Poole, D.; Pruitt, S. R.; Rendell, A. P.; Roskop, L. B.; Ruedenberg, K.; Sattasathuchana, T.; Schmidt, M. W.; Shen, J.; Slipchenko, L.; Sosonkina, M.; Sundriyal, V.; Tiwari, A.; Galvez Vallejo, J. L.; Westheimer, B.; Włoch, M.; Xu, P.; Zahariev, F.; Gordon, M. S. Recent developments in the general atomic and molecular electronic structure system. *J. Chem. Phys.* **2020,** *152* (15). https://doi.org/10.1063/5.0005188.
17. Chai, J.-D.; Head-Gordon, M. Long-range corrected hybrid density functionals with damped atom–atom dispersion corrections. *Phys. Chem. Chem. Phys.* **2008,** *10* (44), 6615–6620. https://doi.org/10.1039/B810189B.
18. Schäfer, A.; Huber, C.; Ahlrichs, R. Fully optimized contracted Gaussian basis sets of triple zeta valence quality for atoms Li to Kr. *J. Chem. Phys.* **1994,** *100* (8), 5829–5835. https://doi.org/10.1063/1.467146.
19. Nainan, K. C.; Ryschkewitsch, G. E. A new synthesis of $B_3H_8^-$ ion. *Inorganic and Nuclear Chemistry Letters* **1970,** *6* (9), 765–766. https://doi.org/10.1016/0020-1650(70)80095-2.
20. Bykov, A. Y.; Razgonyaeva, G. A.; Mal'tseva, N. N.; Zhizhin, K. Y.; Kuznetsov, N. T. A new method of synthesis of the $B_3H_8^-$ anion. *Russ. J. Inorg. Chem.* **2012,** *57* (4), 471–473. https://doi.org/10.1134/S0036023612040055.
21. Deiseroth, H. J.; Sommer, O.; Binder, H.; Wolfer, K.; Frei, B. CsB_3H_8: Kristallstruktur und Optimierung der Synthese. *Z. Anorg. Allg. Chem.* **1989,** *571* (1), 21–28. https://doi.org/10.1002/zaac.19895710102.
22. Chen, X.-M.; Ma, N.; Zhang, Q.-F.; Wang, J.; Feng, X.; Wei, C.; Wang, L.-S.; Zhang, J.; Chen, X. Elucidation of the Formation Mechanisms of the Octahydrotriborate Anion ($B_3H_8^-$) through the Nucleophilicity of the B–H Bond. *J. Am. Chem. Soc.* **2018,** *140* (21), 6718–6726. https://doi.org/10.1021/jacs.8b03785.
23. Chen, X.; Liu, X.-R.; Wang, X.; Chen, X.-M.; Jing, Y.; Wei, D. A safe and efficient synthetic method for alkali metal octahydrotriborates, unravelling a general mechanism for constructing the delta B3 unit of polyhedral boranes. *Dalton Trans.* **2021,** *50* (39), 13676–13679. https://doi.org/10.1039/D1DT01892B.
24. Dunbar, A. C.; Macor, J. A.; Girolami, G. S. Synthesis and Single Crystal Structure of Sodium Octahydrotriborate, NaB_3H_8. *Inorg. Chem.* **2014,** *53* (2), 822–826. https://doi.org/10.1021/ic402127x.
25. Javanshir, Z.; Mehrani, K.; Ghammamy, Sh.; Saghatforoush, L.; Seyedsadjadi, S.; Hassanijoshaghani, A.; Tavakol, H. Synthesis and characterization of two new fluoroplumbate(II) complexes: tetrabutylammonium fluorodihaloplumbate, $(But)_4N[PbX_2F]$ (X = Cl, I). *Bull. Korean Chem. Soc*. **2008**, *29* (8), 1464–1466.
26. Sethio, D.; Daku, L. M. L.; Hagemann, H.; Kraka, E. Quantitative Assessment of B–B–B, B–Hb–B, and B–Ht Bonds: From BH_3 to $B_{12}H_{12}^{2-}$. *ChemPhysChem* **2019,** *20* (15), 1967–1977. https://doi.org/10.1002/cphc.201900364.

ISSN 2308-8303 (Print) / 2518-1548 (Online)

Information about the authors:
Artem M. Mishchenko, Ph.D. in Chemistry, Laboratory Head at Enamine Ltd.
Maxim A. Nechayev, Laboratory Head at Enamine Ltd.; Junior Scientific Researcher, Institute of Organic Chemistry of the National Academy of Sciences of Ukraine; https://orcid.org/0000-0002-4145-416X.
Andrii I. Subota, Ph.D. in Chemistry, Laboratory Head at Enamine Ltd.;
Andriy V. Kozytskiy, Ph.D. in Chemistry, NMR engineer at Enamine Ltd.; https://orcid.org/0000-0001-8454-7334.
Oleh V. Svaliavyn, Ph.D. in Chemistry, Chemist at Enamine Ltd.; Junior Scientific Researcher, Institute of Organic Chemistry of the National Academy of Sciences of Ukraine.
Yulian L. Lishchenko, Chemist at Enamine Ltd., Postgraduate Student at L. V. Pisarzhevskii Institute of Physical Chemistry of the National Academy of Sciences of Ukraine.
Anastasiia M. Aleksandrova, Ph.D. in Chemistry, Junior Scientific Researcher, Institute of Organic Chemistry of the National Academy of Sciences of Ukraine.
Yuliya V. Rassukana, Dr. Sci. in Chemistry, Professor, Deputy Director for Scientific Work in Institute of Organic Chemistry of the National Academy of Sciences of Ukraine; https://orcid.org/0000-0003-3101-9911.
Dmytro O. Leha (*corresponding author*), Ph.D. in Pharmacy, Department for Education and Advanced Training of Specialists in Chemistry, Enamine Ltd.; Associate Professor of Supramolecular Chemistry Department, Institute of High Technologies, Taras Shevchenko National University of Kyiv; https://orcid.org/0000-0002-4505-3646.

Journal of Organic and Pharmaceutical Chemistry

Original Research

OPEN ACCESS
Freely available online on
http://ophcj.nuph.edu.ua

UDC 547.52+547.539.12

M. O. Pashko[1,2], Yu. L. Yagupolskii[1,2]

[1] Institute of Organic Chemistry of the National Academy of Sciences of Ukraine,
5 Akademik Kuhar str., 02094 Kyiv, Ukraine
[2] Enamine Ltd, 78 Winston Churchill str., 02094 Kyiv, Ukraine

Introduction of the Difluoro(methoxy)methyl Group into the Aromatic Ring and the Study of Its Electronic Properties

Abstract

A simple and efficient method for synthesizing aromatic compounds with a difluoro(methoxy)methyl fragment (CF_2OCH_3) by the fluorodesulfurization of thionoesters has been developed. Systematic screening identified $SnCl_4$/DAST as the optimal reagent combination, providing excellent selectivity and high yields of target products. A series of aromatic difluoro(methoxy)methyl compounds was synthesized under these conditions. Further studies of the electronic properties of the difluoro(methoxy)-methyl group using ^{19}F NMR allowed us to determine its Hammett constants for inductive (σ_I) and resonance (σ_R) effects. The results show that CF_2OCH_3 acts as a moderately electron-withdrawing substituent, underscoring its potential as a versatile group for designing organic molecules with precisely tuned electronic characteristics.

Keywords: difluoro(methoxy)methyl; fluorodesulfurization; Hammett constants

М. О. Пашко[1,2], Ю. Л. Ягупольський[1,2]

*[1] Інститут органічної хімії Національної академії наук України,
вул. Академіка Кухаря, 5, м. Київ, 02094, Україна*
[2] ТОВ НВП «Єнамін», вул. Вінстона Черчилля, 78, м. Київ, 02094, Україна

Введення дифторо(метокси)метильної групи в ароматичне кільце та дослідження її електронних властивостей

Анотація

Розроблено простий та ефективний метод синтезу ароматичних сполук із дифторо(метокси)метильним фрагментом (CF_2OCH_3) шляхом фтородесульфуризації тіонових естерів. Під час систематичного пошуку умов реакції було визначено, що оптимальним поєднанням реагентів є $SnCl_4$/DAST, яке забезпечує відмінну селективність процесу та високі виходи цільових продуктів. З використанням цих умов було синтезовано серію ароматичних дифторо(метокси)метильних похідних. Подальше дослідження електронних властивостей дифторо(метокси)метильної групи за допомогою ^{19}F ЯМР дозволило визначити її константи Гаммета для індуктивного (σ_I) та резонансного (σ_R) ефектів. Отримані результати свідчать, що дифторо(метокси)метильна група є помірно електроноакцепторним замісником, що робить її цікавим структурним фрагментом для побудови органічних молекул із необхідними електронними характеристиками.

Ключові слова: дифторо(метокси)метил; фтородесульфуризація; константи Гаммета

Citation: Pashko, M. O.; Yagupolskii, Yu. L. Introduction of the difluoro(methoxy)methyl group into the aromatic ring and the study of its electronic properties. *Journal of Organic and Pharmaceutical Chemistry* **2024**, *22* (4), 10–16.
https://doi.org/10.24959/ophcj.24.321167
Received: *3 September 2024*; **Revised:** *24 November 2024*; **Accepted:** *3 December 2024*

Funding: The author received no specific funding for this work.
Conflict of interests: The authors have no conflict of interests to declare.

ISSN 2308-8303 (Print) / 2518-1548 (Online)

■ Introduction

The development of methodologies for introducing difluoro(alkoxy)methyl fragments (CF_2OR) into organic molecules has gained prominence in the chemical community, owing to their distinctive impact on the physicochemical and biological properties of compounds [1, 2]. In particular, the difluoro(methoxy)methyl group (CF_2OCH_3) combines the electron-withdrawing properties of a CF_2 moiety with the ambiguous electronic nature of a methoxy substituent, potentially resulting in an intriguing balance of field (inductive) and resonance effects.

Traditionally, the synthesis of difluoro(alkoxy)-methyl ethers has relied on aggressive reagents, such as SF_4 [3], BrF_3 [4], or HF with oxidant systems [5], which typically demand elevated temperatures and pressures, and often involve toxic or explosive conditions. More moderate protocols employing DAST and related reagents [6] can enable the fluorodesulfurization under milder conditions, but they may be limited by compatibility issues with certain functional groups. Recent literature has described the use of silver(I) salts (AgF) [7] for similar transformations although this approach is quite sensitive to the purity of the AgF reagent.

Despite progress in the synthesis of difluoro(alkoxy)methyl compounds, the electronic properties of the CF_2OCH_3 group, particularly in terms of its Hammett constants, have remained largely unexplored. The first objective of our study, therefore, was to develop a convenient method for accessing aryl-CF_2OCH_3 derivatives by utilizing thionoesters as precursors to install the difluoro(methoxy)-methyl group. The second goal was to study the electronic characteristics of the CF_2OCH_3 group and determine its Hammett constants (σ_I and σ_R) comparing these values with those of related fluorinated substituents [8]. The Hammett analysis was performed *via* the ^{19}F NMR approach [9, 10, 13].

■ Results and discussion

Optimization of the aryl-CF_2OCH_3 synthesis

We selected *O*-methyl benzothioate (**3**) as a model substrate to evaluate the transformation of a methyl thionoester into a difluoro(methoxy)methyl group. Thionoesters were prepared from the corresponding aryl bromides using *O*-methyl carbonochloridothioate (**2**), following a reported procedure [11]. According to the literature, there are three main strategies for converting thionoesters into difluoro-(alkoxy)methyl compounds: (1) using DAST or related fluorinating reagents [6]; (2) using oxidizing agents for the fluorination [5, 12]; (3) performing the nucleophilic fluorine substitution with *S*-selective metal fluorides (or their salts) in the presence of additional fluoride sources [7]. It is important to note that methods not relying on DAST or morphDAST were very sensitive to the presence of water; in many experiments, methyl benzoate (**5**) appeared as an impurity or even the main product. After testing various conditions for forming the difluoro(methoxy)-methyl group, we found that the best results came from using DAST with small (catalytic) amounts of tin chlorides ($SnCl_2$ or $SnCl_4$). This approach, in our opinion, is the most effective since it tolerates trace moisture and uses readily available reagents.

Using the $SnCl_4$/DAST method to convert methyl thionoesters into difluoro(methoxy)methyl derivatives, we synthesized a series of aromatic compounds **4a–l** containing the CF_2OCH_3 group (**Figure 1**).

Determination of Hammett Constants

Compounds **4e** and **4f** were used to measure Hammett constants *via* the ^{19}F NMR method. This method is known to be simple and often used for studying electronic properties [13]. The ^{19}F NMR spectra were recorded in the presence of small amounts of hexafluorobenzene (to calibrate chemical shifts) and monofluorobenzene. From the difference in ^{19}F chemical shifts between monofluorobenzene

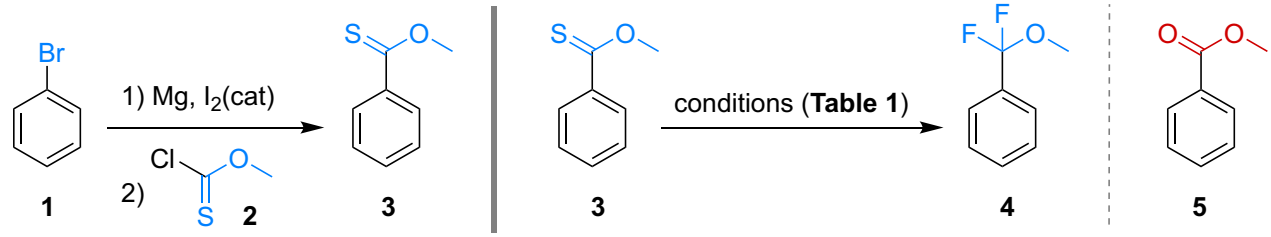

Scheme 1. The synthetic approach to the synthesis of difluoro(methoxy)methyl compounds

Table 1. Screening fluorination conditions for forming the difluoro(methoxy)-methyl group

Reagents	Conditions	Result
morpDAST 2 equiv.	DCM, rt, 16 h	No reaction
$SbCl_3$ 0.05 equiv., morphDAST 2 equiv.	DCM, rt, 16 h	Conversion – 100 %, 15 % of **5**
SbF_3 0.05 equiv., morphDAST 2 equiv.	DCM, rt, 16 h	No reaction
PCl_3 0.05 equiv., morphDAST 2 equiv.	DCM, rt, 16 h	No reaction
PBr_3 0.05 equiv., morphDAST 2 equiv.	DCM, rt, 16 h	No reaction
$SiCl_4$ 0.05 equiv., morphDAST 2 equiv.	DCM, rt, 16 h	No reaction
$SnCl_4$ 0.05 equiv., morphDAST 2 equiv.	DCM, rt, 16 h	Conversion – 100 %
$SnCl_2$ 0.05 equiv., morphDAST 2 equiv.	DCM, rt, 16 h	Conversion – 100 %
NBS 3 equiv., NEt_3*3HF 3 equiv.	DCM, rt, 16 h	Conversion – 100 %, 60 % of **5**
$SnCl_2$ 0.05 equiv., morphDAST 2 equiv.	DCM, rt, 16 h	Conversion – 100 %
$SnCl_4$ 0.05 equiv., DAST 2 equiv.	DCM, rt, 2 h	Conversion – 100 %
$SnCl_2$ 0.05 equiv., DAST 2 equiv.	DCM, rt, 2 h	Conversion – 100 %
DAST 2 equiv.	DCM, rt, 36 h	Conversion – 100 %
CsF 3 equiv., $HgCl_2$ 0.1 equiv.	THF, rt, 16 h	Starting material. Product traces in ^{19}F
TBAF 3 equiv., $HgCl_2$ 0.1 equiv.	THF, rt, 16 h	Starting material. Product traces in ^{19}F
CsF 3 equiv., $Hg(OAc)_2$ 0.1 equiv.	THF, 60 °C, 2 h	Conversion – 80 %, **5** was formed
CsF 3 equiv., $Hg(OAc)_2$ 0.1 equiv., NEt_3*3HF 2 equiv.	THF, rt, 0.25 h	Conversion – 100 %, **5** was formed. Product traces in ^{19}F
CsF 3 equiv., $HgCl_2$ 0.1 equiv., NEt_3*3HF 2 equiv.	THF, 60 °C, 2 h	Conversion – 100 %, 70 % of **5**
AgF 3 equiv.	MeCN, rt, 3 h	Conversion – 100 %, 40 % of **5**

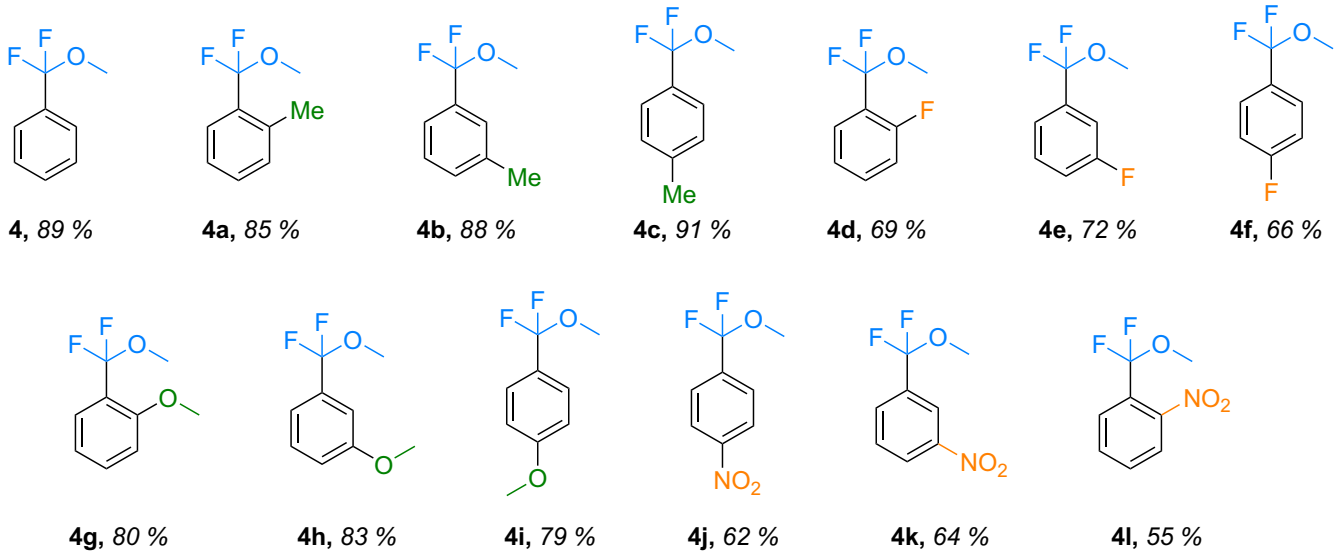

4, *89 %* **4a**, *85 %* **4b**, *88 %* **4c**, *91 %* **4d**, *69 %* **4e**, *72 %* **4f**, *66 %*

4g, *80 %* **4h**, *83 %* **4i**, *79 %* **4j**, *62 %* **4k**, *64 %* **4l**, *55 %*

Figure 1. The synthesis of a series of aromatic compounds **4a–l** containing the CF_2OCH_3 group

and the target samples, we calculated the Hammett constants using equations (1) and (2) [10, 14]. To ensure that the fluorine atom was not shielded by intermolecular interactions, additional ^{19}F spectra were taken at lower concentrations; the chemical shift difference remained nearly the same (**Table 2**). Based on these results, we calculated the inductive (σ_I) and resonance (σ_R) Hammett constants for the difluoro(methoxy)-methyl group as $\sigma_I = 0.2163$ and $\sigma_R = 0.0686$.

$$\Delta\delta_m^{19}F = -7.1 \times \sigma_I + 0.6 \quad (1)$$

$$\Delta\delta_p^{19}F = -7.1 \times \sigma_I - 29.5 \times \sigma_R + 0.6 \quad (2)$$

These positive values of Hammett constants indicate that the CF_2OCH_3 group acts as a moderate electron acceptor through both inductive and resonance effects. Comparing these Hammett constants with those of similar groups suggests that CF_2OCH_3 lies near CHF_2 within the series CF_3, CHF_2, CH_2F, and CH_3 (**Table 3**).

■ Conclusions

A convenient method for synthesizing aromatic compounds bearing the difluoro(methoxy) methyl group (CF_2OCH_3) *via* the fluorodesulfurization of thionoesters has been developed. By screening various fluorination conditions, an

ISSN 2308-8303 (Print) / 2518-1548 (Online)

Table 2. ^{19}F NMR data for **4e** and **4f** at different concentrations.

	Concentration	$\delta^{19}F(C_6H_5F)$	$\delta^{19}F(Ar)$	$\delta^{19}F(CF_2OMe)$	$\delta^{19}F(C_6H_5F) - \delta^{19}F(Ar)$ ($\Delta\delta_m^{19}F$)
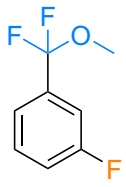 **4e**	c	-113.006	-112.07	-72.007	-0.936
	c/2	-113.008	-112.071	-72.009	-0.937
	c/4	-113.014	-112.078	-72.017	-0.936
	c/8	-113.019	-112.083	-72.023	-0.936
	c/16	-113.019	-112.083	-72.023	-0.936
	c/32	-113.022	-112.087	-72.033	-0.935
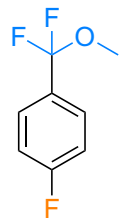 **4f**	c	-113.005	-110.046	-71.307	-2.959
	c/2	-113.014	-110.055	-71.317	-2.959
	c/4	-113.018	-110.059	-71.321	-2.959
	c/8	-113.019	-110.059	-71.323	-2.96
	c/16	-113.019	-110.059	-71.322	-2.96
	c/32	-113.019	-110.059	-71.322	-2.96

Table 3. Hammett constants for CF_2OCH_3 and similar groups [15]

Group	σ_I	σ_R
CF_2OCH_3	0.22	0.07
CH_3	-0.08	-0.15
CH_2F	0.13	-0.02
CHF_2	0.26	0.06
CF_3	0.39	0.1
CH_2OCH_3	0.09	-0.05

$SnCl_4$/DAST combination has proven to be optimal in terms of both selectivity and yield.

The compounds **4e** and **4f** synthesized served as models to study the electronic effects of this group. The Hammett constant measurements (σ_I and σ_R) by ^{19}F NMR have shown that the difluoro(methoxy)methyl group acts as a moderate electron acceptor through both inductive and resonance pathways ($\sigma_I = 0.22$, $\sigma_R = 0.07$). The comparison with similar substituents (CF_3, CHF_2, CH_2F, CH_2OCH_3 and CH_3) suggests that CF_2OCH_3 occupies an intermediate position and is closest in overall electronic effect to CHF_2.

These findings indicate that CF_2OCH_3 can be used as an effective tool for the targeted modulation of the electronic properties of aromatic compounds. The described mild-condition synthesis of the difluoro(methoxy)methyl fragment from thionoesters broadens the scope for incorporating this group into a diverse range of molecules. Determining the electronic features of the CF_2OCH_3 group opens up promising opportunities for its further application in medicinal chemistry, materials science, and other areas of organic synthesis.

Experimental part

General information and materials

The solvents were purified according to the standard procedures. All starting materials were obtained from Enamine Ltd. NMR spectra were recorded on a Bruker Avance 500 spectrometer (at 500 MHz for ^1H and 126 MHz for ^{13}C nucleus) and Varian Unity Plus 400 spectrometers (at 400 MHz for ^1H, 101 MHz for ^{13}C nucleus). Tetramethylsilane (^1H, ^{13}C) was used as an internal standard. GCMS analyses were performed using an Agilent 5890 Series II 5972 GCMS instrument (electron impact (EI) ionization (70 eV)). Column chromatography was performed with silica gel (200–300 mesh). The elemental analysis was carried out in the Analytical Laboratory of the Institute of Organic Chemistry, NAS of Ukraine.

The general procedure for the fluorodesulfurization (on the example of thionoester 3)

A stirred solution of methyl benzenecarbothioate (1.0 g, 6.58 mmol) in CH_2Cl_2 (30 mL) was cooled to 0°C. DAST (2.12 g, 13.16 mmol, 1.74 mL, 2.0 equiv.) was added dropwise, followed by $SnCl_4$ (85.45 mg, 328.95 μmol, 0.05 equiv.). The reaction mixture was then allowed to warm to room temperature and stirred for 2 h. It was quenched with saturated aqueous $NaHCO_3$, and the resulting mixture was extracted with CH_2Cl_2. The combined organic layers were dried over Na_2SO_4, filtered, and concentrated *in vacuo* to give a crude residue. The residue was purified by silica gel column chromatography (hexanes) to give [difluoro(methoxy)methyl]benzene as a colorless liquid (0.93 g, 89% yield).

(Difluoro(methoxy)methyl)benzene (4)

A colorless liquid. Yield – 0.93 g (89%). Anal. Calcd for $C_8H_8F_2O$, %: C 60.76, H 5.10. Found, %: C 61.10, H 5.04. ^{1}H NMR (500 MHz, Chloroform-*d*), *δ*, ppm: 7.61 (2H, d, *J* = 7.4 Hz), 7.43 (3H, dt, *J* = 14.5, 6.9 Hz), 3.72 (3H, s). ^{13}C{^{1}H} NMR (126 MHz, Chloroform-*d*), *δ*, ppm: 133.71 (t, *J* = 32.6 Hz), 129.94, 127.75, 124.89 (t, *J* = 3.8 Hz), 122.60 (t, *J* = 257.9 Hz), 50.06 (t, *J* = 8.0 Hz). ^{19}F{^{1}H} NMR (376 MHz, Chloroform-*d*), *δ*, ppm: -72.84. GC-MS (EI), m/z: 158 $[M]^{+\cdot}$.

1-(Difluoro(methoxy)methyl)-2-methylbenzene (4a)

A colorless liquid. Yield – 0.88 g (85%). Anal. Calcd for $C_9H_{10}F_2O$, %: C 62.78, H 5.85. Found, %: C 62.80, H 5.84. ^{1}H NMR (500 MHz, Chloroform-*d*), *δ*, ppm: 7.63 (1H, d, *J* = 7.7 Hz), 7.34 (1H, t, *J* = 7.5 Hz), 7.23 (2H, d, *J* = 8.2 Hz), 3.71 (3H, s), 2.48 (3H, d, *J* = 1.9 Hz). ^{13}C{^{1}H} NMR (126 MHz, Chloroform-*d*), *δ*, ppm: 136.10, 131.70 (t, *J* = 30.5 Hz), 131.08, 129.84, 125.31 (t, *J* = 5.9 Hz), 124.87, 122.99 (t, *J* = 259.6 Hz), 49.92, 19.12. ^{19}F{^{1}H} NMR (376 MHz, Chloroform-*d*), δ, ppm: -73.38. GC-MS (EI), m/z: 172 $[M]^{+\cdot}$.

1-(Difluoro(methoxy)methyl)-3-methylbenzene (4b)

A colorless liquid. Yield – 0.92 g (89%). Anal. Calcd for $C_9H_{10}F_2O$, %: C 62.78, H 5.85. Found, %: C 62.47, H 5.88. ^{1}H NMR (400 MHz, Chloroform-*d*), *δ*, ppm: 7.45 (2H, d, *J* = 9.2 Hz), 7.31 (2H, dt, *J* = 13.7, 7.5 Hz), 3.74 (3H, s), 2.41 (3H, s). ^{13}C{^{1}H} NMR (101 MHz, Chloroform-*d*), *δ*, ppm: 138.15, 134.01 (t, *J* = 32.7 Hz), 131.22, 128.23, 125.97, 123.16 (t, *J* = 258.0 Hz), 122.45, 50.67 (t, *J* = 7.0 Hz), 21.35. ^{19}F{^{1}H} NMR (376 MHz, Chloroform-*d*), *δ*, ppm: -73.39. GC-MS (EI), m/z: 172 $[M]^{+\cdot}$.

1-(Difluoro(methoxy)methyl)-4-methylbenzene (4c)

A colorless liquid. Yield – 0.94 g (91%). Anal. Calcd for $C_9H_{10}F_2O$, %: C 62.78, H 5.85. Found, %: C 63.14, H 5.88. ^{1}H NMR (500 MHz, Chloroform-*d*), *δ*, ppm: 7.51 (2H, d, *J* = 7.9 Hz), 7.22 (2H, d, *J* = 7.9 Hz), 3.71 (3H, s), 2.39 (3H, s). ^{13}C{^{1}H} NMR (126 MHz, Chloroform-*d*), *δ*, ppm: 140.03, 130.85 (t, *J* = 32.7 Hz), 128.40, 124.81 (t, *J* = 3.8 Hz), 122.84 (d, *J* = 258.0 Hz), 50.10, 20.75. ^{19}F{^{1}H} NMR (376 MHz, Chloroform-*d*), *δ*, ppm: -71.32. GC-MS (EI), m/z: 172 $[M]^{+\cdot}$.

1-(Difluoro(methoxy)methyl)-2-fluorobenzene (4d)

A colorless liquid. Yield – 0.72 g (69%). Anal. Calcd for $C_8H_7F_3O$, %: C 54.55, H 4.01. Found, %: C 54.27, H 4.05. ^{1}H NMR (500 MHz, Chloroform-*d*), *δ*, ppm: 7.61 (1H, t, *J* = 7.6 Hz), 7.44 (1H, q, *J* = 7.1 Hz), 7.17 (1H, t, *J* = 7.8 Hz), 7.13 (1H, dd, *J* = 10.8, 8.4 Hz, 1H), 3.73 (3H, s). ^{13}C{^{1}H} NMR (126 MHz, Chloroform-*d*), *δ*, ppm: 159.37 (d, *J* = 254.3 Hz), 133.90 (d, *J* = 8.9 Hz), 131.97 (d, *J* = 8.3 Hz), 126.96 (d, *J* = 4.8 Hz), 123.10 (d, *J* = 3.8 Hz), 121.13 (t, *J* = 258.0 Hz), 116.04 (d, *J* = 21.0 Hz), 50.15. ^{19}F{^{1}H} NMR (376 MHz, Chloroform-*d*), *δ*, ppm: -72.29 (d, *J* = 14.3 Hz), -115.11 (t, *J* = 14.2 Hz). GC-MS (EI), m/z: 176 $[M]^{+\cdot}$.

1-(Difluoro(methoxy)methyl)-3-fluorobenzene (4e)

A colorless liquid. Yield – 0.75 g (72%). Anal. Calcd for $C_8H_7F_3O$, %: C 54.55, H 4.01. Found, %: C 54.16, H 4.03. ^{1}H NMR (400 MHz, Chloroform-*d*), *δ*, ppm: 7.43–7.35 (2H, m), 7.35–7.27 (1H, m), 7.14 (1H, ddd, *J* = 10.5, 5.5, 2.6 Hz), 3.71 (3H, d, *J* = 1.7 Hz). ^{13}C{^{1}H} NMR (101 MHz, Chloroform-*d*), *δ*, ppm: 162.41 (d, *J* = 246.8 Hz), 136.28 (td, *J* = 33.5, 7.7 Hz), 130.09 (d, *J* = 8.0 Hz), 122.22 (t, *J* = 256.8 Hz), 121.16 (q, *J* = 3.6 Hz), 117.54 (d, *J* = 21.1 Hz), 112.99 (dt, *J* = 23.9, 3.8 Hz), 50.77 (t, *J* = 7.1 Hz). ^{19}F{^{1}H} NMR (376 MHz, Chloroform-*d*), *δ*, ppm: -72.61, -112.66. GC-MS (EI), m/z: 176 $[M]^{+\cdot}$.

1-(Difluoro(methoxy)methyl)-4-fluorobenzene (4f)

A colorless liquid. Yield – 0.68 g (66%). Anal. Calcd for $C_8H_7F_3O$, %: C 54.55, H 4.01. Found, %: C 54.29, H 4.05. ^{1}H NMR (500 MHz, Chloroform-*d*), *δ*, ppm: 7.60 (2H, dd, *J* = 8.5, 5.3 Hz), 7.09 (2H, t, *J* = 8.5 Hz), 3.71 (3H, s). ^{13}C{^{1}H} NMR (101 MHz, Chloroform-*d*), *δ*, ppm: 163.90 (d, *J* = 249.9 Hz), 130.29 (td, *J* = 32.8, 2.8 Hz), 127.68 (dt, *J* = 8.4, 3.7 Hz), 122.67 (t, *J* = 257.7 Hz), 115.30 (d, *J* = 22.0 Hz), 50.66 (t, *J* = 7.0 Hz). ^{19}F{^{1}H} NMR (376 MHz, Chloroform-*d*), *δ*, ppm: -71.91, -110.65. GC-MS (EI), m/z: 176 $[M]^{+\cdot}$.

1-(Difluoro(methoxy)methyl)-2-methoxybenzene (4g)

A colorless liquid. Yield – 1.03 g (80%). Anal. Calcd for $C_9H_{10}F_2O_2$, %: C 57.45, H 5.36. Found, %: C 57.66, H 5.35. ^{1}H NMR (500 MHz, Chloroform-*d*), *δ*, ppm: 7.59 (1H, dd, *J* = 7.9, 1.7 Hz), 7.41 (1H, td, *J* = 7.9, 1.8 Hz), 6.97 (2H, d, *J* = 7.9 Hz), 3.88 (3H, s), 3.69 (3H, s). ^{13}C{^{1}H} NMR (126 MHz, Chloroform-*d*), *δ*, ppm: 156.89, 131.49, 126.92 (t, *J* = 5.5 Hz), 122.06 (t, *J* = 258.7 Hz), 121.56 (t, *J* = 31.4 Hz), 119.40, 111.58, 55.47, 50.05. ^{19}F{^{1}H} NMR (376 MHz, Chloroform-*d*), *δ*, ppm: -73.39. GC-MS (EI), m/z: 188 $[M]^{+\cdot}$.

1-(Difluoro(methoxy)methyl)-3-methoxybenzene (4h)

A colorless liquid. Yield – 0.86 g (83%). Anal. Calcd for $C_9H_{10}F_2O_2$, %: C 57.45, H 5.36. Found, %:

ISSN 2308-8303 (Print) / 2518-1548 (Online)

C 57.44, H 5.40. ^{1}H NMR (400 MHz, Chloroform-*d*), *δ*, ppm: 7.35 (1H, t, *J* = 8.0 Hz), 7.22 (1H, d, *J* = 7.6 Hz), 7.15 (1H, d, *J* = 2.0 Hz), 7.01 (1H, dd, *J* = 8.3, 2.6 Hz), 3.84 (3H, s), 3.73 (2H, s). ^{13}C{^{1}H} NMR (101 MHz, Chloroform-*d*), *δ*, ppm: 159.48, 129.48, 122.89 (t, *J* = 258.4 Hz), 121.97, 119.49, 116.47, 110.73 (d, *J* = 3.8 Hz), 55.34, 50.73 (t, *J* = 7.1 Hz). ^{19}F{^{1}H} NMR (376 MHz, Chloroform-*d*), *δ*, ppm: -73.39. GC-MS (EI), m/z: 188 $[M]^{+\cdot}$.

1-(Difluoro(methoxy)methyl)-4-methoxybenzene (4i)

A colorless liquid. Yield – 0.82 g (79%). Anal. Calcd for $C_9H_{10}F_2O_2$, %: C 57.45, H 5.36. Found, %: C 57.79, H 5.30. ^{1}H NMR (500 MHz, Chloroform-*d*), *δ*, ppm: 7.54 (2H, d, *J* = 8.5 Hz), 6.91 (2H, d, *J* = 8.7 Hz), 3.82 (3H, d, *J* = 1.1 Hz), 3.70 (3H, s). ^{13}C{^{1}H} NMR (101 MHz, Chloroform-*d*), *δ*, ppm: 161.12, 126.98 (t, *J* = 3.6 Hz), 126.51 (t, *J* = 33.0 Hz), 123.28 (t, *J* = 257.0 Hz), 113.55, 55.31, 50.64 (t, *J* = 7.1 Hz). ^{19}F{^{1}H} NMR (376 MHz, Chloroform-*d*), *δ*, ppm: -71.51. GC-MS (EI), m/z: 188 $[M]^{+\cdot}$.

1-(Difluoro(methoxy)methyl)-4-nitrobenzene (4j)

A yellow liquid. Yield – 0.64 g (62%). Anal. Calcd for $C_8H_7F_2NO_3$, %: C 47.30, H 3.47, N 6.90. Found, %: C 46.64, H 3.51, N 6.79. ^{1}H NMR (500 MHz, Chloroform-*d*), *δ*, ppm: 8.26 (1H, dd, *J* = 9.3, 2.6 Hz), 7.86–7.67 (1H, m), 3.75 (1H, s). ^{13}C{^{1}H} NMR (101 MHz, Chloroform-*d*), *δ*, ppm: 149.19, 139.92 (t, *J* = 33.7 Hz), 126.85 (t, *J* = 3.5 Hz), 123.61, 121.83 (t, *J* = 248.5 Hz), 51.01 (t, *J* = 7.1 Hz). ^{19}F{^{1}H} NMR (376 MHz, Chloroform-*d*), *δ*, ppm: -72.69. GC-MS (EI), m/z: 203 $[M]^{+\cdot}$.

1-(Difluoro(methoxy)methyl)-3-nitrobenzene (4k)

A yellow liquid. Yield – 0.66 g (64%). Anal. Calcd for $C_8H_7F_2NO_3$, %: C 47.30, H 3.47, N 6.90. Found, %: C 47.61, H 3.48, N 6.82. ^{1}H NMR (400 MHz, Chloroform-*d*), δ, ppm: 8.48 (1H, s), 8.33 (1H, dd, *J* = 8.2, 2.2 Hz), 7.95 (1H, d, *J* = 7.8 Hz), 7.63 (1H, t, *J* = 8.0 Hz), 3.78 (3H, d, *J* = 1.2 Hz). ^{13}C{^{1}H} NMR (101 MHz, Chloroform-*d*), *δ*, ppm: 148.06, 135.96 (t, *J* = 34.3 Hz), 131.47 (t, *J* = 3.2 Hz), 129.65, 125.37, 121.70 (t, *J* = 258.7 Hz), 121.04, 50.99 (t, *J* = 7.0 Hz). ^{19}F{^{1}H} NMR (376 MHz, Chloroform-*d*), *δ*, ppm: -72.72. GC-MS (EI), m/z: 203 $[M]^{+\cdot}$.

1-(Difluoro(methoxy)methyl)-2-nitrobenzene (4l)

A yellow liquid. Yield – 0.57 g (55%). Anal. Calcd for $C_8H_7F_2NO_3$, %: C 47.30, H 3.47, N 6.90. Found, %: C 46.61, H 3.50, N 6.80. ^{1}H NMR (400 MHz, Chloroform-*d*), *δ*, ppm: 7.86–7.72 (1H, m), 7.64 (3H, dtd, *J* = 9.2, 6.0, 2.5 Hz), 3.71 (3H, s). ^{13}C{^{1}H} NMR (101 MHz, Chloroform-*d*), *δ*, ppm: 148.21, 131.75, 131.56, 129.01, 127.79 (t, *J* = 4.9 Hz), 123.92, 120.84 (t, *J* = 260.1 Hz), 51.18 (t, *J* = 7.0 Hz). ^{19}F{^{1}H} NMR (376 MHz, Chloroform-*d*), *δ*, ppm: -72.75. GC-MS (EI), m/z: 203 $[M]^{+\cdot}$.

References

1. Meanwell, N. A. Fluorine and Fluorinated Motifs in the Design and Application of Bioisosteres for Drug Design. *J. Med. Chem.* **2018,** *61* (14), 5822–5880. https://doi.org/10.1021/acs.jmedchem.7b01788.
2. Leroux, F.; Jeschke, P.; Schlosser, M. α-Fluorinated Ethers, Thioethers, and Amines: Anomerically Biased Species. *Chem. Rev.* **2005,** *105* (3), 827–856. https://doi.org/10.1021/cr040075b.
3. Burmakov, A. I.; Kunshenko, B. V.; Lyalin, V. V.; Muratov, N. N.; Omarov, V. O.; Yagupolskii, L. M. Reactions of organic compounds with SF_4•HF, SF_4•HF•Cl_2(Br_2) and SF_4•HF•S_2Cl_2 systems. *J. Fluorine Chem.* **1992,** *58* (2), 174. https://doi.org/10.1016/S0022-1139(00)80622-3.
4. Rozen, S.; Mishani, E. Conversion of esters to α,α-difluoro ethers using bromine trifluoride. *J. Chem. Soc., Chem. Commun.* **1993,** 23, 1761–1762. https://doi.org/10.1039/C39930001761.
5. Kuroboshi, M.; Hiyama, T. A Facile Synthesis of α,α-Difluoroalkyl Ethers and Carbonyl Fluoride Acetals by Oxidative Desulfurization-Fluorination. *Synlett* **1994**, *1994* (04), 251–252. https://doi.org/10.1055/s-1994-22815.
6. Lepri, S.; Buonerba, F.; Maccaroni, P.; Goracci, L.; Ruzziconi, R. Are carboxylic esters really refractory to DAST? On the fluorination of α-hydroxyesters with DAST. *J. Fluorine Chem.* **2015,** *171*, 82–91. https://doi.org/10.1016/j.jfluchem.2014.09.007.
7. Newton, J.; Driedger, D.; Nodwell, M. B.; Schaffer, P.; Martin, R. E.; Britton, R.; Friesen, C. M. A Convenient Synthesis of Difluoroalkyl Ethers from Thionoesters Using Silver(I) Fluoride. *Chem. Eur. J.* **2019,** *25* (70), 15993–15997. https://doi.org/10.1002/chem.201904132.
8. Hansch, C.; Leo, A.; Taft, R. W. A survey of Hammett substituent constants and resonance and field parameters. *Chem. Rev.* **1991,** *91* (2), 165–195. https://doi.org/10.1021/cr00002a004.
9. Yagupolskii, L. M. Aromatic compounds with new fluorine-containing substituents. *J. Fluorine Chem.* **1987,** *36* (1), 1–28. https://doi.org/10.1016/S0022-1139(00)82050-3.
10. Taft, R. W.; Price, E.; Fox, I. R.; Lewis, I. C.; Andersen, K. K.; Davis, G. T. Fluorine Nuclear Magnetic Resonance Shielding in p-Substituted Fluorobenzenes. The Influence of Structure and Solvent on Resonance Effects. *J. Am. Chem. Soc.* **1963,** *85* (20), 3146–3156. https://doi.org/10.1021/ja00903a022.
11. Pashko, M.; Pashkov, K.; Granat, D.; Yagupolskii, Yu.; Ryabukhin, S.; Volochnyuk, D. Methyl chlorothioformate as a convenient reagent for the thionoesters synthesis. *ChemRxiv*, **2024**. https://doi.org/10.26434/chemrxiv-2024-s379b.
12. Newton, J. J.; Britton, R.; Friesen, C. M. Base-Catalyzed Transesterification of Thionoesters. *J. Org. Chem.* **2018,** *83* (20), 12784–12792. https://doi.org/10.1021/acs.joc.8b02260.
13. Yagupolskii, L. M.; Yagupolskaya, L. N. Ob elektronnoy prirode ftorsoderzhashchikh zamestiteley. *Doklady Akademii nauk SSSR*, **1960**, *134* (6), 1381–1383.

14. Taft, R. W.; Price, E.; Fox, I. R.; Lewis, I. C.; Andersen, K. K.; Davis, G. T. Fluorine Nuclear Magnetic Resonance Shielding in meta-Substituted Fluorobenzenes. The Effect of Solvent on the Inductive Order. *J. Am. Chem. Soc.* **1963,** *85* (6), 709–724. https://doi.org/10.1021/ja00889a015.
15. Yagupol'skii, L. M.; Il'chenko, A. Ya.; Kondratenko, N. V. The Electronic Nature of Fluorine-containing Substituents. *Russian Chemical Reviews*, **1974**, *43* (1), 32–47. https://doi.org/10.1070/RC1974v043n01ABEH001787.

Information about the authors:
Mykhailo O. Pashko, Ph.D. Student, Institute of Organic Chemistry of the National Academy of Sciences of Ukraine; Team Leader, Enamine Ltd.
Yurii L. Yagupolskii (*corresponding author*), Dr.Sci. in Chemistry, Professor, Head of the Organofluorine Compounds Chemistry Department, Institute of Organic Chemistry of the National Academy of Sciences of Ukraine; Scientific Advisor, Enamine Ltd.; https://orcid.org/0000-0002-5179-4096; e-mail for correspondence: yagupolskii@ioch.kiev.ua.

ISSN 2308-8303 (Print) / 2518-1548 (Online)

Journal of Organic and Pharmaceutical Chemistry

Original Research

OPEN ACCESS
Freely available online on
http://ophcj.nuph.edu.ua

UDC 547.79

I. I. Myrko
Danylo Halytsky Lviv National Medical University, 69 Pekarska str., 79010 Lviv, Ukraine

Synthesis and Anti-inflammatory Activity of Some New 6-Aryltriazolo[3,4-*b*][1,3,4]thiadiazole Derivatives

Abstract

A series of 6-aryl[1,2,4]triazolo[3,4-*b*][1,3,4]thiadiazole derivatives has been synthesized. Their anti-inflammatory activity has been studied *in vivo* in a carrageenan model of the paw inflammatory edema in rats. 3-(2-Fluorophenyl)-6-phenyl-[1,2,4]triazolo-[3,4-*b*][1,3,4]thiadiazole (**3c**) and 3-(2-fluorophenyl)-6-(4-methoxy-phenyl)[1,2,4]triazolo[3,4-*b*][1,3,4]thiadiazole (**3d**) have been identified as hit compounds with the anti-exudative activity. The crucial role of the fluorine atom in the anti-inflammatory activity has been determined, which value considerably correlates with the calculated values of lipophilicity and solubility.

Keywords: [1,2,4]triazolo[3,4-*b*][1,3,4]thiadiazole; anti-inflammatory activity; cyclooxygenase; docking

І. І. Мирко
Львівський національний медичний університет імені Данила Галицького,
вул. Пекарська, 69, м. Львів, 79010, Україна

Синтез та протизапальна активність деяких нових похідних 6-арил[1,2,4]триазоло[3,4-*b*][1,3,4]тіадіазолу

Анотація

Синтезовано ряд похідних 6-арил[1,2,4]триазоло[3,4-*b*][1,3,4]тіадіазолу. Для цих сполук досліджено *in vivo* протизапальну активність на карагеніновій моделі запального набряку лапи щура. 3-(2-Фторофеніл)-6-феніл-[1,2,4]триазоло[3,4-*b*]-[1,3,4]тіадіазол (**3c**) та 3-(2-фторофеніл)-6-(4-метоксифеніл)[1,2,4]триазоло[3,4-*b*][1,3,4]тіадіазол (**3d**) було ідентифіковано як сполуки-хіти з антиексудативною активністю. Виявлено важливу роль атома Фтору в протизапальній активності, величина якої корелює з розрахованими значеннями ліпофільності та розчинності.

Ключові слова: [1,2,4]триазоло[3,4-*b*][1,3,4]тіадіазол; протизапальна активність; циклооксигеназа; докінг

Citation: Myrko, I. I. Synthesis and anti-inflammatory activity of some new 6-aryltriazolo[3,4-*b*][1,3,4]thiadiazole derivatives. *Journal of Organic and Pharmaceutical Chemistry* **2024**, *22* (4), 17–24.
https://doi.org/10.24959/ophcj.24.321751
Received: *115 September 2024*; **Revised:** *1 December 2024;* **Accepted:** *5 December 2024*

Funding: The author received no specific funding for this work.
Conflict of interests: The author has no conflict of interests to declare.

■ Introduction

Inflammation is a universal physiological response to injury that can be caused by infectious, allergic, toxic, physical, and neurogenic factors. It is one of the most common diseases that can be fatal [1]. Nonsteroidal anti-inflammatory drugs (NSAIDs) represent a class of important therapeutic agents. They are used as anti-inflammatory, antipyretic, and analgesic medicines. However, NSAIDs may cause serious side effects, including gastrointestinal bleeding, peptic ulcer disease, hypertension, edema, and kidney disease [2]. Some NSAIDs have also been associated with an increased risk of myocardial infarction [3]. Therefore, novel anti-inflammatory and analgesic compounds with improved safety profiles still need to be invented.

Currently, the synthesis and biological activities of various 1,2,4-triazole and 1,3,4-thiadiazole derivatives and their *N*-bridged heterocyclic analogs are the subject of intensive research [4–7]. 1,2,4-Triazole and 1,3,4-thiadiazole rings are known to be unique pharmacophores in several drugs and natural products. The favorable properties of triazole and thiadiazole rings, including

moderate dipole properties, hydrogen bonding ability, optimal lipophilicity and rigidity, are responsible for their biological activities [4–7]. Thiadiazole is the bioisostere of pyrimidine and oxadiazole [7].

[1,2,4]Triazolo[3,4-*b*][1,3,4]thiadiazoles, including 1,2,4-triazole and 1,3,4-thiadiazole rings, are attractive heterocyclic compounds for medical chemists. They are important analogs of bioactive compounds with diverse pharmacological effects, including the anti-inflammatory one [8–18]. Among [1,2,4]triazolo[3,4-*b*][1,3,4]thiadiazole derivatives, some selective inhibitors of the cyclooxygenase COX-2 isoform were found [18, 19].

The aim of this work was to synthesize new [1,2,4]triazolo[3,4-b][1,3,4]thiadiazole derivatives and study their anti-exudative potential.

■ Results and discussion

Synthesis of [1,2,4]triazolo[3,4-*b*][1,3,4]-thiadiazole targeted derivatives

The synthesis of the targeted [1,2,4]triazolo-[3,4-b][1,3,4]thiadiazole derivatives was carried out by the reaction of 1-amino-4*H*-[1,2,4]triazol-3-thiols **1a–c** with commercially available benzoic acid **2a** and its substituted derivatives **2b–d** (**Scheme**). The reaction was performed in $POCl_3$ under reflux. The resulting compounds are light yellow substances that are highly soluble in DMFA, DMSO, and dioxane, moderately soluble in ethanol and acetic acid, and insoluble in water and non-polar solvents.

The anti-inflammatory activity of compounds **3a–f** synthesized was evaluated by the carrageenan-induced paw edema method [19]. The compounds were tested in the dose of 50 mg kg^{-1}, and the activity was compared to the reference drugs – Ibuprofen, Diclofenac, and Ketorolac in the mean therapeutic dose of 10 mg kg^{-1} (**Table 1**).

Compounds **3c** and **3d** were identified as the most active among the substances studied, and their anti-inflammatory effect was equal to or higher than that of the reference drugs. A significant effect was also observed in the case of compound **3b**. All active compounds possess a fluorine atom in the aromatic cycle in position 6 of the [1,2,4]triazolo[3,4-*b*][1,3,4]thiadiazole moieties.

Compounds containing heterocyclic rings substituted with fluorinated phenyl moiety are

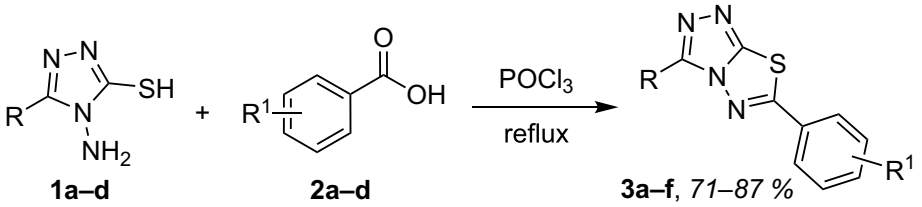

1a: R = C_6H_5; **1b**: R = 2-F-C_6H_4; **1c**: R = 4-Cl-$C_6H_4CH_2$; **1d**: R = 4-MeO-$C_6H_4CH_2$

2a: R^1 = H; **2b**: R^1 = 4-CF_3; **2c**: R^1 = 4-MeO; **2d**: R^1 = 3,4-*di*-MeO

3a: R = C_6H_5, R^1 = H; **3b**: R = C_6H_5, R^1 = 4-CF_3; **3c**: R = 2-F-C_6H_4, R^1 = H;

3d: R = 2-F-C_6H_4, R^1 = 4-MeO; **3e**: R = 4-Cl-$C_6H_4CH_2$, R^1 = H;

3f: R = 4-MeO-$C_6H_4CH_2$, R^1 = 3,4-*di*-MeO

Scheme. The synthesis of [1,2,4]triazolo[3,4-*b*][1,3,4]thiadiazoles **3a–f**

Table 1. The anti-inflammatory activity of compounds **3a–f** synthesized compared to Ibuprofen, Diclofenac and Ketorolac

Compound	Paw edema volume, (mL) ± SEM*	Inhibition, %	Activity relative to Ibuprofen, %	Activity relative to Diclofenac, %	Activity relative to Ketorolac, %
Control	2.20 ± 0.05	-	-	-	-
3a	1.73 ± 0.04	21.4	53.5	49.1	55.4
3b	1.48 ± 0.05	32.7	81.8	75.0	84.7
3c	1.24 ± 0.03	43.6	109.0	100.0	113.0
3d	1.27 ± 0.05	42.3	105.8	97.0	109.6
3e	1.64 ± 0.02	25.5	63.8	58.5	66.1
3f	1.94 ± 0.03	11.8	29.5	27.1	30.6
Ibuprofen	1.32 ± 0.03	40.0	100	-	-
Diclofenac	1.24± 0.03	43.6	-	100	-
Ketorolac	1.35± 0.04	38.6	-	-	100

Note: *SEM denotes the standard error of the mean

ISSN 2308-8303 (Print) / 2518-1548 (Online)

well-recognized anti-inflammatory and analgesic agents [20–24]. There are many reports that the incorporation of fluorine into a molecule results in increased binding affinity to the target protein [25–29]. In addition, an increase in the rate of absorption and transport of the drug *in vivo* was observed [27–29].

The consensus values for lipophilicity and water solubility [30] calculated using the SwissADME web resource [31] correlate with the anti-inflammatory activity of highly active fluorinated compounds (**Figure 1**). An increase in lipophilicity and a decrease in solubility lead to the loss of the anti-inflammatory effect. It should be noted that fluoro-substituted derivatives are also among the anti-inflammatory drugs available in the pharmaceutical market (Celecoxib, Fluproquazone).

Cyclooxygenase (COX) enzymes are involved in the synthesis of various prostanoids, which participate in physiological and pathological mechanisms of inflammation. There are two isoforms of COX enzymes: COX-1 and COX-2. COX-1 is a regulatory enzyme with physiological and homeostatic functions, whereas COX-2 stimulates the synthesis of prostaglandins, which cause pathological conditions, such as inflammation. Side effects of NSAIDs are caused by the inhibition of the physiological function of COX-1, while selective COX-2 inhibitors cause the anti-inflammatory activity without the risk of side effects. Compounds **3b–d** were docked [32, 33] into the binding site pockets of COX-1 and COX-2. The molecular docking studies were conducted using Autodock Vina [32] for docking simulations and a Discovery Studio Visualizer [33] for visualization and interpretation. The protein structures were retrieved from the Protein Data Bank (PDB): Cyclooxygenase 2 (PDB ID 1PXX) and Cyclooxygenase 1 (PDB ID 1HT5). Proteins were prepared by removing water molecules, adding hydrogen atoms, assigning partial charges, and converting the protein to the PDBQT format using AutoDock Tools. Ligands were drawn using ChemDraw and prepared by adding hydrogens, assigning charges, and optimizing their geometry through the energy minimization using Open Babel, then converted to the PDBQT format. AutoDock Vina was then utilized to perform the docking simulation, with a grid box size of 20 Å defined to encompass the protein's active site and an exhaustiveness value of 8 to ensure a thorough search. A Discovery Studio Visualizer was used to visualize and analyze the docked complexes, identifying key interactions.

These compounds exhibited stronger interactions at the COX-2 binding site than the COX-1 active site pocket. Binding scores and information about amino acids involved in interactions of the docked compounds **3b–d** on the active sites of COX-1 and COX-2 enzymes are provided in **Table 2** and visualized in **Figures 2–4**.

Compounds **3b–d** are characterized by Pi-Sigma and Pi-Alkyl interactions of amino acid fragments, which contain alkyl residues with aromatic cycles or a heterocyclic system (**Table 2**). In addition, an important role in bonding is played by Pi-Cation, Pi-Sulfur, Pi-Pi Stacked, Pi-Pi T-shaped, and various hydrogen bonds. (Conventional Hydrogen Bond, Carbon Hydrogen Bond, Pi-Donor Hydrogen Bond) (**Table 2**).

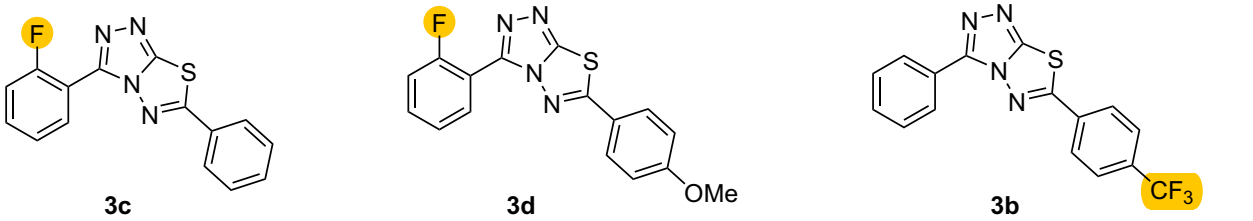

Activity relative to ibuprofen = 109.0 %
Consensus Log $P_{o/w}$ = 3.66
Water solubility = 8.01e-03 mg mL^{-1}

Activity relative to ibuprofen = 105.8 %
Consensus Log $P_{o/w}$ = 3.59
Water solubility = 7.93e-03 mg mL^{-1}

Activity relative to ibuprofen = 81.8 %
Consensus Log $P_{o/w}$ = 4.32
Water solubility = 2.08e-03 mg mL^{-1}

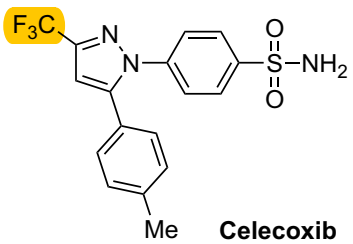

Celecoxib

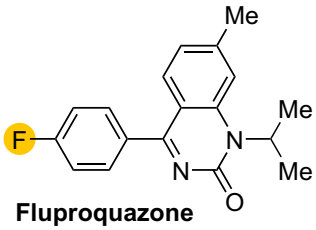

Fluproquazone

Figure 1. Bioactive fluorinated compounds **3b–d** and anti-inflammatory drugs

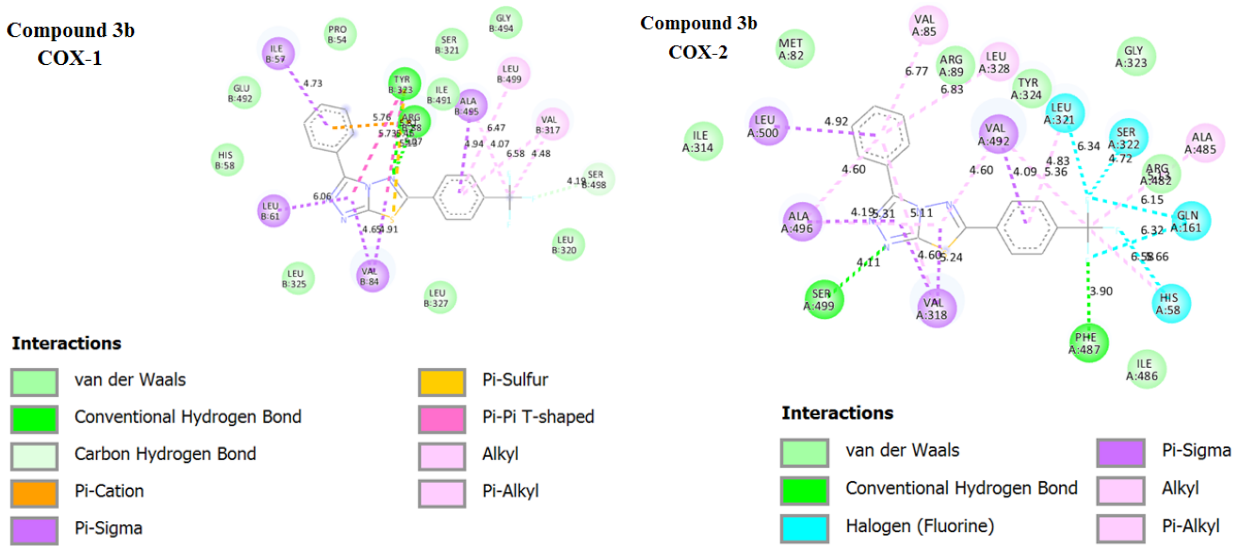

Figure 2. The binding mode of compound **3b** into the binding sites of COX-1 and COX-2

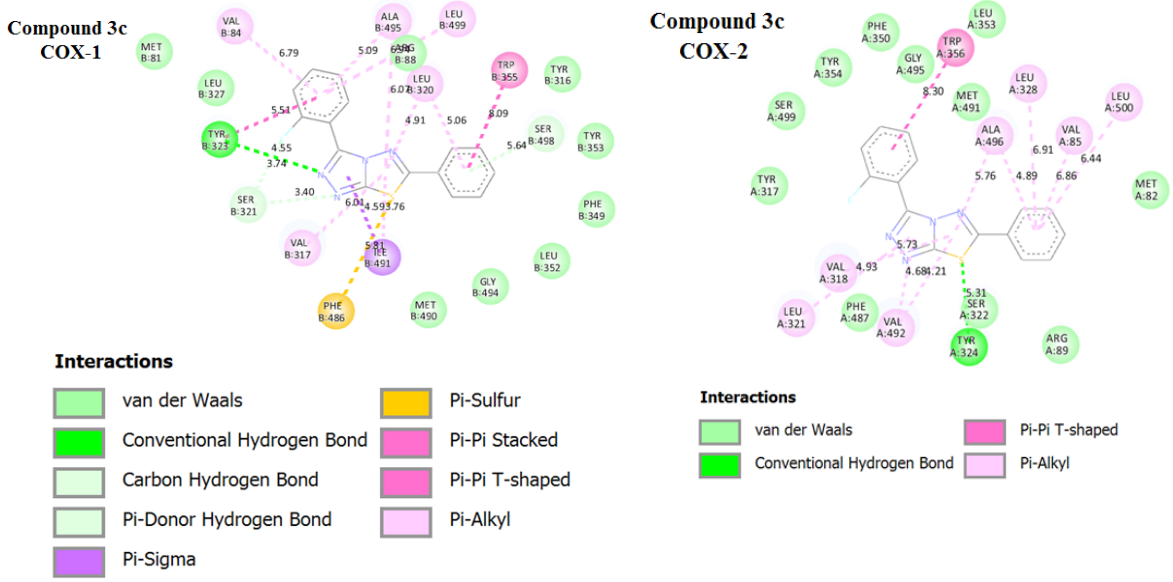

Figure 3. The binding mode of compound **3c** into the binding sites of COX-1 and COX-2

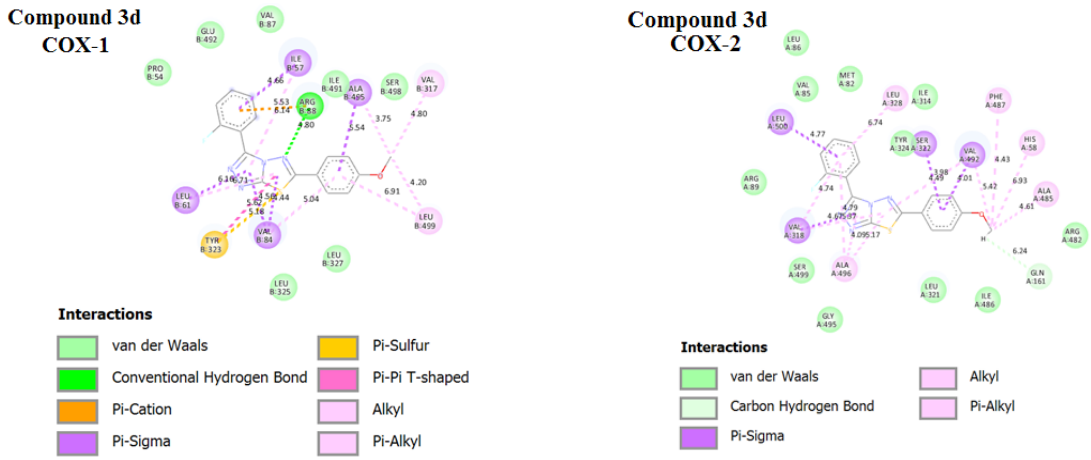

Figure 4. The binding mode of compound **3d** into the binding sites of COX-1 and COX-2

ISSN 2308-8303 (Print) / 2518-1548 (Online)

Table 2. Binding scores and amino acids involved in interactions of the docked compounds **3b-d** on the active sites of COX-1 and COX-2 enzymes*

Compound	Binding energy, kcal mol^{-1}		Interacting residues			
			Conventional Hydrogen Bond, Carbon Hydrogen Bond, Pi-Donor Hydrogen Bond	Pi-Cation, Pi-Sulfur	Pi-Pi Stacked, Pi-Pi T-shaped	Pi-Alkyl, Pi-Sigma
3b	COX-1	-7.4	Arg B:88 Tyr B:323 Ser B:498	Arg B:88 Tyr B:323	Tyr B:323	Leu B:499 Val B:317 Ile B:57 Leu B:61 Val B:84 Ala B: 495
	COX-2	-9.6	Ser A:499 Phe A:487	–	–	Ala A:496 Val A:85 Val A:318 Val A:492 Leu A:328 Leu A:321 Ala A:485 His A:58 Leu A:500 Ala A:496 Val A:318 Val A:492
3c	COX-1	-7.5	Tyr B:323 Ser B:321 Ser B:498	Phe B:486	Tyr B:323 Trp B:355	Val B:84 Val B:317 Ala B: 495 Leu B:320 Leu B:499 Ile B:491
	COX-2	-8.8	Tyr A:324		Trp A:356	Leu A:321 Val A:318 Val A:492 Ala A:496 Leu A:328 Val A:85 Leu A:500
3d	COX-1	-6.6	Arg B:88	Tyr B:323	Tyr B:323	Leu B:61 Ile B:57 Val B:84 Leu B:499 Val B:317 Leu B:61 Ile B:57 Val B:84 Ala B:495
	COX-2	-8.9	Gln A:161	–	–	Val A:318 Ala A:496 Leu A:328 Val A:492 Phe A:487 His A:58 Ala A:485 Leu A:500 Val A:318 Ser A:322 Val A:492

Note: *Colors of the amino acids involved in the interactions correspond to those shown in **Figures 2-4**

The calculated binding energy of compounds **3b–d** is similar to the binding energy for such non-steroidal anti-inflammatory drugs as Ibuprofen, Diclofenac, Ketorolac, and Celecoxib. The selectivity of binding to cyclooxygenases was not observed (**Table 3**).

■ Conclusions

In order to develop new effective anti-inflammatory agents, a series of [1,2,4]triazolo[3,4-*b*]-[1,3,4]thiadiazoles has been synthesized. Among them, 3-(2-fluorophenyl)-6-phenyl-[1,2,4]triazolo-[3,4-*b*][1,3,4]thiadiazole (**3c**) and 3-(2-fluorophenyl)-6-(4-methoxy-phenyl)-[1,2,4]triazolo[3,4-b][1,3,4]-thiadiazole (**3d**) have shown the best activity.

■ Experimental part

The ^{1}H NMR spectra presented in this work were obtained on a Varian instrument at an operating frequency of 400 MHz with DMSO-d_6 as a solvent and tetramethylsilane as an internal standard. Elemental analyses were performed using a Carlo Erba 1106 instrument. Melting points were determined on a Boetius melting point apparatus.

4-Amino-5-(4-R-benzyl)-4*H*-[1,2,4]triazol-3-thiols **1a,b** were obtained according to the procedure described in [34].

The general procedure for the synthesis of [1,2,4]triazolo[3,4-*b*][1,3,4]thiadiazole derivatives 3a–f

The corresponding 4-amino-5-R-4*H*-[1,2,4]triazol-3-thiol **1a–d** (5 mmol) and benzoic acids **2a–d** (5 mmol) were dissolved in $POCl_3$ (10 mL). The reaction mixture was refluxed for 8 h, cooled to room temperature, and poured into a mixture of NaOH (20 g), water (50 mL), and ice (50 g). In 1 hour, the precipitate was filtered off and recrystallized from an ethanol-DMFA mixture giving light yellow powders.

3,6-Diphenyl-[1,2,4]triazolo[3,4-b][1,3,4]thiadiazole (**3a**)

Yield – 75 %. M. p. 159–160 °C. ^{1}H NMR (400 MHz, DMSO-d_6), δ, ppm: 7.81–7.48 (6H, m, ArH), 8.07 (2H, d, J = 7.1 Hz, ArH), 8.32 (2H, d, J = 7.3 Hz, ArH). Anal. Calcd for $C_{15}H_{10}N_4S$, %: C 64.73, H 3.62, N 20.13. Found, %: C 64.77, H 3.72, N 20.20.

3-Phenyl-6-(4-trifluoromethylphenyl)-[1,2,4]-triazolo[3,4-b][1,3,4]thiadiazole (**3b**)

Yield – 87 %. M. p. 188–200 °C. ^{1}H NMR (400 MHz, DMSO-d_6), δ, ppm: 7.82–7.47 (3H, m, ArH), 8.02 (2H, d, J = 8.2 Hz, ArH), 8.26–8,34 (4H, m, ArH). Anal. Calcd for $C_{16}H_9F_3N_4S$, %: C 55.49, H 2.62, N 16.18. Found, %: C 55.62, H 2.73, N 16.22.

3-(2-Fluorophenyl)-6-phenyl-[1,2,4]triazolo[3,4-b][1,3,4]thiadiazole (**3c**)

Yield – 84%. M. p. 175–176 °C. ^{1}H NMR (400 MHz, DMSO-d_6), δ, ppm: 7.53–7.44 (2H, m, ArH), 7.61 (2H, t, J = 7.7 Hz, ArH), 7.71–7.64 (2H, m, ArH), 7.97 (2H, d, J = 8.0 Hz, ArH), 8.07 (1H, t, J = 7.5 Hz, ArH). Anal. Calcd for $C_{15}H_9FN_4S$, %: C 60.80, H 3.06, N 18.91. Found, %: C 60.75, H 2.99, N 18.70.

3-(2-Fluorophenyl)-6-(4-methoxyphenyl)-[1,2,4]triazolo[3,4-b][1,3,4]thiadiazole (**3d**)

Yield – 81 %. M. p. 181–183 °C. ^{1}H NMR (400 MHz, DMSO-d_6), δ, ppm: 3.85 (3H, s, CH_3O), 7.14 (2H, d, J = 7.4 Hz, ArH), 7.56–7.41 (2H, m, ArH), 7.67 (1H, d, J = 6.2 Hz, ArH), 7.92 (2H, d, J = 7.3 Hz, ArH), 8.06 (1H, t, J = 7.5 Hz, ArH). Anal. Calcd for $C_{16}H_{11}FN_4OS$, %: C 58.89, H 3.40, N 17.17. Found, %: 58.95, H 3.45, N 17.10.

3-(4-Chlorobenzyl)-6-phenyl-[1,2,4]triazolo-[3,4-b][1,3,4]thiadiazole (**3e**)

Yield – 71 %. M. p. 192–193 °C. ^{1}H NMR (400 MHz, DMSO-d_6), δ, ppm: 4.47 (2H, s, CH_2), 7.40 (4H, s, ArH), 7.60–7.72 (2H, m, ArH), 7.93 (2H, d, J = 6.7 Hz, ArH). Anal. Calcd for $C_{16}H_{11}ClN_4S$, %: C 58.81, H 3.39, N 17.14. Found, %: 58.69, H 3.44, N 17.21.

6-(3,4-Dimethoxyphenyl)-3-(4-methoxybenzyl)-[1,2,4]triazolo[3,4-b][1,3,4]thiadiazole (**3f**)

Yield – 72 %. M. p. 201–202 °C. ^{1}H NMR (400 MHz, DMSO-d_6), δ, ppm: 3.70 (3H, s, CH_3O), 3.85 (3H, s, CH_3O), 3.86 (3H, s, CH_3O), 4.36 (2H, s), 6.88 (2H, d, J = 8.6 Hz, ArH), 7.14 (1H, d, J = 8.5 Hz, ArH), 7.30 (2H, d, J = 8.5 Hz, ArH), 7.37 (1H, d, J = 1.9 Hz, ArH), 7.48 (1H, dd, J = 8.4, 2.0 Hz, ArH). Anal. Calcd for $C_{19}H_{18}N_4O_3S$, %: C 59.67, H 4.74, N 14.65. Found, %: 59.79, H 4.61, N 14.54.

Table 3. The binding energy, kcal mol^{-1} of the docked compounds **3b–d** and Ibuprofen, Diclofenac, Ketorolac, and Celecoxib on the active sites of COX-1 and COX-2 enzymes

Target protein	Compound						
	3b	**3c**	**3d**	Ibuprofen	Diclofenac	Ketorolac	Celecoxib
COX-1	-7.4	-7.5	-6.6	-7.6	-7.7	-8.6	-5.2
COX-2	-9.6	-8.8	-8.9	-7.4	-8.4	-8.7	-10.2

ISSN 2308-8303 (Print) / 2518-1548 (Online)

The method for studying the anti-inflammatory activity *in vivo* [19]

All *in vivo* procedures on animals comply with the standards of the European Convention for the Protection of Vertebrate Animals Used for Research and Scientific Purposes (Strasbourg, 1985), the Council Directive 2010/63/EU and the Law of Ukraine No. 3447-IV "On the Protection of Animals from Cruelty" as amended by 440-IX of 14.01.2020.

We conducted a study of the anti-inflammatory activity using the method of carrageenan-induced paw edema in rats. White Wistar rats weighing 180-250 g were used for this study. The laboratory animals were divided into 10 groups. Each group consisted of 5 rats. To test the anti-inflammatory activity of 6 compounds synthesized and 3 reference drugs (Ibuprofen, Diclofenac and Ketorolac), in total, 9 experimental groups were used, and the 10th test group was the control group.

The compounds studied (50 mg/kg of the body weight) and Ibuprofen, Diclofenac, Ketorolac in the mean therapeutic dose (10 mg/kg of the body weight) were dissolved in DMSO and administered intraperitoneally. Only DMSO was administered to the animals from the control group. In 1 hour, a generalized edema was induced by injecting 0.1 mL of 2% carrageenan solution under aseptic conditions under the aponeurosis of the rat hindlimb sole. The inflammatory response was determined by the change in the limb volume using the oncometric method at the beginning of the experiment and 4 hours after administration of the phlogogenic agent. The inhibition of the inflammatory response was calculated as a percentage of the reduction in the paw volume using the following formula:

$$\% \text{ Inhibition} = \frac{V_{control} - V}{V_{control}} \times 100\ \%$$

where $V_{control}$ is the increase in the paw volume in the control group of animals;

V is the increase in the paw volume in animals injected with the test substances.

Acknowledgments

The author thanks Prof. Pinyazhko O. R. and researcher Nektegayev I. O. for their efforts in performing the *in vivo* biological screening.

References

1. Gusev, E.; Zhuravleva, Y. Inflammation: A New Look at an Old Problem. *Int. J. Mol. Sci.* **2022**, *23*, 4596. https://doi.org/10.3390/ijms23094596.
2. Tai, F. W. D.; McAlindon, M. E. Non-steroidal anti-inflammatory drugs and the gastrointestinal tract. *Clinical Medicine* **2021**, *21* (2), 131–134. https://doi.org/10.7861/clinmed.2021-0039.
3. Mitsis, A.; Avraamides, P.; Lakoumentas, J.; Kyriakou, M.; Sokratous, S.; Karmioti, G.; Drakomathioulakis, M.; Theodoropoulos, K. C.; Nasoufidou, A.; Evangeliou, A.; Vassilikos, V.; Fragakis, N.; Ziakas, A.; Tzikas, S.; Kassimis, G. Role of Inflammation Following An Acute Myocardial Infarction: Design of INFINITY. *Biomarkers in Medicine.* **2023**, *17* (23), 971–981. https://doi.org/10.2217/bmm-2023-0491.
4. Aggarwal, R.; Sumran, G. An insight on medicinal attributes of 1,2,4-triazoles. *Eur. J. Med. Chem.* **2020**, *205*, 112652. https://doi.org/10.1016/j.ejmech.2020.112652.
5. Bozorov, K.; Zhao, J.; Aisa, H. A. 1,2,3-Triazole-containing hybrids as leads in medicinal chemistry: A recent overview. *Bioorg. Med. Chem.* **2019**, *27* (16), 3511–3531. https://doi.org/10.1016/j.bmc.2019.07.005.
6. Iraji, A.; Firuzi, O.; Khoshneviszadeh, M.; Tavakkoli, M.; Mahdavi, M.; Nadri, H.; Edraki, N.; Miri, R. Multifunctional iminochromene-2H-carboxamide derivatives containing different aminomethylene triazole with BACE1 inhibitory, neuroprotective and metal chelating properties targeting Alzheimer's disease. *Eur. J. Med. Chem.* **2017**, *141*, 690–702. https://doi.org/10.1016/j.ejmech.2017.09.057.
7. Li, Y.; Geng, J.; Liu, Y.; Yu, S.; Zhao, G. Thiadiazole—a Promising Structure in Medicinal Chemistry. *ChemMedChem.* **2013**, *8* (1), 27–41. https://doi.org/10.1002/cmdc.201200355.
8. Khalili Ghomi, M.; Noori, M.; Nazari Montazer, M.; Zomorodian, K.; Dastyafteh, N.; Yazdanpanah, S.; Sayahi, M. H.; Javanshir, S.; Nouri, A.; Asadi, M.; Badali, H.; Larijani, B.; Irajie, C.; Iraji, A.; Mahdavi, M. [1,2,4]triazolo[3,4-b][1,3,4]thiadiazole derivatives as new therapeutic candidates against urease positive microorganisms: design, synthesis, pharmacological evaluations, and in silico studies. *Scientific reports* **2023**, *13* (1), 10136. https://doi.org/10.1038/s41598-023-37203-z.
9. Mathew, V.; Keshavayya, J.; Vaidya, V. P.; Giles, D. Studies on synthesis and pharmacological activities of 3,6-disubstituted-1,2,4-triazolo[3,4-b]-1,3,4-thiadiazoles and their dihydro analogues. *Eur. J. Med. Chem.* **2007**, *42* (6), 823–840. https://doi.org/10.1016/j.ejmech.2006.12.010.
10. Gilani, S. J.; Khan, S. A.; Siddiqui, N. Synthesis and pharmacological evaluation of condensed heterocyclic 6-substituted 1,2,4-triazolo-[3,4-b]-1,3,4-thiadiazole and 1,3,4-oxadiazole derivatives of isoniazid. *Bioorg. Med. Chem. Lett.* **2010**, *20* (16), 4762–4765. https://doi.org/10.1016/j.bmcl.2010.06.125.
11. Zhang, L.; Zhao, J.; Zhang, B.; Lu, T.; Chen, Y. Discovery of [1,2,4]triazolo[3,4-b][1,3,4]thiadiazole derivatives as novel, potent and selective c-Met kinase inhibitors: Synthesis, SAR study, and biological activity. *Eur. J. Med. Chem.* **2018**, *150*, 809–816. https://doi.org/10.1016/j.ejmech.2018.03.049.
12. Chidananda, N.; Poojary, B.; Sumangala, V.; Kumari, N. S.; Shetty, P.; Arulmoli, T. Facile synthesis, characterization and pharmacological activities of 3,6-disubstituted 1,2,4-triazolo[3,4-b][1,3,4]thiadiazoles and 5,6-dihydro-3,6-disubstituted-1,2,4-triazolo[3,4-b][1,3,4]-thiadiazoles. *Eur. J. Med. Chem*. **2012**, *51*, 124–136. https://doi.org/10.1016/j.ejmech.2012.02.030.
13. Al-Wahaibi, L. H.; Karthikeyan, S.; Blacque, O.; El-Masry, A. A.; Hassan, H. M.; Percino, M. J.; El-Emam, A. A.; Thamotharan, S. Structural and Energetic Properties of Weak Noncovalent Interactions in Two Closely Related 3,6-Disubstituted-[1,2,4]triazolo[3,4-b][1,3,4]thiadiazole Derivatives: *In Vitro* Cyclooxygenase Activity, Crystallography, and Computational Investigations. *ACS Omega* **2022**, *7* (38), 34506–34520. https://doi.org/10.1021/acsomega.2c04252.

14. Maddila, S.; Gorle, S.; Singh, M.; Lavanya, P.; Jonnalagadda, S. B. Synthesis and Anti-Inflammatory Activity of Fused 1,2,4-triazolo-[3,4-b] [1,3,4]thiadiazole Derivatives of Phenothiazine. *Letters in Drug Design & Discovery* **2013**, *10* (10), 977–983. http://dx.doi.org/10.2174/15701808113109990034.
15. Birsen, T.; Sevim Peri, A.; Sule, G.; Selami, G.; Goknur, A. Novel 1,2,4-Triazolo[3,4-b]-1,3,4-thiadiazole Derivatives as Dual Analgesic/Anti-inflammatory and Antimicrobial Agents. *Letters in Drug Design & Discovery* **2012**, *9* (2), 204–212. http://dx.doi.org/10.2174/157018012799079626.
16. Apan, A.; Casoni, D.; Leonte, D.; Pop, C.; Iaru, I.; Mogoșan, C.; Zaharia, V. Heterocycles 52: The Drug-Likeness Analysis of Anti-Inflammatory Thiazolo[3,2-b][1,2,4]triazole and Imidazo[2,1-b][1,3,4]thiadiazole Derivatives. *Pharmaceuticals* **2024**, *17*, 295. https://doi.org/10.3390/ph17030295.
17. Pathak, P.; Shukla, P. K.; Naumovich, V.; Grishina, M.; Verma, A.; Potemkin, V. 1,2,4-Triazole-conjugated 1,3,4-thiadiazole hybrid scaffolds: A potent ameliorant of carrageenan-induced inflammation by lessening proinflammatory mediators. *Arch. Pharm.* **2020**, *353* (1), 1900233. https://doi.org/10.1002/ardp.201900233.
18. Tratrat, C.; Haroun, M.; Paparisva, A.; Kamoutsis, C.; Petrou, A.; Gavalas, A.; Eleftheriou, P.; Geronikaki, A.; Venugopala, K.N.; Kochkar, H.; et al. New Substituted 5-Benzylideno-2-Adamantylthiazol[3,2-b][1,2,4]Triazol-6(5*H*)ones as Possible Anti-Inflammatory Agents. *Molecules* **2021**, *26*, 659. https://doi.org/10.3390/molecules26030659.
19. Atta-ur-Rahman; Choudhary, M. I.; Thomsen, W. J. *Bioassay techniques for drug development*. Harwood academic Publishers, 2005, 203 p.
20. Chawla, G.; Kumar, U.; Bawa, S.; Kumar, J. Syntheses and evaluation of anti-inflammatory, analgesic and ulcerogenic activities of 1,3,4-oxadiazole and 1,2,4-triazolo[3,4-b]-1,3,4-thiadiazole derivatives. *J. Enzyme Inhib. Med. Chem.* **2012**, *27* (5), 658–665. https://doi.org/10.3109/14756366.2011.606543.
21. Luan, M. Z.; Zhang, X. F.; Yang, Y.; Meng, Q. G.; Hou, G. G. Anti-inflammatory activity of fluorine-substituted benzo[h]quinazoline-2-amine derivatives as NF-κB inhibitors. *Bioorg. Chem*. **2023**, *132*, 106360. https://doi.org/10.1016/j.bioorg.2023.106360.
22. Kalkhambkar, R. G.; Kulkarni, G. M.; Kamanavalli, C. M.; Premkumar, N.; Asdaq, S. M.; Sun, C. M. Synthesis and biological activities of some new fluorinated coumarins and 1-aza coumarins. *Eur. J. Med. Chem*. **2008**, *43* (10), 2178–2188. https://doi.org/10.1016/j.ejmech.2007.08.007.
23. Kaur, K.; Kumar, V.; Gupta, G. K. Trifluoromethylpyrazoles as anti-inflammatory and antibacterial agents: A review. *J. Fluor. Chem*. **2015**, *178*, 306–326. https://doi.org/10.1016/j.jfluchem.2015.08.015.
24. Nargund, L. V.; Hariprasad, V.; Reedy, G. R. Synthesis and anti-inflammatory activity of fluorinated phenyl styryl ketones and N-phenyl-5-substituted aryl-3-p-(fluorophenyl) pyrazolins and pyrazoles. *J. Pharm. Sci*. **1992**, *81* (9), 892–894. https://doi.org/10.1002/jps.2600810910.
25. Ali, S.; Bolinger, A. A.; Zhou, J. Highlights on Fluorine-containing Drugs Approved by U.S. FDA in 2023. *Curr. Top. Med. Chem*. **2024**, *24* (10), 843–849. https://doi.org/10.2174/0115680266300245240223070242.
26. Wang, Q.; Bian, Y.; Dhawan, G.; Zhang, W.; Sorochinsky, A. E.; Makarem, A.; Soloshonok, V. A.; Han J. FDA approved fluorine-containing drugs in 2023. *Chin. Chem. Lett.* **2024**, *35* (11), 109780, https://doi.org/10.1016/j.cclet.2024.109780.
27. Sheikhi, N.; Bahraminejad, M.; Saeedi, M.; Mirfazli, S. S. A review: FDA-approved fluorine-containing small molecules from 2015 to 2022. *Eur. J. Med. Chem.* **2023**, *260*, 115758. https://doi.org/10.1016/j.ejmech.2023.115758.
28. Chandra, G.; Singh, D. V.; Mahato, G. K.; Patel, S. Fluorine-a small magic bullet atom in the drug development: perspective to FDA approved and COVID-19 recommended drugs. *Chemical Papers* **2023**, *77* (8), 4085–4106. https://doi.org/10.1007/s11696-023-02804-5.
29. Henary, E.; Casa, S.; Dost, T.L.; Sloop, J.C.; Henary, M. The Role of Small Molecules Containing Fluorine Atoms in Medicine and Imaging Applications. *Pharmaceuticals* **2024**, *17*, 281. https://doi.org/10.3390/ph17030281.
30. Delaney, J. S. ESOL: estimating aqueous solubility directly from molecular structure. *J. Chem. Inf. Comput. Sci*. **2004**, *44* (3), 1000–1005. https://doi.org/10.1021/ci034243x.
31. SwissADME. http://www.swissadme.ch/index.php (accessed Sep 13, 2024).
32. Autodock Vina. https://vina.scripps.edu/ (accessed Jun 21, 2024).
33. Discovery Studio. https://discover.3ds.com/discovery-studio-visualizer-download (accessed Jun 26, 2024).
34. Kamboj, V. K.; Kapoor, A.; Jain, S. Synthesis, Antimicrobial, and Antioxidant Screening of Aryl Acetic Acid Incorporated 1,2,4-Triazolo-1,3,4-Thiadiazole Derivatives. *J. Heterocycl. Chem.* **2019**, *56* (4), 1376–1382. https://doi.org/10.1002/jhet.3513.

Information about the author:
Iryna I. Myrko (*corresponding author*), Assistant Professor, Department of General, Bioinorganic, Physicocolloid Chemistry, Danylo Halytsky Lviv National Medical University; https://orcid.org/0000-0003-3979-543X; e-mail for correspondence: irynaoliinyk@gmail.com.

ISSN 2308-8303 (Print) / 2518-1548 (Online)

Journal of Organic and Pharmaceutical Chemistry

Original Research

OPEN ACCESS
Freely available online on
http://ophcj.nuph.edu.ua

UDC 544.47:547-31/-39:54-39

E. N. Abdullayev[1], A. M. Mishura[1], I. A. Iermolenko[2,3], A. S. Lytvynenko[1], M. A. Kolosov[4], E. G. Shvets[4], K. S. Gavrilenko[2,5], S. V. Kolotilov[1]

[1] L. V. Pisarzhevsky Institute of Physical Chemistry of the National Academy of Sciences of Ukraine, 31 Nauky ave., 03028 Kyiv, Ukraine
[2] Enamine Ltd., 78 Winston Churchill str., 02094 Kyiv, Ukraine
[3] Institute of Organic Chemistry of the National Academy of Sciences of Ukraine, 5 Academik Kukhar str., 02094 Kyiv, Ukraine
[4] V. N. Karazin Kharkiv National University, School of Chemistry, 4 Svobody sq., 61022 Kharkiv, Ukraine
[5] Taras Shevchenko National University of Kyiv, 12 Pavlo Skoropadskyi str., 01033 Kyiv, Ukraine

The Oxidation of Cyclic Ketones by H_2O_2 Catalyzed by Cu(II) and Fe(III) Coordination Polymers

Abstract

It has been shown that the oxidation of ketones – analogs of cyclohexanone – by hydrogen peroxide in the presence of $Cu_3(btc)_2$ (btc^{3-} = 1,3,5-benzenetricarboxylate) occurred mainly by the radical mechanism, rather than by the Baeyer-Villiger reaction mechanism, and led to a mixture of products formed due to the ring cleavage and reduction of the hydrocarbon chain length. Unlike aliphatic ketones, α-tetralone hardly underwent conversion in the reaction with H_2O_2 in the presence of HKUST-1, and the oxidation of the same ketone in the presence of $Fe_2(OH)_3(btc)$ led to the formation of a number of products; among them, 1,4-naphthoquinone was dominant.

Keywords: catalytic oxidation; cyclic ketones; hydrogen peroxide; porous coordination polymers; copper(II); iron(III)

Е. Н. Абдуллаєв[1], А. М. Мішура[1], Є. А. Єрмоленко[2,3], А. С. Литвиненко[1], М. О. Колосов[4], О. Г. Швець[4], К. С. Гавриленко[2,5], С. В. Колотілов[1]

[1] Інститут фізичної хімії ім. Л. В. Писаржевського Національної академії наук України, просп. Науки, 31, м. Київ, 03028, Україна
[2] ТОВ НВП «Єнамін», вул. Вінстона Черчилля, 78, м. Київ, 02094, Україна
[3] Інститут органічної хімії Національної академії наук України, вул. Академіка Кухаря, 5, м. Київ, 02094, Україна
[4] Харківський національний університет імені В. Н. Каразіна, майдан Свободи, 4, м. Харків, 61022, Україна
[5] Київський національний університет імені Тараса Шевченка, вул. Володимирська, 60, м. Київ, 01033, Україна

Окиснення циклічних кетонів H_2O_2, каталізоване координаційними полімерами Cu(II) та Fe(III)

Анотація

З'ясовано, що окиснення кетонів – аналогів циклогексанону – перекисом водню в присутності $Cu_3(btc)_2$ (btc^{3-} = 1,3,5-бензолтрикарбоксилат) проходило переважно за радикальним механізмом, а не за механізмом реакції Баєра-Віллігера, і призводило до суміші продуктів, що утворювалися внаслідок розщеплення кільця та зменшення довжини вуглеводневого ланцюга. На відміну від аліфатичних кетонів, α-тетралон майже не вступав у реакцію з H_2O_2 в присутності HKUST-1, а окиснення цього кетону в присутності $Fe_2(OH)_3(btc)$ призводило до утворення низки продуктів, серед яких домінував 1,4-нафтохінон.

Ключові слова: каталітичне окиснення; циклічні кетони; пероксид водню; пористі координаційні полімери; мідь(II); залізо(III)

Citation: Abdullayev, E. N.; Mishura, A. M.; Iermolenko, I. A.; Lytvynenko, A. S.; Kolosov, M. A.; Shvets, E. G.; Gavrilenko, K. S.; Kolotilov, S. V. The oxidation of cyclic ketones by H_2O_2 catalyzed by Cu(II) and Fe(III) coordination polymers *Journal of Organic and Pharmaceutical Chemistry* **2024**, *22* (4), 25–35.
https://doi.org/10.24959/ophcj.24.315358
Received: *29 September 2024*; **Revised:** *27 November 2024*; **Accepted:** *10 December 2024*

Funding: The authors received no specific funding for this work.
Conflict of interests: The authors have no conflict of interests to declare.

■ Introduction

Oxidation reactions have been widely used in both high-volume organic industry (for example, manufacturing of dicarboxylic acids to produce plastics) and in fine organic synthesis for the preparation of substances for pharmaceuticals (active pharmaceutical ingredients, APIs) and agrochemistry [1–3]. Many currently used methods of organic compounds oxidation involve the application of toxic catalysts based on platinum group metals [4, 5] or oxidizing agents, which contain toxic metals (chromium, manganese, osmium) and, hence, produce toxic wastes [6–8]. Residual impurities formed from reagents or catalysts can also cause contamination of the products, which is critical for the production of APIs. For example, the content of platinum metals in the substance in some cases should not exceed 10^{-6} % by weight [9]. The development of new environmentally friendly methods for the oxidation of organic compounds and studies of the pathways of such processes are the tasks of modern organic and physical chemistry.

The problem of generating large amounts of waste during oxidation can be solved using environmentally friendly oxidants, such as hydrogen peroxide, which produces water and oxygen (in the side reaction of decomposition of H_2O_2) [10, 11]. At the same time, the widespread use of hydrogen peroxide as an oxidant in organic chemistry is limited because of the formation of an unpredictable mixture of products due to multiple parallel processes and/or different mechanisms, which can occur simultaneously [11, 12]. Nevertheless, there are many examples of the successful use of H_2O_2 for the selective oxidation of organic compounds in literature. High selectivity is achieved when the reaction proceeds by a single mechanism, unlike radical oxidation. For example, the oxidation of ketones by the Baeyer-Villiger mechanism in the presence of metal-containing catalysts usually leads to lactones with high yields [13–18]. In contrast, it has been found that hydrogen peroxide can decompose in the presence of $Cu_3(btc)_2$ (btc^{3-} is 3,5-benzenetricarboxylate), forming OH radicals, which cause deep oxidation of organic molecules and the formation of a mixture of products [19]. It has been noted that ·OH radical is one of the most potent oxidants. Thus, the study of the conditions under which the oxidation reaction involving H_2O_2 proceeds by the Baeyer-Villiger or radical mechanism is a problem of high importance for selecting catalysts and determining the scope of their application.

The use of porous coordination polymers (PCP) of the 3d metals as catalysts is of particular interest since these compounds may have high catalytic performance in oxidation processes [12, 20], and their selectivity can be associated with differences in the sorption capacity of PCP with respect to reagents [21–23]. In addition, the use of PCP allows one to carry out reactions in a heterogeneous catalytic mode; this feature significantly simplifies the purification of products from the catalyst (transition metal ions) and makes possible a simple reuse of the catalyst or transfer of the reaction to the flow mode.

The aim of the study was to determine the catalytic properties of two well-known PCPs – 1,3,5-benzenetricarboxylates (btc^{3-}, also known as an anion of trimesic acid) of copper(II) (known as HKUST-1 [24]) and iron(III) [25] – in the process of cyclic ketone oxidation with hydrogen peroxide, and to determine their place among the catalysts used for the oxidation of organic compounds with hydrogen peroxide. The PCPs $Cu_3(btc)_2$ and Fe(btc) are widely used and are manufactured and distributed under trademarks Basolite® C300 and Basolite® F300, respectively. Though the synthesis of the first compound is simple and straightforward, the second one usually forms species with a high hydroxide content and corresponds to formula $Fe_2(OH)_3(btc)$. The use of these PCP made it possible to compare the catalytic activity of compounds containing metal ions with different Lewis acidity [26] and oxidative capacity [27].

The study used 1,2,3,4-tetrahydro-1-naphthalenone (I, α-tetralone) as a carbocyclic ketone. This compound is similar to industrially important cyclohexanone, but less volatile. It has

ISSN 2308-8303 (Print) / 2518-1548 (Online)

a simpler NMR spectrum and can be easily analyzed by chromatography without modification. To reveal the peculiarities of oxidation of organic compounds containing several sensitive to oxidation fragments, other ketones, including ethyl 4-oxocyclohexane-1-carboxylate (**II**), *tert*-butyl 4-oxopiperidine-1-carboxylate (**III**), tetrahydro-4*H*-pyran-4-one (**IV**), were also studied (**Figure 1**).

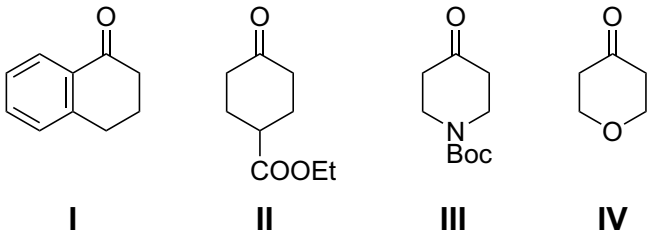

Figure 1. Ketones studied in this work

■ Materials and methods

$Cu_3(btc)_2$ and $Fe_2(OH)_3(btc)$ were obtained by anodic dissolution of the corresponding metals in a solution of 1,3,5-benzenetricarboxylic acid. The method of obtaining $Cu_3(btc)_2$ was described earlier [28]. $Fe_2(OH)_3(btc)$ was obtained by modification of the known method [29]. Two preliminarily cleaned iron rods with a diameter of 2 mm were immersed in a beaker with the electrolyte (0.5 g Bu_4NBF_4 and 0.2 g H_3btc in 20 mL of ethanol) and 3 F of electricity per 1 mol of trimesic acid was passed through the solution at a temperature of 32 °C and a current density of 3.8 A dm^{-2}. The contact area of iron with the electrolyte was 107 mm^2, current – 40 mA, electrolysis time – 2.2 h. During the reaction, the air was blown through the electrolyte with a peristaltic pump throughout the electrolysis and for an additional 2.5 h after its completion. The reaction mixture was then stirred for 12 h. A beige precipitate fell out during the process, which gradually turned light red. After the process, the precipitate was filtered off, washed with water, and dried at 70–80 °C. The CHN analysis: calculated for $Fe_2(OH)_3(btc)(H_2O)_{1,3}$: $C_9H_{8.6}O_{10.3}Fe_2$, %: C 27.50; H 2.20; found C 27.60; H 2.52.

Powder diffraction patterns of the coordination polymers were measured using a DRON-3M X-ray diffractometer, Cu-Kα radiation in the range of angles 2θ = 5–80° with a step of 2θ = 0.05°. The transmission electron microscopy studies were performed using a PEM-125K SELMI microscope with an accelerating voltage of 100 kV. Test samples in the form of alcohol suspensions were applied to copper mesh covered with a film of amorphous carbon and then dried. The CHN analysis was performed using a CarloErba 1106 instrument. Nitrogen adsorption isotherms were measured by the volumetric method using a Sorptomatic 1990 instrument. Optical micrographs were obtained using an XY-B2 trinocular microscope (Ningbo Sunny Instruments Co., Ltd., PRC) equipped with the attached PowerShot G6 Canon camera in the mode of illumination of the sample, the light source was a lamp built into the microscope. The composition of the reaction mixtures in the ketone oxidation processes was determined by ^{1}H NMR (a Bruker Advance 400 spectrometer), gas chromatography with mass spectrometric detection (an Agilent 7890 A chromatograph) and in individual experiments with mass spectrometry (a Shimadzu GCMS QP-2020 instrument using a column type HP-5 and a direct sample inlet (DI) into the ion source).

Mass spectra of mixtures were obtained by the direct introduction of samples into an ion source (DI) on a Shimadzu GCMS QP-2020 instrument (ionization energy 70 eV). In addition to DI, an attempt was made to chromatographically separate mixtures of reaction products followed by the mass spectrometric detection of individual substances (GCMS) using a Shimadzu GCMS QP-2020 instrument, the carrier gas was helium (99.999% vol.), the sample solvent – ethyl acetate, the sample volume – 1 μL, the injector temperature – 150 °C. Column: the stationary phase was 5% diphenylpolysiloxane, 95% dimethylpolysiloxane; the length – 30 m; the inner diameter – 0.25 mm; the thickness of the stationary phase film – 0.25 μm. Column temperature control: the initial temperature was 35 °C; the initial isotherm time – 1 min; the temperature gradient – 15 °C min^{-1}; the final temperature – 200 °C; the time of the final isotherm – 5 min (the detector temperature – 200 °C; the ionization energy – 70 eV). The NIST 17.0 database was used to assign mass spectra.

Ketone oxidation experiments were performed according to the method similar to that described in the literature [11]. A portion of the appropriate PCP and a portion of a ketone (concentrations of reaction mixtures are indicated in the *Results and discussion* section) were added to the solution obtained by mixing acetonitrile with aqueous hydrogen peroxide. In most cases the solutions were prepared by mixing 40 mL of acetonitrile with 7 mL of 35% aqueous solution of H_2O_2 (d = 1.1 g cm^{-1}); the solution obtained contained 1.7 M H_2O_2 and 5.9 M water. The resulting

suspension was stirred at 25 °C for 24 h on a magnetic stirrer. After standing for a certain time, 50 mL of 1.1 M aqueous Na_2SO_3 solution was added to the reaction mixture, the organic compounds were extracted with ethyl acetate (2 portions of 75 mL), the extracts were dried over sodium sulfate, and the solvents were removed on a rotary evaporator under reduced pressure. The reaction products were analyzed as described above.

■ Results and discussion

The powder diffraction pattern of the HKUST-1 sample obtained in this work was similar to the diffraction pattern of the hydrated form of copper(II) benzenetricarboxylate $Cu_3(btc)_2(H_2O)_3 \cdot xH_2O$ [30]. In contrast, there were no distinct reflections on the diffraction pattern of the coordination polymer $Fe_2(OH)_3(btc)$, which was a sign of a disordered structure. The results obtained are in good agreement with the literature – copper(II) 1,3,5-benzenetricarboxylate is almost always characterized by a well-defined crystalline structure, while iron(III) 1,3,5-benzenetricarboxylate, according to X-ray diffraction, is usually referred to as a material with low crystallinity or even amorphous one [31].

The TEM studies showed that the HKUST-1 sample mainly consisted of particles of *ca.* 0.5 μm size (**Figure 2**, *a*). The particle size of $Fe_2(OH)_3(btc)$, determined by optical microscopy, was 0.7–0.8 μm (**Figure 2**, *c*). Particles of $Fe_2(OH)_3(btc)$ were unstable in the electron beam of TEM.

According to nitrogen adsorption data, HKUST-1 was characterized by the value of $S_{BET} = 1435$ m^2 g^{-1}, the volume of micropores according to the Dubinin-Radushkevich equation V_{DR} was equal to 0.533 cm^3 g^{-1} [28]. In the case of $Fe_2(OH)_3(btc)$ the value of S_{BET} was 520 m^2 g^{-1}, the volume of micropores according to the Dubinin-Radushkevich equation was $V_{DR} = 0.196$ cm^3 g^{-1}. The distribution of pores by size was calculated using the Saito-Foley method, the sample $Fe_2(OH)_3(btc)$ had dominating pores size with a diameter of 1.0 nm, and there were pores with a diameter of 1.2–1.4 nm. The values of S_{BET} and

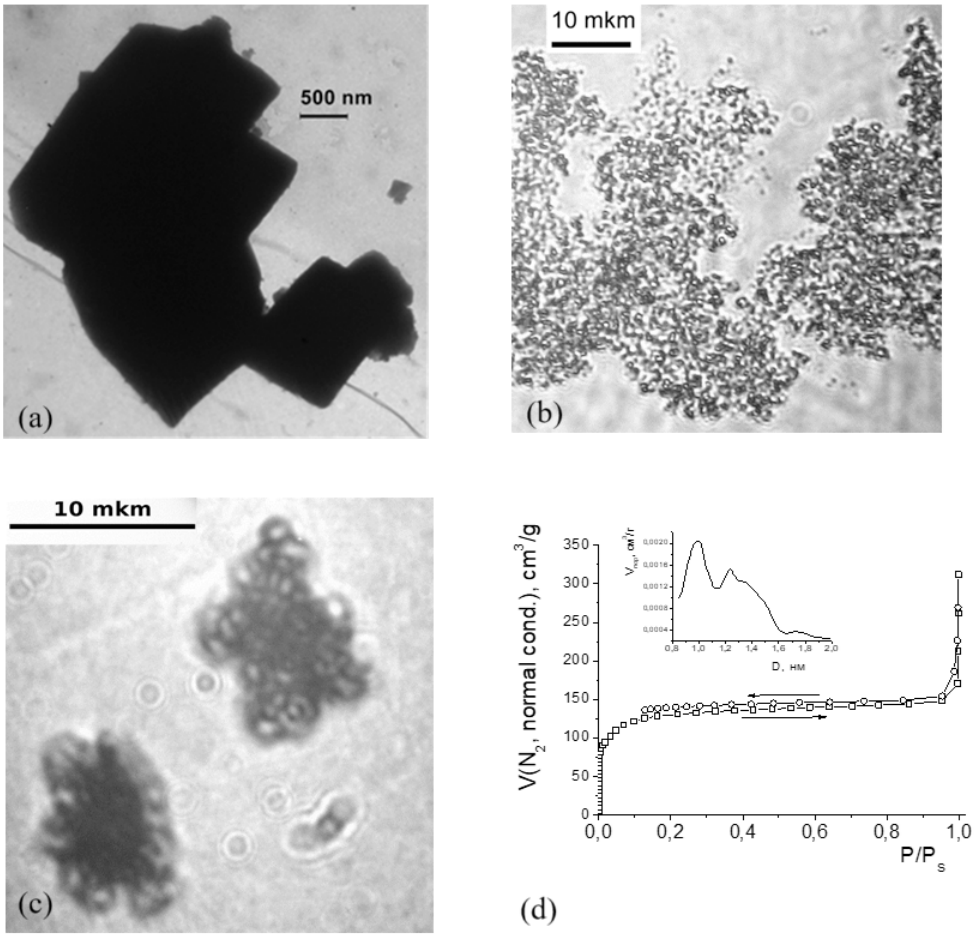

Figure 2. Images of HKUST-1 obtained by TEM (**a**) and optical microscopy (**b**), the image of $Fe_2(OH)_3(btc)$, obtained by optical microscopy (**c**) and nitrogen adsorption isotherm of PCP $Fe_2(OH)_3(btc)$ (**d**)

ISSN 2308-8303 (Print) / 2518-1548 (Online)

V_{DR} for HKUST-1 were close to the upper limit of the range of sorption characteristics typical for these PCPs [24], and in the case of $Fe_2(OH)_3(btc)$ S_{BET} and V_{DR} were significantly lower than the values published for similar compounds [31].

At room temperature, α-tetralone (**I**) was not oxidized by hydrogen peroxide in the presence of HKUST-1 (0.1 M of a ketone, 1.7 M of H_2O_2, $1.5 \cdot 10^{-2}$ M of HKUST-1) as the organic mixture after the experiment contained almost pure starting ketone (hereinafter the "effective concentration" of PCP in the reaction mixture is given as the ratio of the amount of PCP expressed in moles per 1 mol of a metal ion to the volume of the solution. The PCP is suspended as a fine solid). The interaction of **I** with hydrogen peroxide in the presence of HKUST-1 for 3 h at 55 °C also did not lead to the formation of a significant amount of oxidation products: according to the gas chromatography and NMR methods, the reaction mixture contained more than 97% of the initial ketone **I**, and among the minor oxidation products a lactone resulting from the Baeyer-Villiger oxidation could be identified.

Upon the oxidation of **I** (0.14 M) with hydrogen peroxide (1.7 M) in the presence of $Fe_2(OH)_3(btc)$ (1×10^{-3} M) at 25 °C in 5 h, *ca.* 5–8% of quinone was found in the results of two experiments, while about 90% of the initial ketone **I** remained unchanged. At the same time, the formation of several products was detected by gas chromatography. These products could be attributed to the lactone or the products of the compound **I** hydroxylation in the aromatic core, the yield of each of these products did not exceed 2%. Increasing the reaction time to 24 h had little effect on the formation of oxidation products.

The oxidation of organic compounds in the presence of PCPs occurs on the metal ions located in pores and on the outer surface of the catalyst particles. Clearly, not all metal ions are accessible to a substrate in this case. In order to compare the outcome of the oxidation process with the one that occurred in homogeneous conditions, a similar reaction was carried out in the presence of soluble copper(II) salt. In order to reveal if there was any contribution of Lewis acidity of the metal ion (in contrast to possible redox activity), the oxidation in the presence of $AlCl_3$ was tested. It was found that in a similar reaction of the oxidation of **I** in the presence of $CuCl_2$ (0.1 M ketone, 1.7 M of H_2O_2, $1 \cdot 10^{-2}$ M $CuCl_2$, 24 h at 25 °C), 95% of the starting ketone and about 3% of quinone were found in the reaction mixture, and when $CuCl_2$ was replaced with an equimolar amount of $AlCl_3$, 98% of the starting material were found unchanged. It can be concluded that the low yield in the oxidation of **I** in the presence of HKUST-1 was associated with the intrinsic low catalytic activity of Cu^{2+} ions rather than their low accessibility. Moreover, the low Lewis acidity does not cause such low catalytic activity.

The oxidation of ketones **II-IV** in the presence of HKUST-1 at room temperature led to the formation of mixtures of products at the ketone/H_2O_2 ratio of 1:2 (0.05 M of ketone, 0.1 M of H_2O_2, $5 \cdot 10^{-3}$ M of HKUST-1), as well as at a 17-fold excess of H_2O_2 (0.1 M of **II**, 1.7 M H_2O_2, $1 \cdot 10^{-2}$ M of HKUST-1). The mass spectrum (direct injection of the sample into the ion source) of the reaction mixture sample obtained by the oxidation of **II** (0.1 M of **II**, 1.7 M of H_2O_2, $1 \cdot 10^{-2}$ M of HKUST-1 for 24 h at 25 °C with further processing) is shown in **Figure 3** (a). The mass spectrum obtained corresponds to cyclic lactone **IIa** (the Baeyer-Villiger oxidation product, **Figure 4**) and other substances that could form upon its oxidation by the radical mechanism, which led to a decrease in the carbon chain length [32]. The ^{1}H NMR spectrum of the reaction mixture after the oxidation of **II** could also be interpreted with the assumption that the resulting mixture contained lactone **IIa** and the products of its deeper oxidation (the products were determined by comparing the positions of the signals with the calculated values; the positions of the signals in the NMR spectrum were calculated using ACD Labs 10.08 software pack program), however the quantitative composition of the reaction mixture could not be determined. The possible oxidation products are shown in **Figure 3** (b).

The GCMS analysis of the reaction mixture obtained in the experiment of the compound **II** oxidation revealed at least three other compounds with longer retention times compared to **II**; molar fractions of **II** and these 3 products had the ratio of 15:23:17:45. The mass spectrum of the second compound in this series corresponded to cyclohexanone **IIe** (**Figure 3**, *b*), which could be formed due to the hydrolysis and the subsequent decarboxylation of **II**. Taking into account the results of several experiments conducted under different conditions, it can be concluded that most of the oxidation products decompose on the column during chromatographic separation (the release of individual portions of water and CO_2 at certain intervals indicates such decomposition).

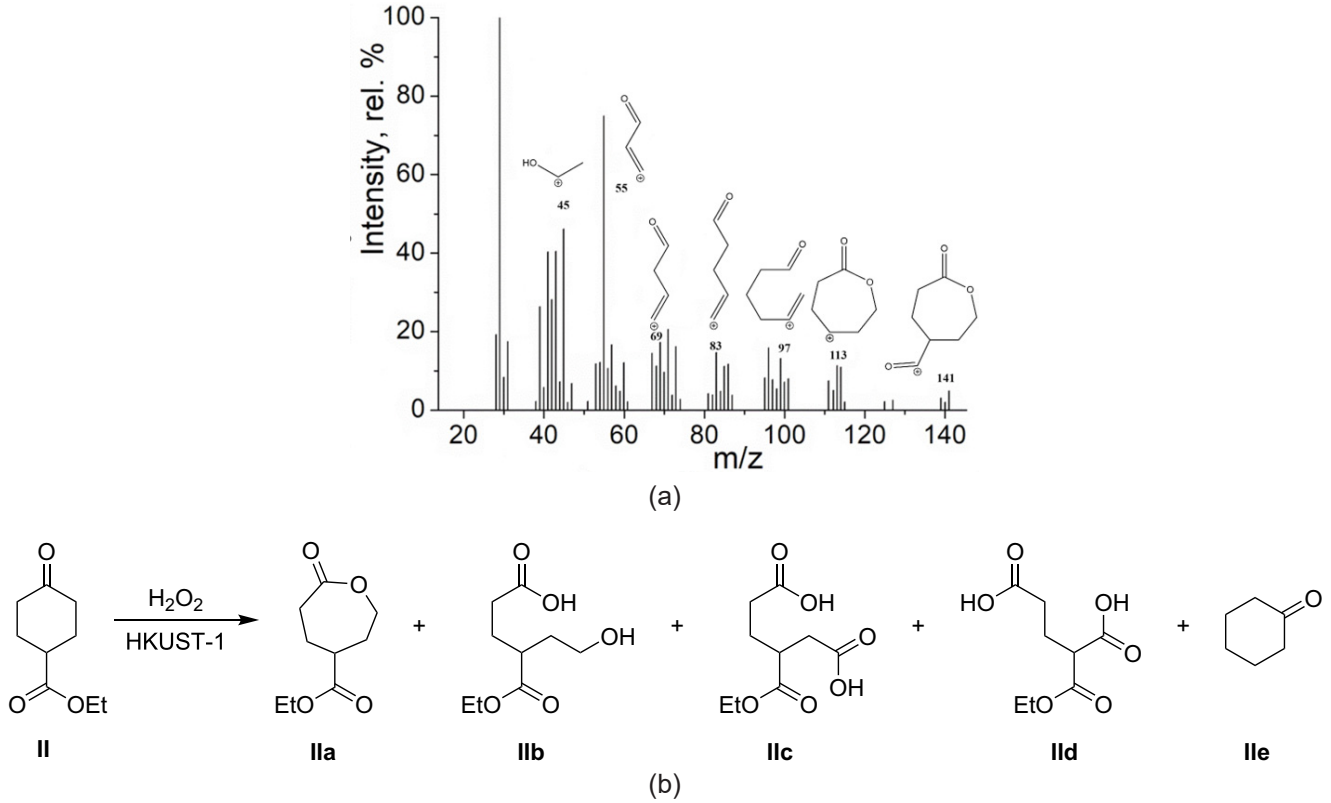

Figure 3. The mass spectrum of the products of the oxidation of **II** by H_2O_2 in the presence of HKUST-1 (**a**) and the scheme showing the oxidation of products **II** (**b**)

At the same time, not all possible products, especially di- and polycarboxylic acids, gave peaks in GCMS due to low volatility, the ability to rearrange and decarboxylation, as well as the tendency to form multicharged ions. Thus, it can be concluded that the oxidation of **II** resulted in the formation of a mixture of products, in which no predominant compounds could be isolated.

In a separate experiment, changes in the composition of the reaction mixture in the process of the oxidation of **II** (0.1 M) with hydrogen peroxide (1.7 M) in the presence of $2 \cdot 10^{-2}$ M of HKUST-1 at 70 °C were monitored. The amount of lactone **IIa** could be estimated by the integral intensity of peak at δ = 4.35 ppm, which corresponded to the CH_2 group near the oxygen atom in the 7-membered lactone cycle, the amount of acid **IId** – by the integral intensity of the signal at δ = 3.65 ppm, which corresponded to the CH group in the malonate fragment. Taking into account that the positions of the signals of the CH_3 and CH_2 groups in the $-CO_2C_2H_5$ fragment coincided in all oxidation products, the integral intensity of the CH_2 group (δ = 4.10–4.14) could be considered as an indicator of the total content of unreacted **II** and all products of its oxidation, except the products formed upon the hydrolysis of the ester and subsequent reactions. The content of other possible reaction products could not be considered in this calculation since there were no signals in their spectra that did not overlap each other. It can be noted that in the period from 60 to 150 min at 70 °C, the content of lactone **IIa** and acid **IId** remained almost unchanged and was equal to 15 and 20-30%, respectively (**Figure 4**). When the reaction time increased to 180 min, the content of lactone **IIa** and acid **IId** increased to 22 and 50%, respectively (the percentage was calculated relative to the total amount of all compounds in the mixture having the ethyl group). The stable level of concentrations of **IIa** and **IId** in the reaction mixture over a long period of time can be explained by similar values of the rates of the formation of these substances and subsequent oxidation and agreed well with the above conclusion about the formation of several oxidation products.

The formation of lactone **IIa** was a consequence of the Baeyer-Villiger oxidation of the ketone, which took place at the acidic sites of the catalyst [4, 5]. Further oxidation occurred, most likely, by the radical mechanism, and led to a shortening of the hydrocarbon chain [12, 33]. At the same time, it should be noted that the formation of carboxylic acids (such as **IIc** and **IId**) could take place without the formation of lactone **IIa** and the product of its hydrolysis **IIb** as intermediates.

ISSN 2308-8303 (Print) / 2518-1548 (Online)

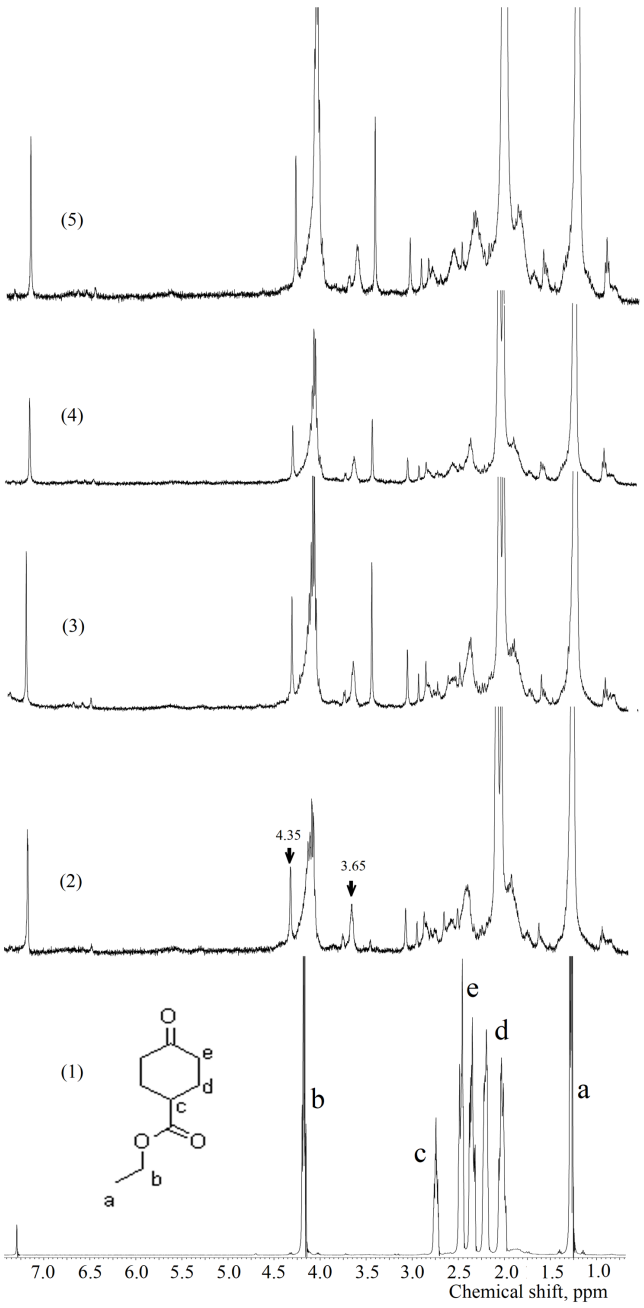

Figure 4. The change of ^{1}H NMR spectra of the reaction mixture in the process of oxidation of **II** (0.1 M) with hydrogen peroxide (1.7 M) in the presence of $2 \cdot 10^{-2}$ M of HKUST-1 at 70 °C along with the spectrum of the starting compound: (**1**) starting **II**, (**2**) in 60 min, (**3**) in 90 min, (**4**) in 120 min, and (**5**) in 150 min

The reaction of **III** with H_2O_2 in the presence of HKUST-1 under the same conditions as in the case of **II** (0.1 M of ketone, 1.7 M of H_2O_2, $1 \cdot 10^{-2}$ M of HKUST-1, 24 h at 25 °C) led to the formation of a mixture of products. The DI-mass spectrum of this mixture contained several peaks. Some of them could be assigned to 4-piperidinone and lactone formed upon oxidation of **III** and elimination of the *tert*-butoxycarbonyl group (**Figure 5**, *b*). The NMR spectrum of the reaction mixture contained signals that could be attributed to the starting material, lactone, and products of the subsequent oxidation with cleavage of the cycle, similar to the oxidation of **II**. It was not possible to reliably identify all the signals in the NMR spectrum, but several characteristic features of the spectrum could be noted. Thus, the spectrum of the mixture of the reaction products contained at least four signals of the *tert*-butyl group in the range of δ = 1.44–1.53 ppm instead of one signal of such a group in the starting ketone at δ = 1.45 ppm and the similar group in lactone at δ = 1.53 ppm (calculated value; signal of *tert*-butanol formed upon the hydrolytic cleavage of the Boc group was observed at δ = 1.28 ppm). The increase in the number of signals was an indicator of the formation of at least four compounds containing the unchanged fragment -N–C(=O)–O*t*Bu, upon the oxidation of **III**. A signal at δ = 4.6 ppm could be attributed to the CH_2 group near the O atom in a 7-membered lactone cycle. In addition, there were new signals at δ = 8.01, 7.25 and 5.14 ppm in the spectrum of the reaction mixture, which could be attributed to nitrone **IIIc** and its tautomer **IIId**.

The reaction of **IV** with H_2O_2 in the presence of HKUST-1 under the same conditions led to the formation of a mixture. The DI-mass spectrum of this mixture corresponded to the lactone formed upon the Bayer-Villiger oxidation of **IV** (**Figure 6**). However, the formation of the compounds with a lower molecular weight could not be excluded.

Higher conversions of **II**–**IV** in reactions with H_2O_2 compared to the conversion of **I** may be explained by a higher reactivity of the aliphatic ketones, which is possibly due to steric effects (the presence of a bulk benzene ring near the carbonyl group in aromatic ketones) or differences in the electronic structure of such ketones. A similar dependence of the conversion on the nature of the ketone was observed in the process of oxidation of ketones by H_2O_2 in the presence of tungsten-containing heteropolyacids [34].

The catalytic oxidation of ketones by H_2O_2 can occur by the Baeyer-Villiger mechanism or by the radical mechanism (**Figure 7**). However, a clear dependence on the nature of the catalyst cannot be found. Generally, it can be noted that the use of mild Lewis acids like Sn-, Ge-containing silicates, MoO_3, or complexes of Pt(II) resulted in the Baeyer-Villiger oxidation. The same effect was also found in the case of strong Lewis acids like $AlCl_3$. All catalysts shown on **Figure 7**, which favored radical oxidation, contained redox-active

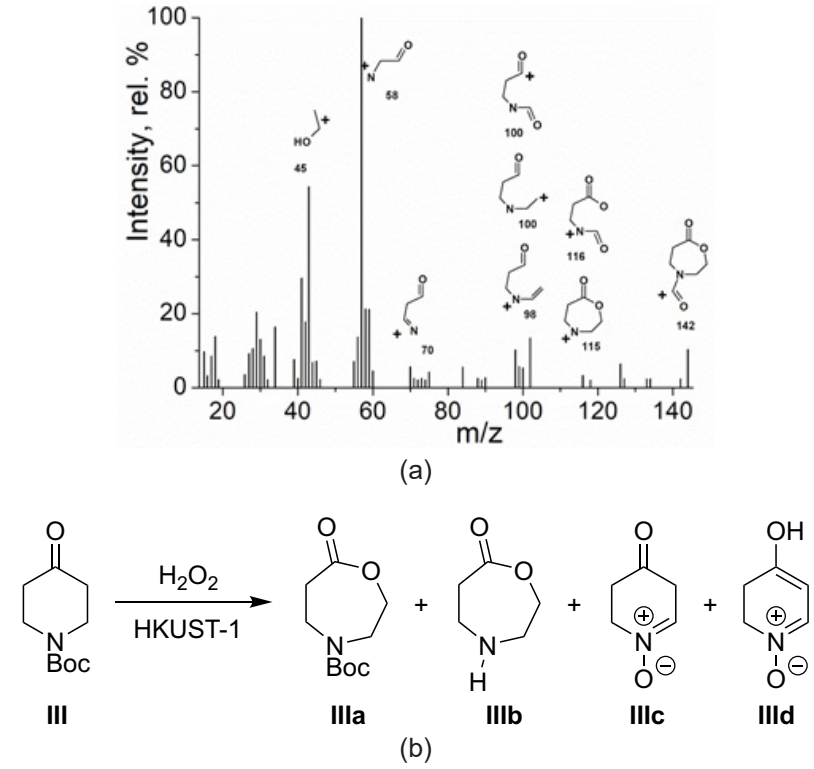

Figure 5. The mass spectrum of the products of oxidation of **III** by H_2O_2 in the presence of HKUST-1 (a) and the scheme showing products of oxidation of **III** (b)

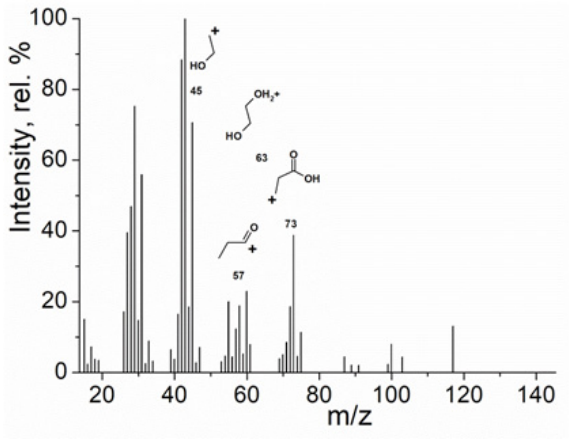

Figure 6. The mass spectrum of the products of oxidation of **IV** by H_2O_2 in the presence of HKUST-1

sites. However, a potentially redox-active catalyst Co(III) salen was found to catalyze the Baeyer-Villiger oxidation (probably, as its redox potential falls out of the suitable range for generation of radicals from H_2O_2) [15]. Notably, the Baeyer-Villiger oxidation can be followed by the radical oxidation [35] in the presence of the same catalyst. The PCPs, studied herein, seem to be able to catalyze the Baeyer-Villiger oxidation, but there are evidences of radical oxidation pathway in the presence of such catalysts.

Generally, soft Lewis acids are considered as the most efficient catalysts for the Bayer-Villiger oxidation [5, 36]. There are examples of the Baeyer-Villiger ketone oxidation catalyzed by coordination compounds of Cu(II) [23, 37, 38] and

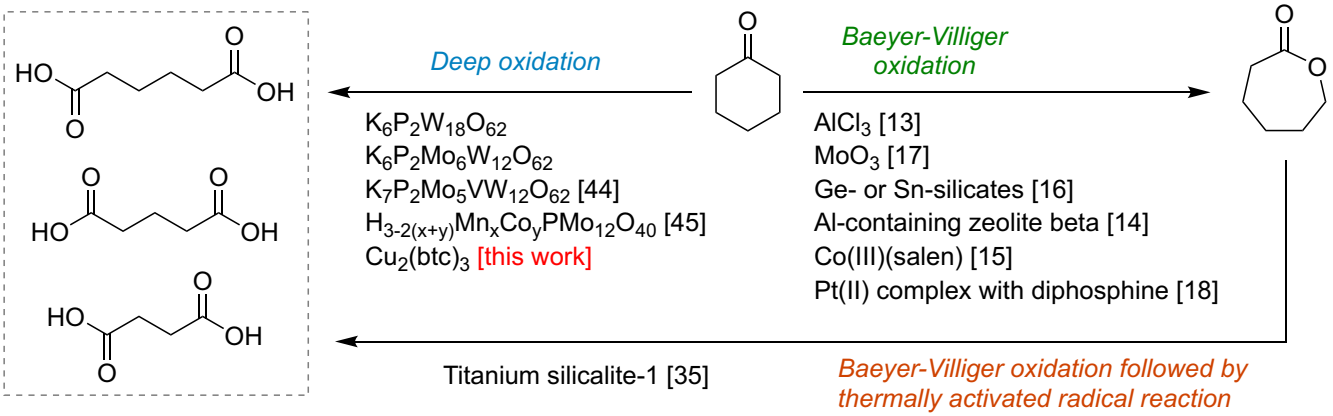

Figure 7. The catalytic oxidation of ketones by H_2O_2 in the presence of different catalysts

ISSN 2308-8303 (Print) / 2518-1548 (Online)

Fe(III) by oxygen [39]. $Cu(OTf)_2$ was found to be an efficient catalyst for the Baeyer-Villiger oxidation of cyclic ketones by *m*CPBA [17]. Several Fe- and Cu-containing systems were found to be efficient catalysts of the Baeyer-Villiger oxidation in the O_2/benzaldehyde system, such as Fe–Sn–O catalysts for the oxidation of cyclohexanone to ε-caprolactone [40], iron(III)-containing mesoporous silica (MCM-41) [41], a $Cu\text{-}SiO_2$ catalyst with highly dispersed copper species and various metal valences for the oxidation of cyclohexanone to ε-caprolactone [42], a bifunctional hybrid catalyst originated from copper tetrasulfophthalocyanine (CuPcTs) and hydrotalcite [43]

Conclusions

The oxidation of cyclohexanone analogs with hydrogen peroxide in the presence of a porous coordination polymer HKUST-1 led to the formation of a mixture of products containing the corresponding lactones (formed by the Baeyer-Villiger process) and other compounds formed by a deeper oxidation of the organic compounds with cleavage of the ring and reduction of the hydrocarbon chain length. Unlike aliphatic ketones, α-tetralone underwent almost no conversion in the reaction with H_2O_2 in the presence of HKUST-1, and the oxidation of the same ketone in the presence of $Fe_2(OH)_3(btc)$ led to the formation of a number of products with low yields. Among them, 1,4-naphthoquinone was dominant (in contrast to cyclic lactone – the expected Baeyer-Villiger oxidation product). The oxidation of ketones in the presence of the PCPs studied occurred mainly by the radical mechanism, which can be explained by insufficient Lewis acidity of Cu^{2+} and Fe^{3+} ions in the environment of oxygen atoms.

References

1. Valange, S.; Vedrine, J. C. General and Prospective Views on Oxidation Reactions in Heterogeneous Catalysis. *Catalysts* **2018**, *8* (10), 483. https://doi.org/10.3390/catal8100483.
2. Trusau, K. I.; Kirillova, M. V.; André, V. A.; Usevich, I.; Kirillov, A. M. Mild Oxidative Functionalization of Cycloalkanes Catalyzed by Novel Dicopper(II) Cores. *Mol. Catal.* **2021**, *503*, 111401. https://doi.org/10.1016/j.mcat.2021.111401.
3. Tereshchenko, O. D.; Perebiynis, M. Y.; Knysh, I. V.; Vasylets, O. V.; Sorochenko, A. A.; Slobodyanyuk, E. Y.; Rusanov, E. B.; Borysov, O. V.; Kolotilov, S. V.; Ryabukhin, S. V.; Volochnyuk, D. M. Electrochemical Scaled-up Synthesis of Cyclic Enecarbamates as Starting Materials for Medicinal Chemistry Relevant Building Blocks. *Adv. Synth. Catal.* **2020**, *362* (15), 3229–3242. https://doi.org/10.1002/adsc.202000450.
4. Strukul, G.; Scarso, A. Metal-Catalyzed Baeyer-Villiger Oxidations. In *Applied Homogeneous Catalysis with Organometallic Compounds: A Comprehensive Handbook in Four Volumes, Third Edition*; B. Cornils, WA Herrmann, M. Beller, R. Paciello Eds., Wiley – VCH Verlag GmbH & Co. KGaA, 2018, Chapter 29, pp 1485–1508. https://doi.org/10.1002/9783527651733.ch29.
5. Michelina, R. A.; Sgarbossa, P.; Scarso, A.; Strukul. G. The Baeyer – Villiger Oxidation of Ketones: A Paradigm for the Role of Soft Lewis Acidity in Homogeneous Catalysis. *Coord. Chem. Rev.* **2010**, *254* (5–6), 646–660. https://doi.org/10.1016/j.ccr.2009.09.014.
6. González-Núñez, M. E.; Mello, R.; Olmos, A.; Acerete, R.; Asensio, G. Oxidation of Alcohols to Carbonyl Compounds with $CrO_3{\cdot}SiO_2$ in Supercritical Carbon Dioxide. J. Org. Chem. **2006**, *71* (3), 1039–1042. https://doi.org/10.1021/jo052137j.
7. Bridges, L.; Mohamed, R. A. M.; Khan, N. A.; Brusseau, M. L.; Carroll, K. C. Comparison of Manganese Dioxide and Permanganate as Amendments with Persulfate for Aqueous 1,4-Dioxane Oxidation. *Water* **2020**, *12* (11), 3061. https://doi.org/10.3390/w12113061.
8. Fujii, H.; Ogawa, R.; Jinbo, E.; Tsumura, S.; Nemoto, T.; Nagase, H. Novel Oxidation Reaction of Tertiary Amines with Osmium Tetroxide. *Synlett* **2009**, 14, 2341–2345. https://doi.org/10.1055/s-0029-1217811.
9. Guideline for elemental impurities (Doc. Ref. EMA/CHMP/ICH/353369/2013), Committee for Human Medicinal Products, European Medicines Agency, Amsterdam, 2019.
10. Lee, J.; Lee, J. C. An Efficient Oxidation of Alcohols by Aqueous H_2O_2 with 1,3-Dibromo-5,5-Dimethylhydantoin. *Lett. Org. Chem.* **2018**, *15* (10), 895–898. https://doi.org/10.2174/1570178615666180613080548.
11. Coelho, J. V.; Oliveira, L. C. A.; Moura, F. C. C.; de Souza, P. P.; Silva, C. A.; Batista, K. B.; da Silva, M. J. β-Pinene Oxidation by Hydrogen Peroxide Catalyzed by Modified Niobium – MCM. *Applied Catal. A: General* **2012**, *419–420*, 215–220. https://doi.org/10.1016/j.apcata.2012.01.032.
12. Shul'pin, G. B.; Shul'pina, L. S. Oxidation of Organic Compounds with Peroxides Catalyzed by Polynuclear Metal Compounds. *Catalysts* **2021**, *11* (2), 186. https://doi.org/10.3390/catal11020186.
13. Lei, Z.; Ma, G.; Wei, L.; Yang, Q.; Su, B. Clean Baeyer–Villiger Oxidation Using Hydrogen Peroxide as Oxidant Catalyzed by Aluminium Trichloride in Ethanol. *Catal. Lett.* **2008**, *124* (3-4), 330–333. https://doi.org/10.1007/s10562-008-9470-0.
14. Ohno, R.; Taniya, K.; Tsuruya, S.; Ichihashi, Y.; Nishiyama, S. Oxidation of Cyclohexane with Hydrogen Peroxide Over Zeolites with Various Si/Al Ratios. *Catal. Today* **2013**, *203*, 60–65. https://doi.org/10.1016/j.cattod.2012.03.007.
15. Uchida, T.; Katsuki, T. Cationic Co(III)(salen)–Catalyzed Enantioselective Baeyer–Villiger Oxidation of 3–Arylcyclobutanones Using Hydrogen Peroxide as a Terminal Oxidant. *Tetrahedron Lett.* **2001**, *42* (39), 6911–6914. https://doi.org/10.1016/S0040-4039(01)01445-9.
16. Xu, H.; Jiang, J.; Yang, B.; Wu, H.; Wu, P. Effective Baeyer – Villiger Oxidation of Ketones over Germanosilicates. *Catal. Commun.* **2014**, *55*, 83–86. https://doi.org/10.1016/j.catcom.2014.06.019.
17. Ma, Q.; Xing, W.; Xu, J.; Peng, X. Baeyer–Villiger Oxidation of Cyclic Ketones with Aqueous Hydrogen Peroxide Catalyzed by Transition Metal Oxides. *Catal. Commun.* **2014**, *53*, 5–8. https://doi.org/10.1016/j.catcom.2014.04.017.
18. Frisone, M. D. T.; Pinna, F.; Strukul, G. Baeyer-Villiger oxidation of cyclic ketones with hydrogen peroxide catalyzed by cationic complexes of platinum(II): selectivity properties and mechanistic studies. *Organometallics* **1993**, *12* (1), 148–156. https://doi.org/10.1021/om00025a027.
19. Granato, T.; Testa, F.; Olivo. R. Catalytic Activity of HKUST-1 Coated on Ceramic Foam. *Micropor. Mesopor. Mater.* **2012**, *153*, 236–246. https://doi.org/10.1016/j.micromeso.2011.12.055.

20. Konnerth, H.; Matsagar, B. M. Chen, S. S.; Prechtl, M. H. G.; Shieh, F.-K.; Wu, K. C.-W. Metal – Organic Framework (MOF) – Derived Catalysts for Fine Chemical Production *Coord. Chem. Rev.* **2020**, *416*, 213319. https://doi.org/10.1016/j.ccr.2020.213319.
21. Sotnik, S. A.; Gavrilenko, K. S.; Lytvynenko, A. S.; Kolotilov, S. V. Catalytic Activity of Copper(II) Benzenetricarboxylate (HKUST-1) in Reactions of Aromatic Aldehydes Condensation with Nitromethane: Kinetic and Diffusion Study. *Inorg. Chim. Acta* **2015**, *426*, 119–125. https://doi.org/10.1016/j.ica.2014.11.018.
22. Lytvynenko, A. S.; Kolotilov, S. V.; Kiskin, M. A.; Cador, O.; Golhen, S.; Aleksandrov, G. G.; Mishura, A. M.; Titov, V. E.; Ouahab, L.; Eremenko, I. L.; Novotortsev, V. M. Redox-Active Porous Coordination Polymers Prepared by Trinuclear Heterometallic Pivalate Linking with the Redox-Active Nickel(II) Complex: Synthesis, Structure, Magnetic and Redox Properties, and Electrocatalytic Activity in Organic Compound Dehalogenation in Heterogeneous Medium. *Inorg. Chem.* **2014**, *53* (10), 4970–4979. https://doi.org/10.1021/ic403167m.
23. Yurchenko, D. V.; Lytvynenko, A. S.; Abdullayev, E. N.; Peregon, N. V.; Gavrilenko, K. S.; Gorlova, A. O.; Ryabukhin, S. V.; Volochnyuk, D. M.; Kolotilov, S. V. Catalytic oxidation of benzoins by hydrogen peroxide on nanosized HKUST-1: influence of substituents on the reaction rates and DFT modeling of the reaction path. *Molecules* **2023**, *28* (2), 747. https://doi.org/10.3390/molecules28020747.
24. Chowdhury, P.; Bikkina, C.; Meister, D.; Dreisbach, F.; Gumma, S. Comparison of Adsorption Isotherms on Cu-BTC Metal Organic Frameworks Synthesized from Different Routes. *Micropor. Mesopor. Mater.* **2009**, *117* (1–2), 406–413. https://doi.org/10.1016/j.micromeso.2008.07.029.
25. Hu, X.; Lou, X.; Li, C.; Ning, Y.; Liao, Y.; Chen, Q.; Mananga, E. S.; Shen, M.; Hua, B. Facile Synthesis of the Basolite F300 – like Nanoscale Fe-BTC Framework and Its Lithium Storage Properties. *RSC Adv.* **2016**, *6* (115), 114483–114490. https://doi.org/10.1039/C6RA22738D.
26. Misono, M.; Ochiai, E.; Saito, Y.; Yoneda, Y. A New Dual Parameter Scale for the Strength of Lewis Acids and Bases with the Evaluation of their Softness. *J. Inorg. Nucl. Chem.* **1967**, *29* (11), 2685–2691. https://doi.org/10.1016/0022-1902(67)80006-X.
27. Razavi, S. A. A.; Chen, W.; Zhou, H.-C.; Morsali, A. Tuning Redox Activity in Metal-Organic Frameworks: From Structure to Application. *Coord. Chem. Rev.* **2024**, *517*, 216004. https://doi.org/10.1016/j.ccr.2024.216004.
28. Lagoshniak, D. A.; Mishura, A. M.; Kurmach, M. M.; Lytvynenko, A. S.; Grabovaya, N. V.; Gavrilenko, K. S.; Manoilenko, O. V.; Kolotilov, S. V. Influence of the Structures of the Carboxylate Porous Coordination Polymers as Stationary Phases for Liquid Chromatography on the Separation Efficiency of the Aniline Derivatives. *Russ. J. Coord. Chem.* **2020**, *46* (7), 458–465. https://doi.org/10.1134/s1070328420070040.
29. Achmann, S.; Hagen, G.; Kita, J.; Malkowsky, I. M.; Kiener, C.; Moos, R. Metal-Organic Frameworks for Sensing Applications in the Gas Phase. *Sensors* **2009**, *9,* 1574–1589. https://doi.org/10.3390/s90301574.
30. Schlichte, K.; Kratzke, T.; Kaskel, S. Improved Synthesis, Thermal Stability and Catalytic Properties of the Metal – Organic Framework Compound $Cu_3(BTC)_2$ *Micropor. Mesopor. Mater.* **2004**, *73* (1–2), 81–88. https://doi.org/10.1016/j.micromeso.2003.12.027.
31. Torres, N.; Galicia, J.; Plasencia, Y.; Cano, A.; Echevarría, F.; Desdin-Garcia. L. F. Implications of Structural Differences between Cu-BTC and Fe-BTC on their Hydrogen Storage Capacity. *Colloids Surf., A* **2018**, *549*, 138–146. https://doi.org/10.1016/j.colsurfa.2018.04.016.
32. Hamann, H. J.; Bunge, A.; Liebscher, J. Reaction of Epoxyketones with Hydrogen Peroxide – Ethane-1,1-dihydroperoxide as a Surprisingly Stable Product. *Chem. Eur. J.* **2008**, *14* (23), 6849–6851. https://doi.org/10.1002/chem.200800932.
33. Ros, D.; Gianferrara, T.; Crotti, C.; Farnetti, E. Iron-Catalyzed Oxidation of 1-Phenylethanol and Glycerol with Hydrogen Peroxide in Water Medium: Effect of the Nitrogen Ligand on Catalytic Activity and Selectivity. *Front. Chem.* **2020**, *8* (810), 1–13. https://doi.org/10.3389/fchem.2020.00810.
34. Li, X.; Cao, R.; Lin, Q. Solvent – Free Baeyer–Villiger Oxidation with H_2O_2 as Oxidant Catalyzed by Multi-SO_3H Functionalized Heteropolyanion – Based Ionic Hybrids. *Catal. Commun.* **2015**, *63*, 79–83. https://doi.org/10.1016/j.catcom.2014.12.028.
35. Cavani, F.; Raabova, K.; Bigi, F.; Quarantelli, C. A Rationale of the Baeyer–Villiger Oxidation of Cyclohexanone to ε-Caprolactone with Hydrogen Peroxide: Unprecedented Evidence for a Radical Mechanism Controlling Reactivity. *Chem. Eur. J.* **2010**, *16* (43), 12962–12969. https://doi.org/10.1002/chem.201001777.
36. Gorban, O.; Danilenko, I.; Nosolev, I.; Abdullayev, E.; Islamov, A.; Gavrilenko, K.; Doroshkevich, A.; Shvets, O.; Kolotilov, S. Impact of chemical and physical modification of zirconia on structure, surface state, and catalytic activity in oxidation of α-tetralol. *J. Nanopart. Res.*, **2022**, *24*, 197. https://doi.org/10.1007/s11051-022-05566-5.
37. Bolm, C.; Schlingloff, G.; Weickhardt, K. Optically Active Lactones from a Baeyer–Villiger-Type Metal-Catalyzed Oxidation with Molecular Oxygen. *Angew. Chem. Int. Ed. Engl.* **1994**, *33* (18), 1848–1849. https://doi.org/10.1002/anie.199418481.
38. Duc, D. X.; Nguyet, N. T. Microwave – Assisted Claisen – Schmidt Condensation Between Arylmethyl Ketones and Aryl Aldehydes Catalyzed by $Cu(OTf)_2$ under Solvent – Free Conditions: Synthesis of Chalcones. *Vietnam J. Sci. Techn.* **2020**, *58* (6A), 1–9.
39. Cao, Q.; Yin, Q.; Chen, Q.; Dong, Z. B.; Han, B. H. Fluorinated Porous Conjugated Polyporphyrins through Direct C–H Arylation Polycondensation: Preparation, Porosity, and Use as Heterogeneous Catalysts for Baeyer – Villiger Oxidation. *Chem. Eur. J.* **2017**, *23* (41), 9831–9837. https://doi.org/10.1002/chem.201700916.
40. Sun, J.; Zhu, Q.; Guo, X.; Jin, H.; He, G.; Ma, L.; Zhang, R.; Gu, Q.; Yang, S. Baeyer –Villiger Co – oxidation of Cyclohexanone with Fe – Sn – O Catalysts in an O_2/ Benzaldehyde System. *Green Process. Synth.* **2021**, *10* (1), 677–686. https://doi.org/10.1515/gps-2021-0045.
41. Kawabata, T.; Ohishi, Y.; Itsuki, S.; Fujisaki, N.; Shishido, T.; Takaki, K.; Zhang, Q.; Wang, Y.; Takehira, K. Iron – containing MCM – 41 catalysts for Baeyer – Villiger oxidation of ketones using molecular oxygen and benzaldehyde. *J. Mol. Catal. A: Chem.* **2005**, *236* (1–2), 99–106. https://doi.org/10.1016/j.molcata.2005.03.027.
42. Chen, L.; Liu, Y.; Chi, J.; Xiong, W.; Liu, P.; Hao, F. A Highly Efficient Bifunctional Copper Catalyst for Baeyer–Villiger Oxidation of Cyclohexanone: Two Different Active Centers and the Reaction Path Investigation. *Appl. Surf. Sci.* **2023**, *638* (158045). https://doi.org/10.1016/j.apsusc.2023.158045.
43. Zhou, W.; Chen, Y.; Qian, J.; Sun, F.; He, M.; Chen, Q. Copper Tetrasulfophthalocyanine Intercalated Hydrotalcite as an Efficient Bifunctional Catalyst for the Baeyer–Villiger Oxidation. *Catal. Lett.* **2016**, *146* (10), 2157–2164. https://doi.org/10.1007/s10562-016-1823-5.
44. Moudjahed, M.; Dermeche, L.; Idrissou, Y.; Mazari, T.; Rabia, C. Dawson – Type Polyoxometalates as Green Catalysts for Adipic Acid Synthesis. *J. Mol. Catal. A: Chem.* **2016**, *414*, 72–77. https://doi.org/10.1016/j.molcata.2015.12.014.
45. Mouanni, S.; Mazari, T.; Amitouche, D.; Benadji, S.; Dermeche, L.; Roch-Marchal, C.; Rabia, C. Preparation and Characterization of $H_{3-2(x+y)}Mn_xCo_yPMo_{12}O_{40}$ Heteropolysalts. Application to Adipic Acid Green Synthesis from Cyclohexanone Oxidation with Hydrogen Peroxide. *Comptes Rendus Chimie* **2019**, *22*, 327–336. https://doi.org/10.1016/j.crci.2019.01.003.

ISSN 2308-8303 (Print) / 2518-1548 (Online)

Information about the authors:
Emir N. Abdullayev, Engineer of the Department of Porous Compounds and Materials, L. V. Pisarzhevsky Institute of Physical Chemistry of the National Academy of Sciences of Ukraine.
Andrii M. Mishura, Leading Engineer of the Department of Free Radicals, L. V. Pisarzhevsky Institute of Physical Chemistry of the National Academy of Sciences of Ukraine.
Ievgenii A. Iermolenko, Ph.D. Student of Institute of Organic Chemistry of the National Academy of Sciences of Ukraine; Chemist, Enamine Ltd.
Anton S. Lytvynenko, Ph.D. in Chemistry, Research Fellow of the Department of Porous Compounds and Materials, L. V. Pisarzhevsky Institute of Physical Chemistry of the National Academy of Sciences of Ukraine; https://orcid.org/0000-0001-5528-9989.
Maksim O. Kolosov, Ph.D. in Chemistry, Deputy Dean for Research, School of Chemistry, V. N. Karazin Kharkiv National University; https://orcid.org/0000-0002-6714-0513.
Olena G. Shvets, Ph.D. in Chemistry, Junior Researcher, School of Chemistry, V. N. Karazin Kharkiv National University; https://orcid.org/0000-0003-4791-2114.
Kostyantyn S. Gavrilenko, Ph.D. in Chemistry, Senior Researcher, Faculty of Chemistry, Taras Shevchenko National University of Kyiv; Manager, Enamine Ltd.; https://orcid.org/0000-0001-7487-6660.
Sergiy V. Kolotilov (*corresponding author*), Corresponding Member of the National Academy of Sciences of Ukraine, Dr.Sci. in Chemistry, Deputy Director for Research, L. V. Pisarzhevsky Institute of Physical Chemistry of the National Academy of Sciences of Ukraine; https://orcid.org/0000-0002-4780-4378; e-mail for correspondence: s.v.kolotilov@gmail.com.

Journal of Organic and Pharmaceutical Chemistry

Original Research

OPEN ACCESS
Freely available online on
http://ophcj.nuph.edu.ua

UDC 577.15:5615.2:547.2333.4

M. Ye. Blazheyevskiy[1], O. V. Kovalska[1], V. V. Diadchenko[2]

[1] National University of Pharmacy of the Ministry of Health of Ukraine,
53 Hryhorii Skovoroda str., 61002 Kharkiv, Ukraine
[2] Military Institute of Armored Forces of the National Technical University "Kharkiv Polytechnic Institute",
2 Kyrpychova str., 61002 Kharkiv, Ukraine

The Use of Tetramethylbenzidine as an Indicator in the Enzymatic Quantitative Determination of Ethonium

Abstract

The study considers the possibility of using 3,3',5,5'-tetramethylbenzidine (TMB) as an indicator in the enzymatic analysis for the quantitative determination of quaternary ammonium compounds on the example of ethonium. The feasibility of using TMB as an indicator in the kinetic photometric method has been confirmed. Kinetic curves showing the relationship between the optical density and the ethonium concentration have been constructed. The reaction rates of acetylcholinesterase inhibition by ethonium have been estimated using the tangents of the angles of these curves with TMB as an indicator. The degree of enzyme inhibition has been calculated, and a linear relationship between the ethonium concentration and the degree of inhibition has been determined. This method was applied to determine the ethonium content in 0.1 % ethonium gel. The relative standard deviation of the method does not exceed 2.5 %. The approach suggested offers a reliable and accurate method for the quantitative analysis of ethonium in dosage forms.

Keywords: ethonium; quaternary ammonium compounds; cholinesterase; acetylcholine

М. Є. Блажеєвський[1], О. В. Ковальська[1], В. В. Дядченко[2]

*[1] Національний фармацевтичний університет Міністерства охорони здоров'я України,
вул. Григорія Сковороди, 53, м. Харків, 61002, Україна*
*[2] Національний технічний університет «Харківський політехнічний інститут»,
вул. Кирпичова, 2, м. Харків, 61002, Україна*

Використання тетраметилбензидину як індикатора в ензиматичному методі кількісного визначення етонію

Анотація

У дослідженні розглянуто можливість використання 3,3',5,5'-тетраметилбензидину (ТМБ) як індикатора в ензиматичному аналізі для кількісного визначення четвертинних амонієвих сполук на прикладі етонію. Підтверджено можливість застосування ТМБ як індикатора в кінетичному фотометричному методі. Побудовано кінетичні криві, що демонструють залежність між оптичною густиною та концентрацією етонію. Швидкість реакції інгібування ацетилхолінестерази етонієм було оцінено за тангенсами кутів цих кривих, із цим ТМБ використано як індикатор. Розраховано ступінь інгібування ферменту, а також визначено лінійну залежність між концентрацією етонію та ступенем інгібування. Цей метод застосовували для визначення вмісту етонію в 0,1 % гелі етонію. Відносне стандартне відхилення методу не перевищує 2,5 %. Запропонований підхід забезпечує надійний та точний метод кількісного аналізу етонію в лікарських формах.

Ключові слова: етоній; холінестераза; ацетилхолін; четвертинні амонієві сполуки

Citation: Blazheyevskiy, M. Ye.; Kovalska, O. V.; Diadchenko, V. V. The Use of Tetramethylbenzidine as an Indicator in the Enzymatic Quantitative Determination of Ethonium. *Journal of Organic and Pharmaceutical Chemistry* **2024**, *22* (4), 36–42.
https://doi.org/10.24959/ophcj.24.321795
Received: *15 August 2024*; **Revised:** *25 November 2024*; **Accepted:** *11 December 2024*

Funding: The authors received no specific funding for this work.
Conflict of interests: The authors have no conflict of interests to declare.

ISSN 2308-8303 (Print) / 2518-1548 (Online)

■ Introduction

3,3′,5,5′-Tetramethylbenzidine (TMB) is a widely used chromogen that is valued for its non-carcinogenic nature and, upon oxidation, gives products with high absorption coefficients. This makes TMB a key component in enzyme-based assays, offering superior sensitivity and low detection limits compared to many commercially available chromogenic reagents. Notably, TMB is the most widely used chromogenic substrate in ELISA procedures that use horseradish peroxidase conjugates. The TMB substrate develops a soluble blue reaction product that can be read at 370 or 655 nm [1].

Additionally, many recent reports support and justify the wide incorporation of TMB into analytical practice [2]. Thus, *Sil et al.* proposed a one-step simple method for nanolevel detection of ascorbic acid based on the inhibitory activity of ascorbic acid on horseradish peroxidase and hydrogen peroxide supported by redox properties of TMB [3]. TMB was also used for the uric acid detection with MnO_2 nanosheets. In mildly acidic conditions, MnO_2 oxidizes TMB to its blue oxidation product applied to human urine samples, achieving recovery rates of 93.1–102.4% with a relative standard deviation below 3% [4]. In 2022, *Zhang et al.* developed a colorimetric detection system for Cu^{2+} ions based on TMB and $Ag(S_2O_3)_2^{3-}$ in an aqueous solution. Unlike Ag nanoparticles, which could not oxidize TMB, $Ag(S_2O_3)_2^{3-}$ catalyzed the reaction effectively, with optimal conditions achieved at 800 μM for TMB, 400 μM for $Na_2S_2O_3$, for 40 min, and at 25 °C. This system, with a detection range of 1–100 μM and a limit of 100 nM, shows promise for monitoring the water quality [5]. Important biogenic thiols, such as glutathione (GSH), cysteine (CySH), and homocysteine (HcySH), were analyzed using TMB as a chromogen in a simple spectrophotometric method. Detection limits for GSH, CySH, and HcySH were 1.04, 0.82, and 2.09 μM, respectively, with successful application of the method to human serum samples, achieving recovery rates of 97–112% [6]. *Chandra and colleagues* reported the synthesis of fluorescent carbon quantum dots (M-CQDs) through a simple hydrothermal treatment of mustard seeds [7]. M-CQDs demonstrated peroxidase-like activity, catalyzing the oxidation of TMB in the presence of H_2O_2, thus mimicking the natural horseradish peroxidase activity. The process enabled the colorimetric detection of H_2O_2 in the range of 0.02–0.20 mM with a detection limit of 0.015 mM. Additionally, reduction of oxidized TMB with ascorbic acid allowed for a selective and sensitive detection of ascorbic acid in the range of 10–70 μM, with a detection limit of 3.26 μM. The method was successfully applied to the ascorbic acid detection in fresh fruits. Further advancements in TMB-based systems include the application of oxidized TMB nanobelts enhancing the colorimetric and paper-based sensing of H_2O_2 [8], peroxidase-like nanoenzymes, such as Fe_3O_4 nanoparticles [9], $CoFe_2O_4$ nanoparticles [10], single-atom iron nanozyme [11], MOF-818 nanozyme containing trinuclear copper centers [12], $Ce_2(WO_4)_3$ nanosheets [13], Fe_3O_4@AuNPs [14], etc., all enhancing the H_2O_2 detection sensitivity through the formation of oxidized TMB. The versatility of TMB is reflected in its increasing popularity, with 2,889 publications between 2015 and 2024 in the Scopus® database (www.scopus.com). Notably, the number of publications surged by 1.5 times between 2019 and 2024, demonstrates the growing impact of TMB on analytical chemistry (**Figure 1**).

Previously, our laboratory developed a novel biochemical kinetic-spectrophotometric method for detecting cholinesterase inhibitors from the group of quaternary ammonium compounds (QACs) using the oxidation of *p*-phenetidine by hydrogen peroxide as the indicator reaction [15], including a recent paper reporting the quantification of Ethonium [16]. Considering all the advantages that TMB can provide for the quantification of this group of pharmaceuticals and its central role in the development of sensitive and effective analytical methods, in this study we present the results of using TMB as a chromogen for the quantitative analysis of the QAC Ethonium in a 0.5% gel formulation. The enzyme-kinetic method based on the inhibition of cholinesterase activity and the use of oxidation of TMB with hydrogen peroxide as an indicator reaction was applied.

■ Materials and methods

Reagents and equipment

The following reagents were used in the study:

- ETONIY® (Aethonium) powder (substance) produced by OJSC Farmak, Kyiv, Ukraine. $C_{30}H_{62}Cl_2N_2O_4$; CAS: 21954-74-5; MW 585.736 g mol^{-1};
- 0.5% Ethonium gel, 50 mL, batch No. 74 (Apr 2023) manufactured by APTEKA PAVLOVA

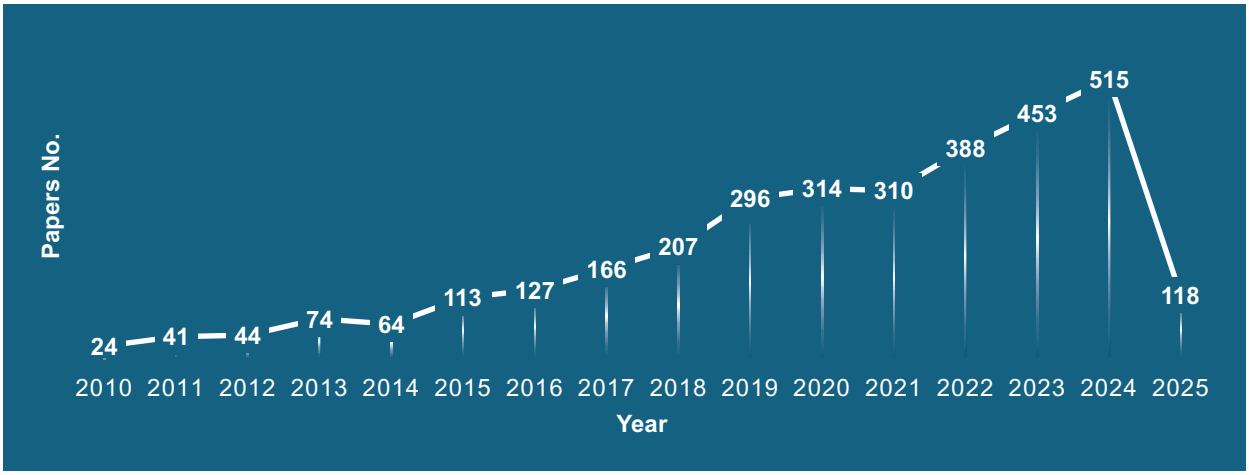

Figure 1. The number of papers per year for the query "3,3',5,5'-tetramethylbenzidine" (title, abstract, keywords) according to the Scopus® database (2010-2025)

Ltd (Odesa, Ukraine) with the composition of ethonium (active pharmaceutical ingredient) 0.5 g; glycerol – 20.0 g; propylene glycol – 20.0 g; PEG 400 – 50.0 g; PEG 1500 – 10.0 g; purified water – 10.0 ml. The content of the active substance, according to the certificate, is 4.4525% (*w*/*w*);

- 3,3',5,5'-Tetramethylbenzidine dihydrochloride (TMB), $C_{16}H_{20}N_2 \cdot 2HCl$; 98.5 % (Sigma-Aldrich); MW 313.27 g mol^{-1};
- Disodium hydrogen phosphate dodecahydrate ($Na_2HPO_4 \cdot 12H_2O$), puriss. p.a. ("ReaChem", Kharkiv, Ukraine);
- Stabilized hydrogen peroxide, 30–40 % solution, puriss. p.a., (LLC Inter-Synthes, Boryslav, Ukraine) with the content of hydrogen peroxide determined using permanganatometry according to the State Pharmacopoeia of Ukraine [17];
- Acetylcholine chloride (Pharm Grade), 0.2 g per amp/5 mL, manufactured by the State Science Center of Virology and Biotechnology "Vector";
- A dry cholinesterase (EC 3.1.1.8) powder from horse serum (SMU "Biomed"), 80 mg in an ampoule (VI class, activity 28 AU mg^{-1}). The catalytic activity of 1 activity unit (AU) is manifested in such an amount of this enzyme preparation that converts 1 μmol of the substrate in 1 min under specified reaction conditions.
- Ethanol 96% *v*/*v* (USP, BP, Ph.Eur.) pure, pharma grade.
- High-purity double distilled water was used throughout the experiment.

The pH measurements were performed with a combined glass electrode (SP20B) together with an EAL-1M3.1 reference standard silver chloride electrode.

The absorbance measurements were performed on an SF-26 spectrophotometer (λ = 420 nm, l = 10 mm).

Preparation of solutions

0.2 M Phosphate buffer solution (pH 8.35)

Disodium hydrogen phosphate dodecahydrate (35.75 g) was dissolved in a 500 mL flask using double-distilled water. 0.1 M Solution of hydrochloric acid (19 mL) was then added. The pH of the final solution was controlled potentiometrically.

0.02 M TMB solution

The substance of TMB (0.6265 g) was dissolved in 40% (*v*/*v*) ethanol solution in a 100 mL volumetric flask and diluted to the volume with the same solvent. The mixture was heated to 45 °C for complete dissolution and was stored in a tightly closed dark glass bottle in a cool place.

10% Hydrogen peroxide solution

The solution was prepared from a 30–40% solution of hydrogen peroxide by dilution with the required amount of double distilled water. The content of hydrogen peroxide in a 10% working solution was determined by permanganatometry.

Cholinesterase (ChE) solution

The accurately weighed content of an ampoule containing the cholinesterase powder (80 mg) was dissolved in double-distilled water (20.0 mL) when heating gently on a water heater. The shelf life of the solution was 1 day.

Acetylcholine chloride (ACh) solution

The solution with the initial concentration of $5.4 \cdot 10^{-3}$ mol L^{-1} was prepared by dissolving the ampoule content (0.2 g of acetylcholine) in 200 mL of double-distilled water. For this purpose, the ampoule was opened, and 4.0 mL of water was pipetted and added to the ampoule, and then shaken until acetylcholine was completely dissolved.

ISSN 2308-8303 (Print) / 2518-1548 (Online)

Then the solution was transferred into a 200 mL volumetric flask and diluted to the volume with double-distilled water.

0.1% Ethonium solution

1.0000 g of the Ethonium substance was dissolved in a 1 L flask using double-distilled water, the solution was heated to 40–45°C, 9.0 g of sodium chloride was added to the solution, and diluted to the volume.

Stock Solution of Ethonium (ET), 1×10^{-4} M

The accurately weighed powder of the Ethonium substance (0.058574 g) was dissolved in 500 mL of double-distilled water in a 1000 mL volumetric flask. The solution was diluted to the volume with the same solvent at +20 °C and mixed thoroughly.

Ethonium Work Standard (WS) solution, $1\cdot10^{-5}$ M

The accurately weighed powder of the ethonium substance (0.58574 g) was dissolved in 500 mL of ethanol solution in double-distilled water ($EtOH/H_2O$ 30:70 *v*/*v*) in a 1 L volumetric flask and diluted to the volume at +20 °C and mixed thoroughly. Using a pipette, 10 mL of the resulting solution was taken and transferred to a 1 L volumetric flask and diluted to the volume with double-distilled water.

Ethonium WS Solution, 1×10^{-6} M

A 10 mL aliquot of *Stock Solution* of the drug (1×10^{-4} mol L^{-1}) was transferred into a 1 L volumetric flask and diluted to the volume with double-distilled water at +20 °C.

The procedure for constructing the kinetic curves

Part 1 – working experiments «ACh + (ChE + ET)»

The buffer solution (2.00 mL, pH 8.35) was added to each of the five 20 mL graduated test tubes with a ground joint stopper. Then 0.50, 1.50, 3.00, 4.50, and 6.00 mL of the ethonium 1×10^{-6} M WS solution was added to the test tubes, followed by 0.50 mL of the cholinesterase solution. The content was thoroughly shaken, and the test tubes were kept in a thermostat at +38 °C for 10 min. After that 1.0 mL of acetylcholine solution and 5.90, 4.90, 1.90, 0.40 mL, and 5.4 mL of double-distilled water were added to the five test tubes, respectively. The content was mixed thoroughly and incubated again for 10 min at 38 °C. Then, a 10% hydrogen peroxide solution (3.20 mL) was added to each of the test tubes, and the latter were incubated for 10 min at +38 °C. After that 3.0 mL of 96% ethanol and 0.50 mL of the TMB solution were added, and the solution was shaken thoroughly and scanned photometrically on a spectrophotometer at a wavelength of 420 nm in a 1 cm cuvette over a 15-minute period. The phosphate buffer was used as a reference solution. The relative rate of the reaction [[(ChE + ET) + ACh] + H_2O_2 + TMB] (*tg*α (Inh), min^{-1}) was determined as the slope of a linear section of the "*optical density (A) vs time (t, min)*" kinetic curve.

Part 2 – control experiments #1 "ACh"

The buffer solution (2.00 mL, pH 8.35) was added to a 20 mL graduated test tube, followed by 6.9 mL of double-distilled water, 1.0 mL of the acetylcholine solution, and 3.2 mL of the hydrogen peroxide solution. The solution was incubated at 38 °C for 10 min. After that 3.0 mL of 96% ethanol and 0.5 mL of the TMB solution were added to the test tube. The solution was shaken thoroughly and scanned photometrically on a spectrophotometer at a wavelength of 420 nm in a 1 cm cuvette over a 15-minute period. The phosphate buffer was used as a reference solution. According to the plotted "*optical density* (*A*) vs *time* (*t*, min)" kinetic curve, the relative rate of the reaction [(ACh + H_2O_2) + TMB] was determined as a slope of a linear section of the curve (*tg*α (ACh), min^{-1}).

Part 3 – control experiments #2 "Ach+ChE"

2.0 mL of the buffer solution, 6.4 mL of double-distilled water, 0.5 mL of the cholinesterase solution, and 1.0 mL of the acetylcholine solution were successively added to a 20 mL test tube with a ground joint stopper and then thermostated at 38 °C for 10 min. Further 3.2 mL of the hydrogen peroxide solution was added, and the mixture was thoroughly shaken and thermostated again at 38 °C for 10 min. After that 3.0 mL of 96% ethanol and 0.5 mL of the TMB solution were added. Then the solution was scanned photometrically on a spectrophotometer at a wavelength of 420 nm in a 1 cm cuvette over a 15 min period. The phosphate buffer was used as a reference solution. According to the plotted "*optical density (A) vs time (t, min)*" kinetic curve, the relative rate of the reaction [(ChE + ACh) + H_2O_2 + TMB] was determined as a slope of a linear section of the curve (*tg*α (ACh + ChE), min^{-1}).

The relative rates of the reactions (expressed as tangents of the angles of slope) were used to calculate the inhibition degree of the enzymatic hydrolysis of ACh (*U*, %) in the presence of ethonium according to the following equation:

$$U(\%) = \frac{[tg\alpha(\text{Inh}) - tg\alpha(\text{Ach} + \text{ChE})]}{[tg\alpha(\text{Ach}) - tg\alpha(\text{Ach} + \text{ChE})]} \times 100\ \%$$

where *tg*α (*Inh*) (min^{-1}) is the relative reaction rate of the TMB oxidation by peroxyacetic

acid formed during the perhydrolysis of unreacted ACh in the working experiment at various concentrations of the inhibitor (ET);

*tg*α (Ach) (min^{-1}) is the relative reaction rate of the TMB oxidation by peroxyacetic acid formed in the reaction of the ACh perhydrolysis in the absence of the inhibitor and ChE (control experiment #1);

*tg*α (Ach + ChE) (min^{-1}) the relative reaction rate of the TMB oxidation by peroxyacetic acid formed in the reaction of the perhydrolysis of unreacted ACh in the presence of ChE and in the absence of the inhibitor (ET) (control experiment #2).

The calculated values of *U* (%) were used to plot the "*inhibition degree (U, %) vs ethonium concentration (c, ng* mL^{-1}*)*" calibration graph (**Figure 3**).

■ Results and discussion

Previously, a study was conducted to analyze the parameters that may affect the effectiveness of the approach proposed [18]. This allowed us to determine the optimal working conditions and concentrations of the reagents used in this study.

Kinetic curves were plotted using experimental data showing the relationship between the optical density and time, as presented in **Figure 2**.

The calibration graph (**Figure 3**) was constructed in the coordinates of the inhibition degree (*U*, %) *vs* the concentration (*c*, ng mL^{-1}). From **Figure 3**, the linear dependence of the inhibition degree on the concentration of the inhibitor was observed in the interval of 4–60% (R = 0.9) corresponding to the concentration of the inhibitor 17–200 ng mL^{-1}. The LOQ was defined as the concentration corresponding to a 4% degree of inhibition, i.e., 17 ng mL^{-1}.

The method for the quantitative determination of ethonium with TMB as an indicator in a "Ethonium 0.5% gel" formulation

0.1 g (accurate weight) of the ethonium gel was dissolved in 1000 mL of double-distilled water. Then 2.0 mL of the phosphate buffer solution, 5.0 mL of the gel solution, and 0.5 mL of the ChE solution were successively added to a 20 mL test tube. The mixture was thoroughly shaken and incubated for 10 min at 38 °C. After that 1.0 mL of the ACh solution and 1.4 mL of double-distilled water were added, and the content was carefully mixed and incubated again for 10 min at 38 °C. Then, 3.2 mL of the hydrogen peroxide solution was added, and the mixture was incubated again at 38 °C for 10 min. After that 3.0 mL of 96% ethanol and 0.5 mL of the TMB solution were added to the test tube. The optical density of the solution was measured at 420 nm in a 1 cm cuvette for 15 min. According to the plot of the "*optical density* vs *time*" dependence, the tangent of the angle of slope for the linear section *tg*α (Inh) was found in min^{-1}. In parallel, two more experiments were carried out. One of them involved acetylcholine and cholinesterase without the inhibitor, another one was performed without the use of cholinesterase enzyme (*control experiments #1* and *#2* described in the previous section). As a result, the

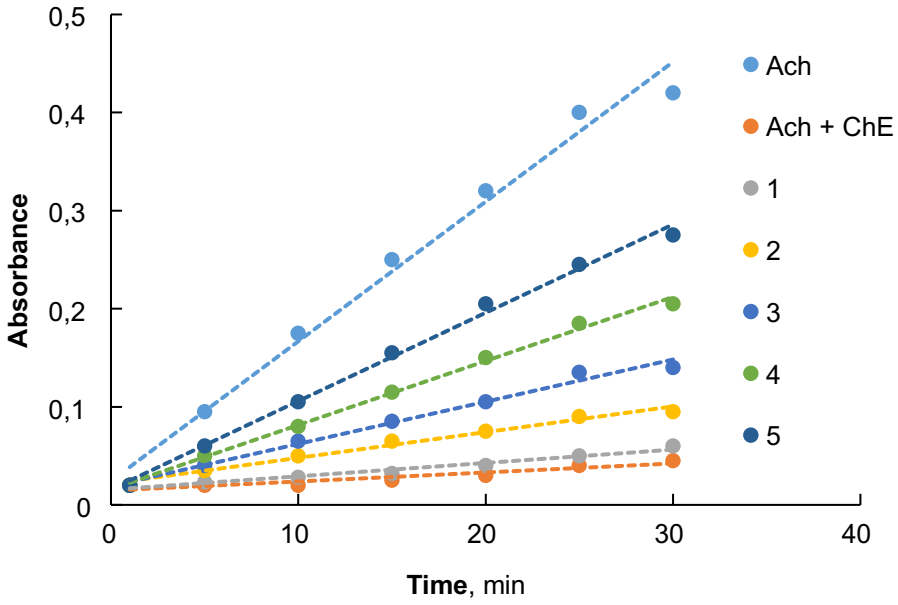

Figure 2. Kinetic curves of the conjugated oxidation of TMB with hydrogen peroxide in the presence of mixtures ACh + ChE + Inh (**1–5**). *c* (Ach) = 3.3×10^{-4} mol L^{-1}; *w*(H_2O_2) =1.92%; c (AChE) = 0.24 mg mL^{-1}. *w* (ET): 17 ng mL^{-1} (**1**); 50 ng mL^{-1} (**2**); 100 ng mL^{-1} (**3**); 150 ng mL^{-1} (**4**); 200 ng mL^{-1} (**5**); *c* (TMB) = 6.25×10^{-4} mol L^{-1}; control experiments *"Ach + ChE"*, control experiments *"ACh"*

ISSN 2308-8303 (Print) / 2518-1548 (Online)

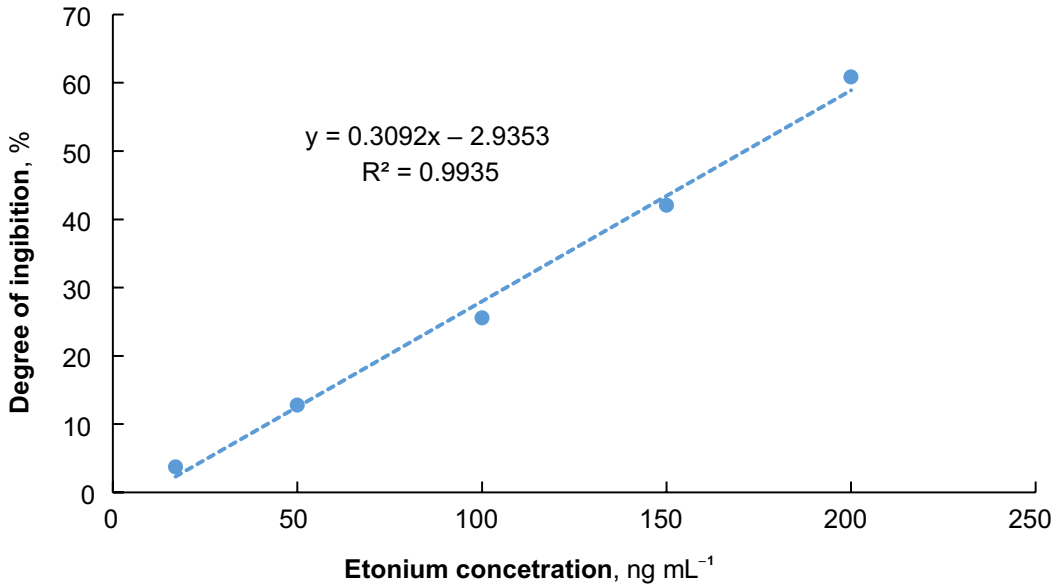

Figure 3. The dependence of the degree of inhibition on the concentration of Ethonium in the system (ACh + (ChE + Ethonium), determined by the indicator reaction of the conjugated oxidation of TMB with hydrogen peroxide in the presence of residual acetylcholine. *c* (ACh) = 3.3×10^{-4} mol L^{-1}; *w* (H_2O_2) = 1.92 %; *c* (AChE) = 0.24 mg mL^{-1}, *c* (TMB) = 6.25×10^{-4} mol L^{-1}

Table. The results of the analysis of 0.5 % ethonium gel and 0.1 % solution according to the proposed procedure by the kinetic-spectrophotometric enzyme method

The substance analyzed	ET found ($\bar{x} \pm \Delta\bar{x}$), %[a]	*RSD*, %	The quality certificate data, %	Accuracy, (δ, %)[b]
0.5 % Ethonium gel, 50 mL, manufactured by APTEKA PAVLOVA Ltd (Odesa, Ukraine)	0.443 ± 0.014	2.54	0.445	–0.45
0.100 % Ethonium solution, 1000 mL, prepared *ex tempore*	0.098 ± 0.003	2.46	0.100	–2.00

Notes: [a] Mean of 5 measurements (*P* = 0.95); [b] $\delta = (\bar{x} - \mu) \times 100\ \% \times \mu^{-1}$; μ is the actual content of ET according to the Certificate

other two tangents *tg*α (Ach + ChE) and *tg*α (ACh), respectively, were determined.

The content of ethonium in the gel formulation, (*w*, %) was calculated by the formula:

$$w\ (\%, \text{w/w}) = \frac{0.00059574[tg\alpha(\text{X}) - tg\alpha(\text{Ach} + \text{ChE})]\times 100\ \%}{g\times[tg\alpha(\text{Ach}) - tg\alpha(\text{Ach} + \text{ChE})]}$$

where 0.00059574 – is the mass of Ethonium in a 10.00 mL aliquot of the Stock Solution of the drug, g;

g – is the mass of the ethonium gel sample taken for the analysis, g;

*tg*α (X) – is the relative reaction rate (the tangent of the angle of slope of the kinetic curve), in the working experiment with the sample solution of the drug studied (the Ach – ChE – Inh (X) + (H_2O_2 – TMB) system), min^{-1};

tgα (Ach + ChE) – is the relative reaction rate in the absence of the inhibitor (ET) (the tangent of the angle of slope of the kinetic curve) in the Ach – ChE + (H_2O_2 – TMB) system, min^{-1};

tgα (ACh) – is the relative reaction rate (the tangent of the angle of slope of the kinetic curve) in the working experiment without the use of the inhibitor and cholinesterase, (the Ach – ChE – Inh (WSS) + (H_2O_2 – TMB) system), min^{-1}.

■ Conclusions

This paper proves the possibility of using tetramethylbenzidine as a promising indicator substance for the quantitative determination of surface-active substances of the class of quaternary ammonium compounds.

The quantitative content of Ethonium as an active ingredient in the 0.5% gel formulation and in the 0.1% solution prepared *ex tempore* was determined by the enzyme-kinetic method using the effect of inhibiting the activity of the enzyme cholinesterase. The inhibition was estimated by the residual acetylcholine using the indicator reaction of the 3,3',5,5'-tetramethylbenzidine oxidation with peracetic acid formed in the perhydrolysis of acetylcholine. As a result, RSD did not exceed 2.5% with accuracy δ = –0.45….–2.00 % (δ < RSD). The LOQ value was 17 ng mL^{-1}.

References

1. 3,3′,5,5′-Tetramethylbenzidine. https://www.sigmaaldrich.com/UA/en/product/sigma/t0440 (accessed Oct 11, 2024).
2. Frey, A.; Meckelein, B.; Externest, D.; Schmidt, M. A. A stable and highly sensitive 3,3′,5,5′-tetramethylbenzidine-based substrate reagent for enzyme-linked immunosorbent assays. *Journal of Immunological Methods* **2000,** *233* (1), 47–56. https://doi.org/10.1016/S0022-1759(99)00166-0.
3. Sil, B. K.; Jamiruddin, M. R.; Haq, M. A.; Aekwattanaphol, N.; K, P. A.; Salendra, L.; Paliwal, H.; Paul, P. K.; Buatong, W.; Srichana, T. Nanolevel of detection of ascorbic acid using horse-radish peroxidase inhibition assay. *Heliyon* **2024,** *10* (10), e30715. https://doi.org/10.1016/j.heliyon.2024.e30715.
4. Huang, L.; Qin, Sh.; Xu, Y.; Shi, Ch.; Jin, Y.; Wang, Y. Enzyme-free colorimetric detection of uric acid on the basis of MnO_2 nanosheets-mediated oxidation of 3,3′,5,5′-tetramethylbenzidine. *Microchemical Journal*, **2023**, *190*, 108719. https://doi.org/10.1016/j.microc.2023.108719.
5. Zhang, Z.; Zhao, W.; Hu, C.; Guo, D.; Liu, Y. Colorimetric copper (II) ions detection in aqueous solution based on the system of 3′3′5′5′-tetramethylbenzidine and AgNPs in the presence of $Na_2S_2O_3$. *Journal of Science: Advanced Materials and Devices* **2022,** *7* (2), 100420. https://doi.org/10.1016/j.jsamd.2022.100420.
6. Lin, M.; Guo, Y.; Liang, Z.; Zhao, X.; Chen, J.; Wang, Y. Simple and fast determination of biothiols using Fe^{3+}-3,3′,5,5′-tetramethylbenzidine as a colorimetric probe. *Microchem. J.* **2019,** *147*, 319–323. https://doi.org/10.1016/j.microc.2019.03.049.
7. Chandra, S.; Singh, V. K.; Yadav, P. K.; Bano, D.; Kumar, V.; Pandey, V. K.; Talat, M.; Hasan, S. H. Mustard seeds derived fluorescent carbon quantum dots and their peroxidase-like activity for colorimetric detection of H_2O_2 and ascorbic acid in a real sample. *Anal. Chim. Acta* **2019,** *1054*, 145–156. https://doi.org/10.1016/j.aca.2018.12.024.
8. Xu, L.; Yang, B.; Guo, L. Oxidized 3,3′,5,5′-tetramethylbenzidine nanobelts enhance colorimetric sensing of H_2O_2. *Talanta* **2024,** *279*, 126584. https://doi.org/10.1016/j.talanta.2024.126584.
9. Baye, A. F.; Thi Nguyen, H.; Kim, H. Fe^0/Fe_3C-assisted Fe_3O_4 redox sites as robust peroxidase mimics for colorimetric detection of H_2O_2. *Sensors and Actuators B: Chemical* **2023,** *377*, 133097. https://doi.org/10.1016/j.snb.2022.133097.
10. Yin, X.; Liu, P.; Xu, X.; Pan, J.; Li, X.; Niu, X. Breaking the pH limitation of peroxidase-like $CoFe_2O_4$ nanozyme via vitriolization for one-step glucose detection at physiological pH. *Sensors and Actuators B: Chemical* **2021,** *328*, 129033. https://doi.org/10.1016/j.snb.2020.129033.
11. Song, G.; Zhang, Z.; Fauconnier, M.-L.; Li, C.; Chen, L.; Zheng, X.; Zhang, D. Bimodal single-atom iron nanozyme biosensor for volatile amine and food freshness detection. *Nano Today* **2023,** *53*, 102025. https://doi.org/10.1016/j.nantod.2023.102025.
12. Yu, K.; Li, M.; Chai, H.; Liu, Q.; Hai, X.; Tian, M.; Qu, L.; Xu, T.; Zhang, G.; Zhang, X. MOF-818 nanozyme-based colorimetric and electrochemical dual-mode smartphone sensing platform for *in situ* detection of H_2O_2 and H_2S released from living cells. *Chem. Eng. J.* **2023,** *451*, 138321. https://doi.org/10.1016/j.cej.2022.138321.
13. Cao, W.; Ju, P.; Wang, Z.; Zhang, Y.; Zhai, X.; Jiang, F.; Sun, C. Colorimetric detection of H2O2 based on the enhanced peroxidase mimetic activity of nanoparticles decorated Ce2(WO4)3 nanosheets. *Spectrochim. Acta, Part A* **2020,** *239*, 118499. https://doi.org/10.1016/j.saa.2020.118499.
14. Liu, Q.; Tang, P.; Xing, X.; Cheng, W.; Liu, S.; Lu, X.; Zhong, L. Colorimetry /SERS dual-sensor of H_2O_2 constructed *via* TMB–Fe_3O_4@ AuNPs. *Talanta* **2022,** *240*, 123118. https://doi.org/10.1016/j.talanta.2021.123118.
15. Blazheevskiy, M. Ye.; Dyadchenko, V. V. Kinetic determination of anticholinesterase compounds by a biochemical method by oxidizing reaction of p-phenetidine as display. *Farmatsevtychnyi zhurnal* **2004**, 2, 52-58.
16. Blazheyevskiy, M. Y.; Kovalska, O. V. The Quantitative Determination of Etonium by the Enzymatic Kinetic-Spectrophotometric Method. *J. Org. Pharm. Chem.* **2024**, *22*, 57-62. https://doi.org/10.24959/ophcj.24.304120.
17. *Derzhavna farmakopeia Ukrainy: v 3 tomakh*, 2 vydannia [The State Pharmacopoeia of Ukraine: in 3 volumes, 2nd ed., *in Ukrainian*]; State Enterprise "Ukrainian Scientific Pharmacopoeial Center for Quality of Medicines": Kharkiv, 2015; Vol. 1.
18. Blazheevskiy, M. E.; Kovalska, O. V.; Dyadchenko, V. V. (National University of Pharmacy, Kharkiv, Ukraine). Sposib vyznachennia aktyvnosti kholinesterazy krovi [Method for determining blood cholinesterase activity, *in Ukrainian*]. Ukraine Patent 117474, 26.06.2017.

Information about the authors:

Olena V. Kovalska (*corresponding author*), Ph.D. in Pharmacy, Associate Professor of Organization, Economy and Pharmacy Management Department, Institute of Advanced Training of Pharmacy Specialists of the National University of Pharmacy of the Ministry of Health of Ukraine; https://orcid.org/0000-0003-0113-7060; e-mail for correspondence: lena05021985@ukr.net; tel. +380970710498.

Mykola Ye. Blazheyevskiy, D.Sci. in Chemistry, Professor of the General Chemistry Department, National University of Pharmacy of the Ministry of Health of Ukraine; https://orcid.org/0000-0002-8032-347X.

Vladyslav V. **Diadchenko**, Ph.D. in Chemistry, Associate Professor, Military Institute of Armored Forces of the National Technical University "Kharkiv Polytechnic Institute". https://orcid.org/0000-0002-5552-3031.

ISSN 2308-8303 (Print) / 2518-1548 (Online)

Journal of Organic and Pharmaceutical Chemistry

Original Research

OPEN ACCESS
Freely available online on
http://ophcj.nuph.edu.ua

UDC 615.322:615.451.1:615.281

O. V. Kovregin[1], T. P. Osolodchenko[2], I. M. Vladymyrova[1]

[1] National University of Pharmacy of the Ministry of Health of Ukraine,
53 Hryhorii Skovoroda str., 61002 Kharkiv, Ukraine

[2] Mechnikov Institute of Microbiology and Immunology of the National Academy of Medical Sciences of Ukraine,
14/16 Hryhorii Skovoroda str., 61057 Kharkiv, Ukraine

The Study of the Antibacterial Effect of the Umbellate Wintergreen Extract

Abstract

The article presents the studies on the antimicrobial effect of the umbellate wintergreen herb extract. The study object was the umbellate wintergreen herb extract obtained with 50 % ethyl alcohol. The sensitivity of microbial strains to the umbellate wintergreen extract was determined by the well diffusion method in Mueller Hinton agar. Five test strains were used as test cultures: *Staphylococcus aureus* ATCC 6538 gram-positive microorganisms, *Bacillus subtilis* ATCC 6633 spore culture, gram-negative *Proteus vulgaris* ATCC 4636, *Escherichia coli* ATCC 25922, and *Pseudomonas aeruginosa* ATCC 9027. The antifungal effect was determined against *Candida albicans* ATCC 885-653. The antibacterial activity of the test substances was assessed by the diameter of the growth inhibition zones. It was found that the extract of the umbellate wintergreen herb exhibited antibacterial properties against test microorganisms where the diameters of the growth inhibition zones were at the level of 20–28 mm. The antibacterial effect of the umbellate wintergreen herb extract was also determined against such clinical strains of microorganisms as *Staphylococcus aureus* 124, *Enterococcus faecalis* 42, *Pseudomonas aeruginosa* 18, *Klebsiella pneumoniae* 64, *Candida albicans* 69. The growth inhibition zones were within 19–24 mm.

Keywords: umbellate wintergreen; liquid extract; antimicrobial effect

О. В. Коврегін[1], Т. П. Осолодченко[2], І. М. Владимирова[1]

*[1] Національний фармацевтичний університет Міністерства охорони здоров'я України,
вул. Григорія Сковороди, 53, м. Харків, 61002, Україна*

*[2] Інститут мікробіології та імунології імені І. І. Мечникова Національної академії медичних наук України,
вул. Григорія Сковороди, 14/16, м. Харків, 61057, Україна*

Дослідження антибактеріальної дії екстракту зимолюбки зонтичної

Анотація

У статті наведено результати дослідження антимікробної дії екстракту трави зимолюбки зонтичної. Об'єктом для дослідження обрали екстракт трави зимолюбки зонтичної, отриманий 50 % спиртом етиловим. Чутливість штамів мікроорганізмів до екстракту зимолюбки визначали методом колодязів на середовищі Мюллера-Хінтона. Як тест-культури використовували 5 тестових штамів: грампозитивні мікроорганізми *Staphylococcus aureus* АТСС 6538, спорову культуру *Bacillus subtilis* АТСС 6633, грамнегативні *Proteus vulgaris* АТСС 4636, *Escherichia coli* АТСС 25922 та *Pseudomonas aeruginosa* АТСС 9027. Антифунгальну дію з'ясовували щодо *Candida albicans* АТСС 885-653. Антибактеріальну активність дослідних речовин оцінювали за діаметром зон затримки зростання. З'ясовано, що екстракт трави зимолюбки зонтичної проявляв антибактеріальні властивості до тестових мікроорганізмів, де діаметри зон затримки зростання були на рівні 20–28 мм. Антибактеріальну дію екстракту зимолюбки також визначали щодо клінічних штамів мікроорганізмів: *Staphylococcus aureus* 124, *Enterococcus faecalis* 42, *Pseudomonas aeruginosa* 18, *Klebsiella pneumoniae* 64, *Candida albicans* 69. Зони затримки зростання були в межах 19–24 мм.

Ключові слова: зимолюбка зонтична; рідкий екстракт; антимікробна дія

Citation: Kovregin, O. V.; Osolodchenko, T. P.; Vladymyrova, I. M. Study of the Antibacterial Effect of Umbellate Wintergreen Extract. *Journal of Organic and Pharmaceutical Chemistry* **2024**, *22* (4), 43–47.
https://doi.org/10.24959/ophcj.24.324652
Received: *21 October 2024;* **Revised:** *4 December 2024;* **Accepted:** *5 December 2024*

Funding: The work was carried out within the framework of the research work of the National University of Pharmacy "Pharmacognostic studies of the medicinal plant raw material and the development of phytotherapeutic agents based on it" (the state registration number 0114U000946).
Conflict of interests: The authors have no conflict of interests to declare.

■ Introduction

Today, the use of the therapeutic potential of medicinal plants is considered a physiological method of prevention and treatment, which affects the normalization of metabolic processes and the restoration of the body's functional capabilities. Medicinal products based on plants can be used for a longer period of time, including in the treatment of chronic diseases [1].

Therefore, the role of phytotherapy in modern medicine is constantly growing, which is due, on the one hand, to the insignificant toxicity and biological safety for the human body of a large number of herbal medicines, and on the other hand, to the peculiarities of the clinical effectiveness of herbal medicines, namely: a wide therapeutic spectrum, a gradual increase in the severity of the expected clinical effect, a complex effect on various pathogenetic links of diseases, and relatively infrequent manifestations of side effects, even with prolonged use [1, 2].

At the present stage, pharmaceutical science continues to be enriched with information about the broad antibacterial significance of plant substances in human life, the possibility of their use for the treatment of diseases caused by microorganisms. Plants of the domestic flora deserve special attention in this aspect [3].

Thus, Chimaphila is a genus of flowering plants of the *Veresaceae* family, which has about 20 species. The Ukrainian name "umbellate" is due to the fact that representatives of its genus are found with green leaves in winter. Umbellate grows in the temperate and cold zones of the Northern Hemisphere, choosing dry pine and spruce forests for life. The species umbellate wintergreen, or wintergreen, a plant used by the natives of North America, is mainly grown in culture [4].

The beneficial properties of umbellate wintergreen were recognized by official medicine during the Civil War in the United States: field doctors used its diuretic and astringent effects. The plant was included in the US Pharmacopoeia in 1820. For centuries, this plant was one of the main medicines of rural residents of America [5, 6].

For the preparation of medicinal products, the herb umbellate wintergreen (*Herbae Chimaphiliae umbellate*) is used, which is harvested during the flowering period. Umbellate wintergreen belongs to unofficial medicinal plants.

The chemical composition is quite rich and specific. The herb contains hyperoside, kaempferol, arbutin, homoarbutin, avicularin, ericolin, the bitter compound ursone, about 20% amyrin, up to 5% tannins, as well as gum, resins, organic acids, mucus, etc. [7].

In alternative medicine, umbellate wintergreen is used as a means to improve diuresis, reduce blood sugar, disinfect the urinary tract, increase the excretion of chloride and nitrogenous salts from the body, improve digestion and appetite, normalize menstruation, etc. [8].

The infusion of the umbellate wintergreen herb is used to treat chronic kidney diseases (nephritis, albuminuria, hematuria), as well as to relieve inflammation and remove sand from the bladder, with urethral stricture, chronic gonorrheal urethritis, for the treatment of the prostate gland, gout, dyspepsia and diabetes mellitus. The infusion of umbellate wintergreen helps with dropsy and edema.

The infusion of umbellate wintergreen is also used as an astringent for inflammatory processes of the gastrointestinal tract and for respiratory tract catarrhs. In addition, the herb has a tonic and restorative effect in diseases caused by excessive physical exertion [6].

The aim of the work was to study the antimicrobial effect of the umbellate wintergreen herb extract on test and clinical strains of microorganisms.

■ Materials and methods

The study of antimicrobial action was conducted at the premises of the State Institution "Mechnikov Institute of Microbiology and Immunology" under the supervision of the head of the Laboratory of Biochemistry and Biotechnology, Candidate of Biology, senior researcher Osolodchenko T. P.

ISSN 2308-8303 (Print) / 2518-1548 (Online)

The study object was the extract of umbellate wintergreen herb. For the study, a dried umbellate wintergreen herb was used (manufacturer TM "Green Pharmacy", Zhytomyr). The umbellate wintergreen extract was obtained at the premises of the LLC "Experimental plant "GNCLS" (Kharkiv) in the period of May–June 2023. The umbellate wintergreen extract was obtained with 50% ethyl alcohol described in detail in the article [9].

The sensitivity of microbial strains to the umbellate wintergreen extract was determined in accordance with the methodological guidelines "Determination of the sensitivity of microorganisms to antibacterial drugs" (Order of the Ministry of Health of Ukraine dated 05.04.2007 No. 167) by the well diffusion method in Mueller Hinton agar ("HIMedia Laboratories Pvt. Ltd, India), which was prepared according to the manufacturer's instructions [10].

A suspension of microorganisms with a certain concentration of microbial cells (optical density) was prepared using a turbidity standard (0.5 units on the McFarland scale). A Densi-La-Meter device (manufactured by PLIVA-Lachema, Czech Republic; wavelength 540 nm) was used. The suspension was prepared according to the instructions for the device and the information sheet on innovations in the healthcare system No. 163-2006 "Standardization for the preparation of microbial suspensions", Kyiv [11]. Synchronization of cultures was carried out using low temperature (4 °C). The sensitivity of fungi was determined on the Sabouraud's medium. The sensitivity of the test substances was determined on two layers of the nutrient medium, which were poured into Petri dishes. The lower layer consisted of agar-agar (10 ml). On it, 3–6 sterile metal cylinders with a diameter of 8 mm and a height of 10 mm were installed. The upper layer (14 ml of the nutrient medium + 1 ml of the microbial solution 0.5 units on the McFarland scale) was poured around the cylinders, which consisted of a nutrient agar medium with the appropriate standard for daily cultivation of the microorganism. After solidification, the wells were removed with sterile tweezers, and the test substance (0.3 ml) was added to the wells. The antibacterial activity of the test substances was assessed by the diameter of the growth inhibition zones [12, 13]:

- 10 mm – a microorganism insensitive to the test substance;
- 10–15 mm – a microorganism weakly sensitive to the test substance;
- 15–25 mm – a microorganism sensitive to the test substance;
- 25 mm and above – a microorganism highly sensitive to the test substance.

■ Results and discussion

According to the results of the study, it was found that the extract of the umbellate wintergreen herb exhibited antibacterial properties against test microorganisms where the diameters of the growth inhibition zones were at the level of 20–28 mm (**Table 1**).

The results of the studies showed that the sample had antibacterial properties against all clinical strains of microorganisms where the growth inhibition zones were within 19–24 mm (**Table 2**).

The data in **Table 3** show that the sample (diluted with sterile distilled water) exhibits antibacterial properties against all test microorganisms in the dilution. High indicators remain in a dilution of 1:4 (from 20–28 mm to 18–24 mm), then the inhibition zones gradually decrease to 14–15 mm. In a dilution of 1:32, the antimicrobial activity is observed in *Staphylococcus aureus* ATCC 25923, *Escherichia coli* ATCC 25922, *Bacillus subtilis* ATCC 6633.

In **Table 4**, the results of the studies demonstrate that the sample (diluted with sterile distilled water) in a dilution of 1:4 exhibits antibacterial properties against all clinical strains of microorganisms. Dilutions of 1:8 and 1:16 show weak antibacterial activity (diameters of the growth inhibition zones are 12–15 mm). No antimicrobial activity is observed in a dilution of 1:32.

The study was conducted to determine the antibacterial activity of the sample for 28 days (**Tables 5** and **6**).

Table 1. The antibacterial effect of the sample on test microorganisms by the agar diffusion method

Sample	Diameters of the growth inhibition zones of microorganisms, mm					
	Staphylococcus aureus ATCC 25923	*Escherichia coli ATCC 25922*	*Pseudomonas aeruginosa ATCC 27853*	*Proteus vulgaris ATCC 4636*	*Bacillus subtilis ATCC 6633*	*Candida albicans ATCC 885-653*
Umbellate wintergreen extract	27, 27, 28	24, 25, 25	23, 24, 25	23, 24, 24	27, 28, 28	20, 21, 22

Table 2. The antibacterial effect of the sample on clinical microorganisms by the agar diffusion method

Sample	Diameters of the growth inhibition zones of microorganisms, mm				
	Staphylococcus aureus 124	*Enterococcus faecalis 42*	*Pseudomonas aeruginosa 18*	*Klebsiella pneumoniae 64*	*Candida albicans 69*
Umbellate wintergreen extract	23, 24, 24	22, 22, 23	20, 21, 21	22, 23, 22	20, 20, 19

Table 3. The antibacterial effect of the sample on test microorganisms in the diluted agar diffusion method

Sample with dilution	Diameters of the growth inhibition zones of microorganisms, mm					
	Staphylococcus aureus ATCC 25923	*Escherichia coli ATCC 25922*	*Pseudomonas aeruginosa ATCC 27853*	*Proteus vulgaris ATCC 4636*	*Bacillus subtilis ATCC 6633*	*Candida albicans ATCC 885-653*
Without dilution	27, 27, 28	24, 25, 25	23, 24, 25	23, 24, 24	27, 28, 28	20, 21, 22
1:2	27, 26, 26	23, 23, 23	21, 22, 22	21, 22, 21	24, 25, 25	18, 19, 19
1:4	24, 23, 23	21, 21, 22	20, 19, 18	20, 18, 19	23, 23, 22	17, 16, 16
1:8	21, 21, 20	19, 19, 20	17, 17, 17	17, 17, 17	20, 20, 19	15, 14, 14
1:16	19, 18, 19	17, 16, 16	14, 15, 15	14, 14, 14	17, 16, 16	13, 13, 12
1:32	15, 16, 16	14, 14, 14	growth	growth	14, 15, 15	growth

Table 4. The antibacterial effect of the sample on clinical microorganisms in the diluted agar diffusion method

Sample with dilution	Diameters of the growth inhibition zones of microorganisms, mm				
	Staphylococcus aureus 124	*Enterococcus faecalis 42*	*Pseudomonas aeruginosa 18*	*Klebsiella pneumoniae 64*	*Candida albicans 69*
Without dilution	23, 24, 24	22, 22, 23	20, 21, 21	22, 23, 22	20, 20, 19
1:2	21, 20, 20	19, 20, 20	19, 18, 19	20, 20, 19	18, 17, 18
1:4	17, 18, 18	17, 16, 17	17, 16, 17	18, 17, 17	16, 15, 16
1:8	15, 14, 14	14, 15, 15	15, 14, 15	15, 16, 16	13, 14, 14
1:16	13, 13, 14	13, 12, 12	13, 13, 12	13, 13, 13	12, 12, 12
1:32	growth	growth	growth	growth	growth

Table 5. The antibacterial activity of the sample for 28 days against test microorganisms

Sample of the umbellate wintergreen extract	Number of days	Diameters of the growth inhibition zones of microorganisms, mm					
		Staphylococcus aureus ATCC 25923	*Escherichia coli ATCC 25922*	*Pseudomonas aeruginosa ATCC 27853*	*Proteus vulgaris ATCC 4636*	*Bacillus subtilis ATCC 6633*	*Candida albicans ATCC 885-653*
	primary	27, 27, 28	24, 25, 25	23, 24, 25	23, 24, 24	27, 28, 28	20, 21, 22
	2 days	27, 27, 27	25, 25, 25	24, 24, 24	24, 24, 24	28, 28, 28	20, 21, 21
	7 days	27, 28, 28	24, 24, 25	23, 24, 24	24, 24, 23	27, 28, 28	22, 21, 21
	14 days	27, 27, 27	25, 24, 25	23, 23, 24	23, 23, 23	27, 27, 28	21, 21, 21
	28 days	27, 27, 28	25, 24, 24	23, 23, 24	24, 23, 23	27, 27, 27	20, 21, 20

Table 6. The antibacterial activity of the sample for 28 days against clinical microorganisms

Sample of the umbellate wintergreen extract	Number of days	Diameters of the growth inhibition zones of microorganisms, mm				
		Staphylococcus aureus 124	*Enterococcus faecalis 42*	*Pseudomonas aeruginosa 18*	*Klebsiella pneumoniae 64*	*Candida albicans 69*
	primary	23, 24, 24	22, 22, 23	20, 21, 21	22, 23, 22	20, 20, 19
	2 days	24, 24, 24	22, 22, 23	21, 21, 21	22, 22, 23	20, 20, 20
	7 days	24, 24, 24	23, 23, 22	21, 21, 21	23, 23, 22	19, 20, 20
	14 days	23, 23, 24	23, 22, 22	20, 21, 20	22, 22, 22	19, 19, 20
	28 days	24, 23, 23	21, 22, 23	20, 20, 21	22, 22, 21	20, 20, 19

ISSN 2308-8303 (Print) / 2518-1548 (Online)

The data in **Tables 5** and **6** indicate that the antibacterial properties of the sample of the umbellate wintergreen extract studied in relation to test and clinical strains of microorganisms do not change within 28 days.

Conclusions

It has been experimentally determined that the sample of the umbellate wintergreen herb liquid extract studied exhibits the antibacterial activity against test strains – *Staphylococcus aureus* ATCC 6538 gram-positive microorganisms, *Bacillus subtilis* ATCC 6633 spore culture, gram-negative *Proteus vulgaris* ATCC 4636, *Escherichia coli* ATCC 25922, and *Pseudomonas aeruginosa* ATCC 9027, *Candida albicans* ATCC 885-653 and clinical strains – *Staphylococcus aureus* 124, *Enterococcus faecalis* 42, *Pseudomonas aeruginosa* 18, *Klebsiella pneumoniae* 64, *Candida albicans* 69.

In dilution, the umbellate wintergreen extract exhibited antibacterial properties against all test microorganisms. High indicators remained in a dilution of 1:4 (from 20–28 mm to 18–24 mm), then the inhibition zones gradually decreased to 14–15 mm. In a dilution of 1:32, the antimicrobial activity was observed against *Staphylococcus aureus* ATCC 25923, *Escherichia coli* ATCC 25922, *Bacillus subtilis* ATCC 6633.

The results of the studies on clinical strains show that the sample in a dilution of 1:4 exhibits antibacterial properties against all clinical strains of microorganisms. Dilutions of 1:8 and 1:16 exhibit a weak antibacterial activity (diameters of the growth inhibition zones is 12–15 mm). No antimicrobial activity is observed in a dilution of 1:32.

References

1. Volianskyi, Yu. L.; Hrytsenko I. S.; Shyrobokov V. P. *Vyvchennya spetsyfichnoyi aktyvnosti protymikrobnykh likars'kykh zasobiv. Metodychni rekomendatsiyi MOZ Ukrayiny* [Study of the specific activity of antimicrobial drugs. Methodological recommendations of the Ministry of Health of Ukraine, *in Ukrainian*]; Zdorovja: Kyiv, 2004; 38 p.
2. Derzhavna farmakopeia Ukrainy, 1 vydannia, 4 dopovnennya [The State Pharmacopoeia of Ukraine, 1st ed., 4th amendment, *in Ukrainian*]; State Enterprise "Ukrainian Scientific Pharmacopoeial Center for Quality of Medicines": Kharkiv, 2011.
3. Manso, T.; Lores, M.; De Miguel, T. Antimicrobial Activity of Polyphenols and Natural Polyphenolic Extracts on Clinical Isolates. *Antibiotics* **2021**, *11* (1), 46. https://doi.org/10.3390/antibiotics11010046.
4. Sherstiuk, M. The Analysis of Vitality Structure of *Chimaphila Umbellata* (L.) W. Barton CENOpopulations in Forest Phytocenoses of the Novgorod-Sivers'k Polissia. *ScienceRise: Biological Science* **2017**, *0* (1 (4)), 40–45. https://doi.org/10.15587/2519-8025.2017.94019.
5. Galván, I. J.; Mir-Rashed, N.; Jessulat, M.; Atanya, M.; Golshani, A.; Durst, T.; Petit, P.; Amiguet, V. T.; Boekhout, T.; Summerbell, R.; Cruz, I.; Arnason, J. T.; Smith, M. L. Antifungal and Antioxidant Activities of the Phytomedicine Pipsissewa, *Chimaphila Umbellata*. *Phytochemistry* **2008**, *69* (3), 738–746. https://doi.org/10.1016/j.phytochem.2007.09.007.
6. Raja, S; Ravindranadh, K; Keerthi, T. A Complete Profile on *Chimaphila Umbellata* – Traditional Uses, Pharmacological Activites and Phytoconstituents. *ijp* **2014**, *6* (4), 464–470.
7. Kovregin, O.; Prokopiuk, V.; Lytkin, D.; Vladymyrova, I. Study of the Influence of the Extract of Pipsissewa on Cell Cultures. *ScienceRise: Pharmaceutical Science* **2024**, 3, 78–85. https://doi.org/10.15587/2519-4852.2024.307291.
8. Ali, U.; Khan, M. M.; Khan, N.; Haya, R. T.; Asghar, M. U.; Abbasi, B. H. *Chimaphila Umbellata*; a Biotechnological Perspective on the Coming-of-Age Prince's Pine. *Phytochem. Rev.* **2024**, *23* (1), 229–244. https://doi.org/10.1007/s11101-023-09880-1.
9. Yu, Y.; Elshafei, A.; Zheng, X.; Cheng, S.; Wang, Y.; Piao, M.; Wang, Y.; Jin, M.; Li, G.; Zheng, M. Chemical Constituents of Chimaphila Japonica Miq. *Biochemical Systematics and Ecology* **2021**, *95*, 104219. https://doi.org/10.1016/j.bse.2020.104219.
10. Marchenko, A.; Maslov, O.; Komisarenko, M.; Ponomarenko, S.; Osolodchenko, T.; Kolisnyk, S. Investigation Relationship between Antimicrobial, Antioxidant Activity and Biologically Active Compounds of Blackberry (Rubus Fruticocus L.) Fresh Fruit Liquid Extracts. *AMI* **2024**, 4, 3–10. https://doi.org/10.5281/zenodo.14275647.
11. Mogana, R.; Adhikari, A.; Tzar, M. N.; Ramliza, R.; Wiart, C. Antibacterial Activities of the Extracts, Fractions and Isolated Compounds from Canarium Patentinervium Miq. against Bacterial Clinical Isolates. *BMC Complement Med Ther* **2020**, *20* (1), 55. https://doi.org/10.1186/s12906-020-2837-5.
12. Zupanets, I. A.; Bezugla, N. P.; Otrishko, I. A.; Ursol, G. M. Modern medicines for herbal medicine: the view of a doctor and a pharmacist. *Ukrainian medical journal* **2023**, *158* (6), 3–8. https://doi.org/10.32471/umj.1680-3051.158.249269.
13. Nakaz Ministerstva okhorony zdorov"ya Ukrayiny vid 05.04.2007 r. No. 167 "Pro zatverdzhennya metodychnykh vkazivok "Vyznachennya chutlyvosti mikroorhanizmiv do antybakterial'nykh preparative" [Order of the Ministry of Health of Ukraine dated 05.04.2007 No. 167 "On approval of methodological guidelines "Determination of the sensitivity of microorganisms to antibacterial drugs", *in Ukrainian*]. https://zakon.rada.gov.ua/rada/show/v0167282-07#Text

Information about the authors:

Oleksiy V. Kovregin, Ph.D. student, Department of Clinical Pharmacology of the Institute for Advanced Training of Pharmacy Specialists, National University of Pharmacy of the Ministry of Health of Ukraine.

Tetyana P. Osolodchenko, Ph.D. in Biology, Head of the Laboratory of Biochemistry and Biotechnology, Senior Researcher, State Institution "Mechnikov Institute of Microbiology and Immunology".

Inna M. Vladymyrova (*corresponding author*), D.Sci. in Pharmacy, Professor, National University of Pharmacy of the Ministry of Health of Ukraine, Ukraine; https://orcid.org/0000-0002-4846-8839; e-mail for correspondence: i.vladimirova@nuph.edu.ua.

Journal of Organic and Pharmaceutical Chemistry

Original Research

OPEN ACCESS
Freely available online on
http://ophcj.nuph.edu.ua

UDC 66.011+542.712:547-304.4+547-316+547-302

V. V. Pendiukh[1,2], A. B. Rozhenko[1]

[1] Institute of Organic Chemistry of the National Academy of Sciences of Ukraine,
5 Akademik Kuhar str., 02094 Kyiv, Ukraine
[2] Enamine Ltd., 78, Winston Churchill str., 02094 Kyiv, Ukraine

Safe and Efficient Preparative Approach to Chiral α-Chloroketones Based on In-Flow Generated Diazomethane

Abstract

α-Chloroketones are valuable semi-products in the organic synthesis and pharmaceutical industry. In particular, they are used as key building blocks for the production of HIV protease inhibitors, such as atazanavir and darunavir. A well-known approach to their synthesis involves the Arndt-Eistert homologation, which relies on the formation of diazoketones followed by their halogenation. However, this process poses significant safety and implementation challenges due to the use of diazomethane (CH_2N_2). The high toxicity, carcinogenicity, and explosion hazard of CH_2N_2 limit its large-scale application and require design of specialized laboratory setups to reduce the risks.

In this study, we present a new continuous-flow diazomethane generator that integrates the membrane technology with a traditional flow reactor setup for a safe and efficient generation of CH_2N_2. The flow technology eliminates the need for storage and handling of diazomethane, while facilitating its direct use in multistep synthesis. As a proof-of-concept, we demonstrate its application in the three-step synthesis of chiral α-chloroketones from *N*-protected amino acids. The approach newly developed offers a safer, more efficient, and scalable alternative to conventional diazomethane-based processes, paving the way for broader industrial applications.

Keywords: flow processes; diazomethane; α-chloroketones; diazoketones; halomethylation; chiral compounds

В. В. Пендюх[1,2], О. Б. Роженко[1]

*[1] Інститут органічної хімії Національної академії наук України,
вул. Академіка Кухаря, 5, м. Київ, 02094, Україна*
[2] ТОВ НВП «Єнамін», вул. Вінстона Черчилля, 78, м. Київ, 02094, Україна

Безпечний та ефективний препаративний підхід до хіральних α-хлорокетонів на основі діазометану, що синтезується в проточному режимі

Анотація

α-Хлорокетони є цінними напівпродуктами в органічному синтезі та у фармацевтичній промисловості. Зокрема, їх використовують як ключові будівельні блоки для отримання інгібіторів ВІЛ протеази, як-от атазанавір і дарунавір. Широко відомий підхід до їх синтезу передбачає гомологізацію Арндта-Айстерта, яка базується на утворенні діазокетонів із подальшим галогенуванням. Однак цей процес створює значні проблеми з безпекою та впровадженням через використання діазометану (CH_2N_2). Висока токсичність, канцерогенність і вибухонебезпечність CH_2N_2 обмежують його широкомасштабне застосування та вимагають створення спеціального лабораторного устаткування для зниження ризиків.

У цьому дослідженні ми репрезентуємо новий проточний генератор діазометану, який об'єднує мембранні технології з класичним реактором проточного синтезу. Ця система забезпечує безпечне та ефективне генерування CH_2N_2, усуваючи потребу у його зберіганні та транспортуванні й одночасно полегшуючи його пряме використання в багатоетапному синтезі. Як доказ концепції ми демонструємо застосування реактора в тристадійному синтезі хіральних α-хлорокетонів із *N*-захищених амінокислот. Нещодавно розроблений підхід пропонує безпечнішу, ефективнішу та придатну до масштабування альтернативу звичайним процесам на основі діазометану, прокладаючи шлях до його більш широкого промислового застосування.

Ключові слова: потокові процеси; діазометан; α-хлорокетони; діазокетони; галогенування; хіральні сполуки

ISSN 2308-8303 (Print) / 2518-1548 (Online)

Citation: Pendiukh, V. V.; Rozhenko, A. B. Safe and efficient preparative approach to chiral α-chloroketones based on in-flow generated diazomethane. *Journal of Organic and Pharmaceutical Chemistry* **2024**, *22* (4), 48–55.
https://doi.org/10.24959/ophcj.24.324406
Supporting information: Copies of ^{1}H and ^{13}C NMR spectra.
Received: *19 September 2024*; **Revised:** *10 December 2024*; **Accepted:** *13 December 2024*

Funding: The work was funded by the National Research Foundation of Ukraine (projects 0120U104008 and 0124U003838).
Conflict of interests: The authors have no conflict of interests to declare.

■ Introduction

Over the past two decades, a series of highly potent, orally bioavailable HIV protease inhibitors have been developed and approved for clinical use [1, 2]. These inhibitors, including atazanavir and darunavir, play a crucial role in highly active antiretroviral therapy (HAART) and are listed by the World Health Organization as essential medicines [3]. Structurally, they belong to the class of peptidomimetics, mimicking natural substrates by incorporating non-hydrolyzable hydroxyethylene or hydroxyethylamine moieties at the protease cleavage site (**Figure 1**). Notably, most FDA-approved HIV protease inhibitors contain a chiral amino alcohol core, which is typically introduced through a nucleophilic ring-opening of the corresponding *N*-protected aminoepoxide [4].

A well-established route for preparing these chiral semi-products involves the transformation of *N*-protected amino acids into α-haloketones, followed by a selective reduction to produce chiral amino epoxides or amino alcohols. Among various methods available for the α-haloketone formation, one of the most straightforward and cost-effective strategies relies on the halomethylation using diazomethane (CH_2N_2) (**Scheme 1**) [5]. This method, involving the condensation of an activated amino acid with CH_2N_2 followed by the α,α-substitution with a hydrogen halide, is known due to its efficiency and diastereoselectivity [6]. However, diazomethane, an extremely versatile reagent in organic synthesis, is also highly toxic, volatile, carcinogenic, and prone to explosive decomposition, which pose significant limitations on its large-scale implementation. Its sensitivity to heat, light, and mechanical shock necessitates careful handling, and even the use of specialized equipment does not guarantee the avoidance of accidents [7]. Therefore, the industrial-scale production of CH_2N_2 could be provided using batch

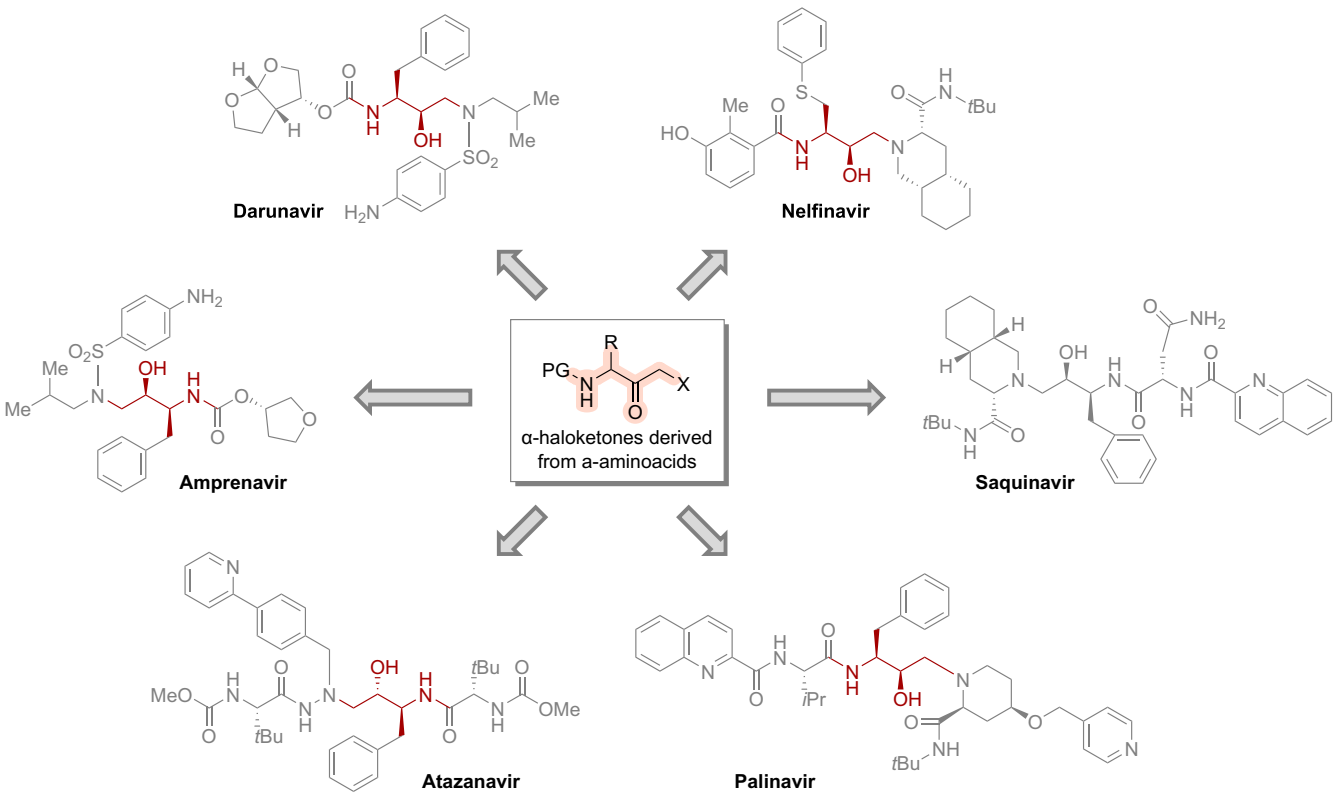

Figure 1. HIV protease inhibitors derived from α-haloketones

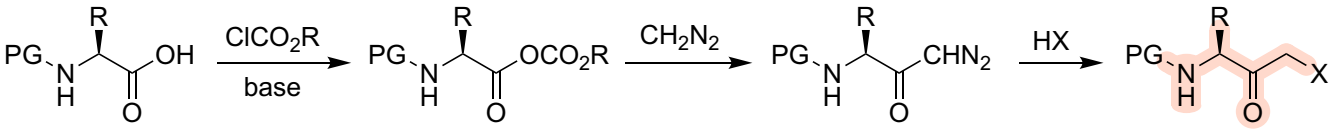

Scheme 1. The diazomethane-based synthesis of α-haloketones from N-protected chiral amino acids

and continuous flow processes, with notable examples including the Aerojet process and other industrial setups utilizing the phase-transfer catalysis or continuous nitrogen stream transport [8]. Despite these advancements, the large-scale application of diazomethane remains restricted due to the challenges of safe storage, transport, and handling. To overcome these limitations, recent developments in flow chemistry have introduced safer, on-demand CH_2N_2 generation methods, integrating the membrane separation technology to minimize the risks associated with its accumulation [9, 10]. Continuous flow systems have long been employed for the large-scale chemical production and are being increasingly adapted for fine chemical and pharmaceutical syntheses [11]. These systems enable controlled multistep transformations, while ensuring greater safety, reproducibility, and efficiency.

In this study, we present the development of a procedure based on a continuous-flow generated diazomethane, applied to the three-step synthesis of α-chloroketones from *N*-protected amino acids. This approach eliminates the need for diazomethane storage and handling while enabling a scalable and efficient synthesis of some key chiral building blocks without racemization. The full continuous process demonstrates high yields and safety improvements, making it a viable alternative to traditional batch methods for producing α-haloketones in pharmaceutical applications.

■ Results and discussion

Generation of Anhydrous Diazomethane

Access to anhydrous diazomethane (CH_2N_2) is essential for the modified Arndt-Eistert reaction, which serves as a key step in the synthesis of chiral amino alcohols – crucial semi-products in the production of HIV protease inhibitors. Ensuring the complete removal of water from CH_2N_2 is critical as even trace moisture can affect the reaction efficiency and selectivity.

Previous studies have employed the reaction between CH_2N_2 and activated organic acids as an indirect method to verify anhydrous conditions [12]. However, our investigations revealed that this technique lacks the required sensitivity. When benzoyl chloride was exposed to CH_2N_2 under controlled conditions, the expected formation of benzoic acid (a marker for water presence) was only detectable by GC-FID when at least 50 vol% of water was added.

To obtain more accurate moisture measurements, we turned to the Karl-Fischer titration, a highly sensitive technique for water quantification [12]. In our setup, a 0.1 M CH_2N_2 solution in the THF:CH_2Cl_2 mixture was generated and subsequently quenched with benzoic acid. A reference Karl-Fischer titration was performed on a pure benzoic acid solution, and this baseline value was subtracted from the reading obtained for the quenched CH_2N_2 solution. The final titration results confirmed that our system successfully produces anhydrous CH_2N_2, with a measured water content of 347 ± 7 ppm, demonstrating that the membrane-based diazomethane generation effectively prevents the moisture contamination.

By ensuring a continuous supply of high-purity CH_2N_2, our method provides a safe, efficient, and scalable alternative to conventional batch approaches, further enhancing its applicability in multistep synthetic processes.

Synthesis of α-Chloroketones

The synthesis of α-chloroketones was carried out *via* a well-established three-step pathway comprising the activation of the *N*-protected amino acid, the formation of the diazoketone semi-product, and the selective halogenation to yield the final product. This methodology, originally optimized for the α-bromoketone synthesis in the previous study [10], was successfully adapted for the α-chloroketone formation by substituting hydrogen bromide (HBr) with hydrogen chloride (HCl) as a halogenating agent.

Step 1: The Activation of N-Protected Amino Acids

In the first step, *N*-protected amino acids **1** were converted into reactive mixed anhydrides **1-act** by the treatment with ethyl chloroformate in the presence of a base, such as triethylamine or *N*-methylmorpholine, in an anhydrous solvent (**Figure 2**, *A*). The procedure was performed under mild reaction conditions that avoided excessive heating or drastic pH changes (*see* **Experimental section**), and it was compatible with

ISSN 2308-8303 (Print) / 2518-1548 (Online)

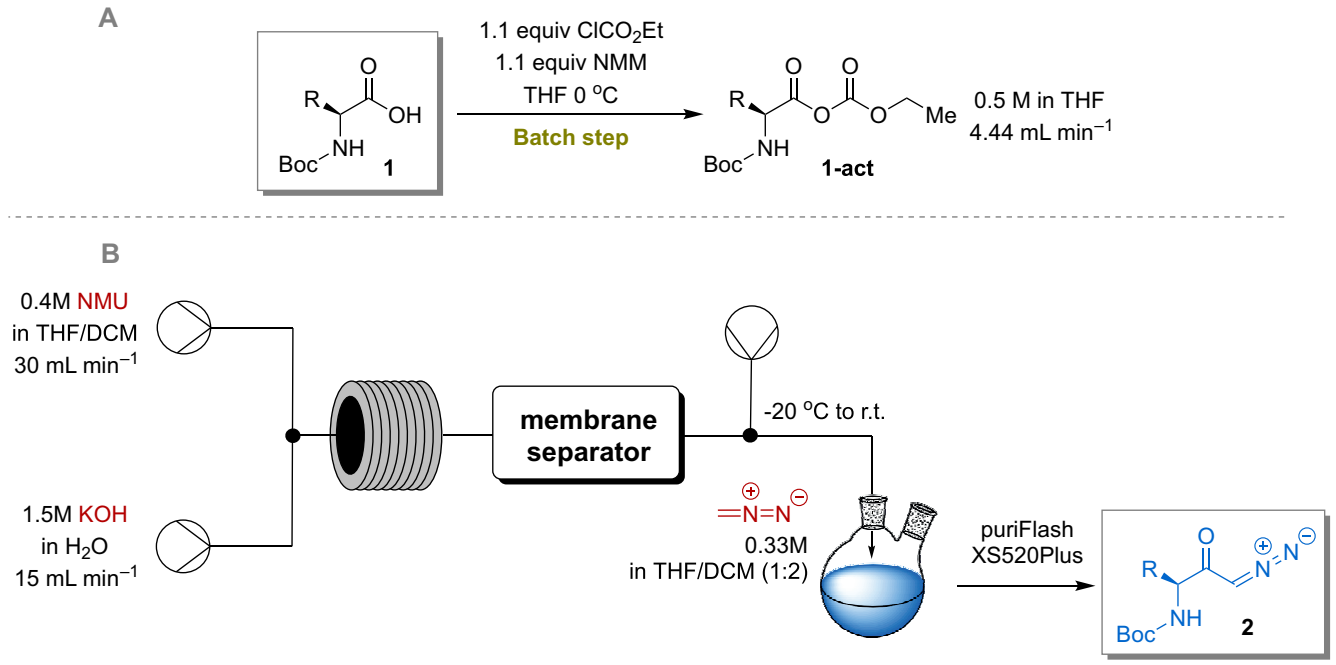

Figure 2. The intermediate synthesis (A) and reactor setup (B)

a broad range of amino acid protecting groups, thereby offering flexibility in the precursor selection. Moreover, the reaction proceeded with a high conversion efficiency, which minimized side reactions and the by-product formation.

Step 2: The Formation of the α-Diazoketone

Once the mixed anhydride was generated, it reacted with anhydrous diazomethane (CH_2N_2) under carefully controlled conditions. By employing a continuous-flow CH_2N_2 generator (**Figure 2**, *B*), a high-purity stream of diazomethane was directed into the reaction mixture, ensuring a rapid and efficient conversion of the mixed anhydride to the corresponding α-diazoketone. The continuous-flow approach enhanced safety by eliminating the need for accumulation and storage of a large amount of diazomethane, provided a high reproducibility through the consistent conversion efficiency across various substrates, and improved the reaction kinetics by facilitating a rapid formation of the diazoketone. The formation of the diazoketone intermediates was confirmed *via* ^{1}H and ^{13}C NMR spectroscopy, with characteristic peaks in agreement with literature reports for similar compounds [9, 10].

Step 3: The Halogenation to α-Chloroketones

In the final step, α-diazoketone semi-products were selectively converted into the corresponding α-chloroketones using aqueous HCl. Chlorination, unlike bromination where rapid elimination side reactions can occur, benefited from the lower nucleophilicity of chloride ions, which enhanced selectivity. Initial attempts focused on developing a fully continuous α-chloroketone synthesis using a flow reactor. However, challenges emerged since the high surface tension of the aqueous HCl phase impeded a reliable flow control, which in turn led to uncontrolled increases in solvent levels. Drawing on insights from previous work, the process was modified by transitioning to a conventional batch synthesis approach. In this modified protocol, a pure isolated diazoketone obtained *via* the continuous-flow process in *Step 2* was used as the starting material for the halogenation. The isolated diazoketone reacted with 3 equiv. of the conc. HCl at room temperature. The complete conversion was achieved within 10 minutes of stirring. It is important to note that increasing the HCl quantity beyond 3 equiv. resulted in the unwanted deprotection of α-chloroketone, underscoring the necessity for the precise reagent control. The final α-chloroketones were isolated with purities exceeding 98%, as confirmed by the HPLC analysis.

The chloroketones prepared by this protocol are shown in **Figure 3** (*B*). The protocol was easily scaled up to 100 g of chloroketone in a single synthetic run. We developed individual protocols for the optical purity control based on the chiral HPLC for all chiral representatives. As a result, we found that the optical purity of the starting amino acids was retained for all chloroketones. It also proves the preservation of the absolute configuration for the intermediate diazoketones.

Comparison with Alternative Methods

The performance of the elaborated method was evaluated against other reported approaches based on the diazoketone formation and

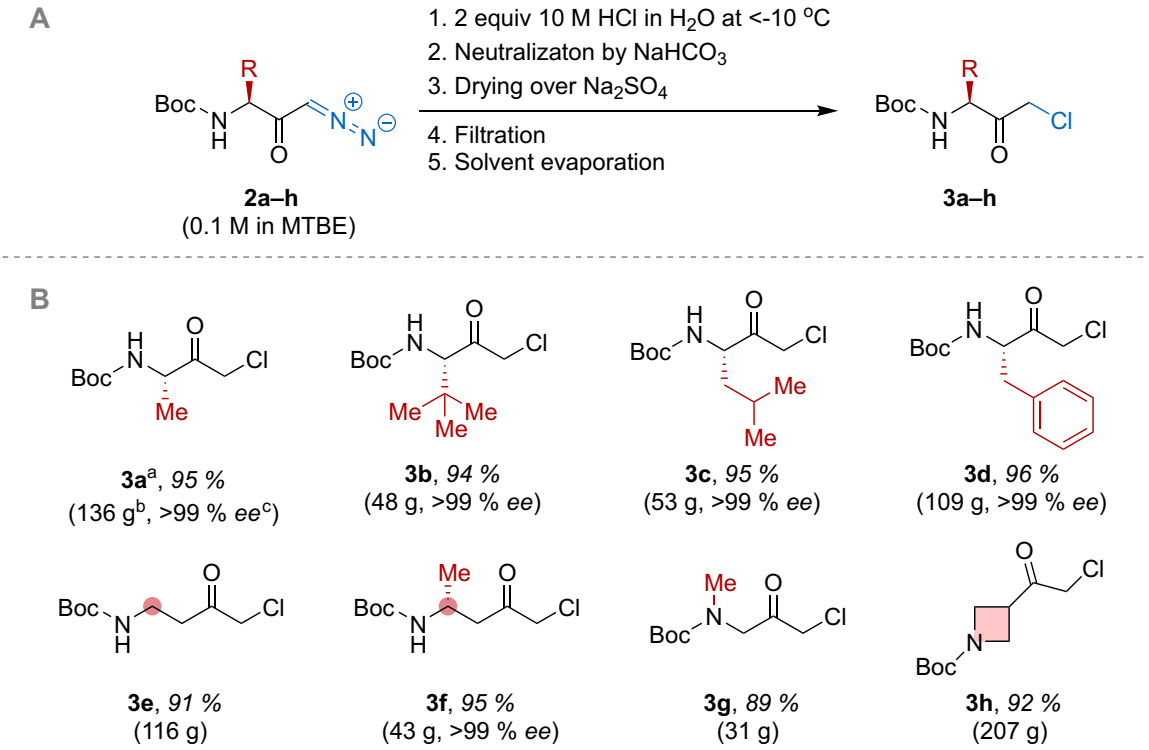

Figure 3. The general scheme for the preparation of chloroketones from diazoketones (*A*); the scope of chloroketones **3a-h** (*B*) prepared. [a] For all chiral products, both enantiomers were independently synthesized (*see* **Experimental section**). [b] The amount of the compound obtained. [c] Measured using chiral HPLC.

halogenation time, yield, purity, and overall safety profile. The classic batch method, which employs pre-made CH_2N_2, typically requires 2–3 hours for the halogenation, with yields of products in the range of 65–75%, the purity between 90–95% and is associated with a high safety risk. The tube-in-tube method described by *Pinho et al.* [13] uses a continuous diazoketone formation and achieves the halogenation in 1–2 hours, with yields of 75–85% and the purity of 95–98%, presenting a moderate safety profile. In contrast, our method, which combines a continuous CH_2N_2 generation in *Step 2* with the batch halogenation in *Step 3*, achieves the diazoketone formation within 30–60 minutes and the halogenation in 10 minutes, resulting in yields of 85–92% and the purity higher than 98% while offering a high safety profile.

■ Conclusion

By adapting our bromoketone synthesis method previously reported for the chloroketone preparation, we have developed a preparative process that combines the continuous-flow generation of α-diazoketones with the subsequent batch halogenation step. This hybrid approach enhances scalability and reproducibility while maintaining a high safety profile by eliminating the need for the hazardous diazomethane accumulation, storage and handling. Taking into account the significant role of α-haloketones in pharmaceutical applications, our methodology represents a noteworthy advance in flow chemistry and a new synthetic employment of easily available diazo compounds.

■ Experimental section

General

The solvents were purified according to standard procedures. All starting materials were obtained from Enamine Ltd. ^{1}H and ^{13}C NMR spectra were recorded on a Bruker Avance 500 spectrometer (500 MHz for ^{1}H and 126 MHz for ^{13}C nuclei) and a Varian Unity Plus 400 spectrometer (400 MHz for ^{1}H and 101 MHz for ^{13}C nuclei). Tetramethylsilane was used as an internal standard. Melting points were measured on the MPA100 OptiMelt automated melting point system. HPLC analyses were performed on an Agilent 1200 chromatograph. A preparative chromatograph puriFlash XS520Plus with a column containing 800 g of silica gel was used for diazoketones purification.

General Methods for the Synthesis of Compounds

The **NMU** precursor was prepared by nitrosation of methylurea using the standard protocol [14].

ISSN 2308-8303 (Print) / 2518-1548 (Online)

The Synthesis of Mixed Anhydrides

In a three-necked flask equipped with a thermometer, a magnetic stirrer, a dropping funnel, and a water seal, 1 equiv. of methylmorpholine was added. The reaction mixture was cooled below −10 °C and then 1 equiv. of ethyl chloroformate was slowly added, keeping the temperature in the flask below 0 °C. The reaction mixture was stirred at this temperature for 30 min. The precipitate formed was filtered off, and the solution of the mixed anhydride was used in the further transformations without isolation.

The Synthesis of Diazoketones

The procedure of diazomethane generation

Solutions of NMU (0.37 M, CH_2Cl_2/THF = 2:1) and KOH (1.5 M, H_2O) were injected into the reaction unit through two channels of the reactor pump unit in a molar ratio of 1:2 (30 and 15 mL min^{-1}). The combined stream passed through the reaction column and then through the membrane separator. The aqueous waste stream leaving the outer tube of the separator was directed into a flask containing acetic acid to decompose any residue of diazomethane in the aqueous solution. The resulting organic solution of diazomethane was transferred from the inner tube to a reactor containing a substrate. The flux of diazomethane (0.45 mol h^{-1}) was directed into a three-necked flask equipped with a magnetic stirrer and an electronic thermometer. The substrate flow kept in a molar ratio of 1:2 in relation to diazomethane was fed into the reactor with a delay of 1 min. After the entire amount of the substrate was added, the reactor was switched to wash the mode, and the reaction mixture was stirred for an additional 2 h. The system was able to operate continuously for 5–6 h (stationary conditions) generating and consuming up to 1.8 mol of diazomethane. After evaporation of solvents under vacuum, diazoketone was purified using a preparative chromatograph puriFlash XS520Plus and hexane with a gradient addition of ethyl acetate up to 30% as an eluent. The total amount of diazoketone after the isolation and purification exceeded 1 mol.

The synthesis of chloroketones

Diazoketone was dissolved in MTBE in a three-necked flask equipped with a thermometer, a magnetic stirrer, a dropping funnel and a water seal. The solution was cooled with ice to a temperature below 10 °C. Two (2) equiv. of the concentrated HCl was slowly added, keeping the temperature in the flask below 10 °C. The reaction mixture was stirred at this temperature for 45 min. The resulting solution was neutralized with aq. $NaHCO_3$ to pH = 7–8, washed with water, dried over Na_2SO_4 and filtered. The solvent was evaporated under reduced pressure. The purity of the chloroketones prepared was >95%, no further purification was necessary.

(*S*)-*tert*-Butyl (4-Chloro-3-oxobutan-2-yl)-carbamate (3a)

A white powder. Yield – 136 g (*95%*). M. p. = 59–60 °C. Anal. Calcd for $C_9H_{16}ClNO_3$, %: C 46.85, H 6.94, N 5.26, Cl 15.40. Found, %: C 46.63, H 6.93, N 5.12, Cl 15.07. ^{1}H NMR (400 MHz, $CDCl_3$), δ, ppm: 1.41 (d, *J* = 7.2 Hz, 3H), 1.46 (s, 9H), 4.08 (d, *J* = 4.0 Hz, 2H), 4.50–4.67 (m, 1H), 5.10 (s, 1H). ^{13}C NMR (151 MHz, $CDCl_3$), δ, ppm: 17.77, 28.28, 31.61, 53.22, 80.30, 155.16, 201.53. $[\alpha]_D$(25°C) = −54.2 (*c* = 0.5, CH_3OH).

(*R*)-*tert*-Butyl (4-Chloro-3-oxobutan-2-yl)-carbamate (3a′)

A white powder. Yield – 37 g (*94%*). M. p. = 59–60 °C. $[\alpha]_D$ = +54.2 (*c* = 0.5, CH_3OH).

(*S*)-*tert*-Butyl (1-Chloro-4,4-dimethyl-2-oxopentan-3-yl)-carbamate (3b)

A white crystalline powder. Yield – 48 g (*94%*). M. p. = 82 °C. Anal. Calcd for $C_{12}H_{22}ClNO_3$, %: C 52.84, H 8.07, N 5.14, Cl 13.03. Found, %: C 52.51, H 7.88, N 4.92, Cl 13.13. ^{1}H NMR (400 MHz, $CDCl_3$), δ, ppm: 0.98 (s, 9H), 1.41 (s, 9H), 4.05–4.23 (m, 2H), 4.30 (d, *J* = 9.0 Hz, 1H), 5.07 (d, *J* = 9.1 Hz, 1H). ^{13}C NMR (151 MHz, $CDCl_3$), δ, ppm: 26.5, 28.3, 34.6, 36.2, 64.0, 80.3, 155.5, 201.5. $[\alpha]_D$(25°C) = −47.0 (c = 0.5, CH_3OH).

(*R*)-*tert*-Butyl (1-Chloro-4,4-dimethyl-2-oxopentan-3-yl)-carbamate (3b′)

A white powder. Yield – 25 g (*94%*). M. p. = 82 °C. $[\alpha]_D$(25 °C) =+48.1 (c = 0.5, CH_3OH).

(*R*)-*tert*-Butyl (1-Chloro-5-methyl-2-oxohexan-3-yl)-carbamate (3c)

A white powder. Yield – 53 g (*95%*). M. p. = 76 °C. Anal. Calcd for $C_{12}H_{22}ClNO_3$, %: C 52.84, H 8.07, N 5.14, Cl 13.03. Found, %: C 52.53, H 7.89, N 4.95, Cl 13.17. ^{1}H NMR (400 MHz, $CDCl_3$), δ, ppm: 0.98 (t, *J* = 6.7 Hz, 6H), 1.46 (s, 10H), 1.56–1.66 (m, 1H), 1.68–1.84 (m, 1H), 3.98–4.24 (m, 2H), 4.55 (s, 1H), 4.92 (d, *J* = 8.0 Hz, 1H). ^{13}C NMR (126 MHz, $CDCl_3$), δ, ppm: 21.1, 22.7, 24.5, 27.8, 31.8, 40.2, 55.6, 79.9, 155.0, 201.3. $[\alpha]_D$(25°C) = −45.4 (c = 1.0, CH_3OH).

(*R*)-*tert*-Butyl (1-Chloro-5-methyl-2-oxohexan-3-yl)-carbamate (3c′)

A white powder. Yield – 23 g (*95%*). $[\alpha]_D$(25°C) = +44.5 (c = 1.0, CH_3OH).

(*S*)-*tert*-Butyl (4-Chloro-3-oxo-1-phenylbutan-2-yl)-carbamate (3d)

A white powder. Yield – 109 g (*96%*). M. p. = 101 °C. Anal. Calcd for $C_{15}H_{20}ClNO_3$, %: C 58.73, H 6.52, N 4.57, Cl 11.58. Found, %: C 58.63, H 6.50, N 4.55, Cl 11.38. ^{1}H NMR (400 MHz, $CDCl_3$), δ, ppm: 1.42 (s, 9H), 3.08 (tt, *J* = 20.7, 10.0 Hz, 2H), 3.79–4.13 (m, 2H), 4.73 (q, *J* = 6.5, 6.1 Hz, 1H), 5.04 (s, 1H), 7.13–7.23 (m, 2H), 7.27 (s, 1H), 7.33 (q, *J* = 9.0, 7.9 Hz, 2H). ^{13}C NMR (151 MHz, $CDCl_3$), δ, ppm: 28.2, 33.2, 37.9, 58.5, 80.5, 127.3, 128.9, 129.1, 135.8, 155.2, 200.8. $[\alpha]_D$(25°C) = −43.7 (c = 0.5, CH_3OH).

(*R*)-*tert*-Butyl (4-Chloro-3-oxo-1-phenylbutan-2-yl)-carbamate (3d′)

A white powder. Yield – 29 g (*97%*). $[\alpha]_D$(25°C) = +55.4 (c = 0.5, CH_3OH).

***tert*-Butyl (4-Chloro-3-oxobutyl)carbamate (3e)**

A colorless liquid. Yield – 116 g (*91%*). Anal. Calcd for $C_9H_{16}ClNO_3$, %: C 46.85, H 6.94, N 6.07, Cl 15.40. Found, %: C 46.71, H 6.90, N 6.17, Cl 15.37. ^{1}H NMR (400 MHz, $CDCl_3$), δ, ppm: 1.44 (s, 9H), 2.91 (t, *J* = 5.8 Hz, 2H), 3.37–3.51 (m, 2H), 3.91 (s, 2H), 4.96 (s, 1H). ^{13}C NMR (126 MHz, $CDCl_3$), δ, ppm: 27.9, 33.6, 34.9, 39.6, 79.0, 155.4, 201.0.

(S)-tert-Butyl (5-Chloro-4-oxopentan-2-yl)carbamate (3f)

A yellow powder. Yield – 43 g (*95%*). M. p. = 73 °C. Anal. Calcd for $C_{10}H_{18}ClNO_3$, %: C 49.08, H 7.36, N 5.73, Cl 14.52. Found, %: C 49.18, H 7.27, N 5.77, Cl 14.12. ^{1}H NMR (400 MHz, $CDCl_3$), δ, ppm: 1.23 (d, *J* = 7.0 Hz, 3H), 1.43 (s, 9H), 2.86 (d, *J* = 5.8 Hz, 2H), 3.92 (q, *J* = 12.6 Hz, 2H), 4.02–4.15 (m, 1H), 4.78 (s, 1H). ^{13}C NMR (126 MHz, $CDCl_3$), δ, ppm: 20.1, 27.9, 34.0, 43.0, 45.7, 79.1, 154.6, 200.1. $[\alpha]_D$(25°C) = −16.8 (c = 0.5, CH_3OH).

(*R*)-*tert*-Butyl (5-Chloro-4-oxopentan-2-yl)carbamate (3f′)

A yellow powder. Yield – 200 g (*95%*). M. p. = 73 °C. $[\alpha]_D$(25°C) = +16.1 (c = 0.5, CH_3OH).

***tert*-Butyl (3-Chloro-2-oxopropyl)(methyl)carbamate (3g)**

An orange oil. Yield – 31 g (*89%*). Anal Calcd for $C_9H_{16}ClNO_3$, %: C 46.85, H 6.94, N 6.07, Cl 15.40. Found, %: C 46.74, H 7.02, N 6.17, Cl 15.37. ^{1}H NMR (400 MHz, $CDCl_3$), δ, ppm: 1.46 (d, *J* = 18.8 Hz, 9H), 2.94 (d, *J* = 7.7 Hz, 3H), 3.91 (d, *J* = 16.9 Hz, 2H), 4.22 (d, *J* = 18.2 Hz, 2H). ^{13}C NMR (151 MHz, $CDCl_3$), δ, ppm: 24.1*, 27.0, 28.2*, 28.3, 30.7*, 31.5, 35.9*, 36.4, 55.9*, 56.3, 80.5*, 80.7, 156.1, 198.4 (rotamers).

***tert*-Butyl 3-(2-Chloroacetyl)azetidine-1-carboxylate (3h)**

A white crystalline powder. Yield – 207 g (*92%*). M. p. = 73 °C. Anal. Calcd for $C_{10}H_{16}ClNO_3$, %: C 49.48, H 6.60, N 5.77, Cl 14.64. Found, %: C 49.45, H 6.50, N 5.72. Cl 14.63. ^{1}H NMR (400 MHz, $CDCl_3$), δ, ppm: 1.44 (s, 9H), 3.82 (pd, *J* = 7.5, 1.2 Hz, 1H), 3.91 (s, 2H), 4.08 (s, 2H), 4.10 (s, 2H). ^{13}C NMR (126 MHz, $CDCl_3$), δ, ppm: 28.3, 32.5, 36.6, 51.1, 80.0, 156.0, 200.2.

References

1. Witte, J. M.; Ayim, E.; Sams, C. J.; Service, J. B.; Kant, C. C.; Bambalas, L.; Wright, D.; Carter, A.; Moran, K.; Rohrig, I. G.; Ferrence, G. M.; Hitchcock, S. R. Diastereoselective Synthesis of the HIV Protease Inhibitor Darunavir and Related Derivatives via a Titanium Tetrachloride-Mediated Asymmetric Glycolate Aldol Addition Reaction. *J. Org. Chem.* **2024**, *89* (13), 9569–9585. https://doi.org/10.1021/acs.joc.4c01057.
2. Singh, G.; Malik, P.; Thakur, Y.; Khurana, S.; Sharma, S.; Sushma; Ritika; Kumar, T. J. D.; Singh, K. N. Development of a Triazole-Linked Bis-Organosilane Compound as Dual-Function Agent: Sensing of Al3+ Ion in Aqueous Environments and Inhibition of HIV-1 Protease. *Journal of Molecular Structure* **2025**, *1319*, 139572. https://doi.org/10.1016/j.molstruc.2024.139572.
3. Banik, B. K.; Das, A. Monocyclic Beta-Lactams: Stereocontrolled Synthesis by Diverse Methods. *Chemistry and Biology of Beta-Lactams*; CRC Press: Boca Raton, 2024. https://doi.org/10.1201/9780367816339.
4. Ahmad, R.; Choudhary, M. Design and Synthesis of Copper(ii) and Nickel(ii) Complexes as Potential Inhibitors against SARS-CoV-2 Viral RNA Binding Protein and Omicron RBD Protein. *New J. Chem.* **2024**, *48* (34), 15053–15076. https://doi.org/10.1039/D4NJ02753A.
5. Laporte, A. A. H.; Masson, T. M.; Zondag, S. D. A.; Noël, T. Multiphasic Continuous-Flow Reactors for Handling Gaseous Reagents in Organic Synthesis: Enhancing Efficiency and Safety in Chemical Processes. *Angew. Chem.* **2024**, *136* (11), e202316108. https://doi.org/10.1002/ange.202316108.
6. Dallinger, D.; Gutmann, B.; Kappe, C. O. The Concept of Chemical Generators: On-Site On-Demand Production of Hazardous Reagents in Continuous Flow. *Acc. Chem. Res.* **2020**, *53* (7), 1330–1341. https://doi.org/10.1021/acs.accounts.0c00199.
7. Hone, C. A.; Kappe, C. O. Membrane Microreactors for the On-Demand Generation, Separation, and Reaction of Gases. *Chem.–Eur. J.* **2020**, *26* (58), 13108–13117. https://doi.org/10.1002/chem.202001942.
8. Movsisyan, M.; Delbeke, E. I. P.; Berton, J. K. E. T.; Battilocchio, C.; Ley, S. V.; Stevens, C. V. Taming Hazardous Chemistry by Continuous Flow Technology. *Chem. Soc. Rev.* **2016**, *45* (18), 4892–4928. https://doi.org/10.1039/C5CS00902B.
9. Mastronardi, F.; Gutmann, B.; Kappe, C. O. Continuous Flow Generation and Reactions of Anhydrous Diazomethane Using a Teflon AF-2400 Tube-in-Tube Reactor. *Org. Lett.* **2013**, *15* (21), 5590–5593. https://doi.org/10.1021/ol4027914.
10. Pendiukh, V. V.; Yakovleva, H. V.; Stadniy, I. A.; Pashenko, A. E.; Rusanov, E. B.; Grabovaya, N. V.; Kolotilov, S. V.; Rozhenko, A. B.; Ryabukhin, S. V.; Volochnyuk, D. M. Practical Synthetic Method for Amino Acid-Derived Diazoketones Shelf-Stable Reagents for Organic Synthesis. *Org. Process Res. Dev.* **2024**, *28* (1), 165–176. https://doi.org/10.1021/acs.oprd.3c00230.

ISSN 2308-8303 (Print) / 2518-1548 (Online)

11. Chen, Y.; Monbaliu, J. M. Continuous-Flow Multistep Synthesis of Active Pharmaceutical Ingredients. In *Methods and Principles in Medicinal Chemistry*; Alza, E., Ed.; Wiley, 2022; pp 233–268. https://doi.org/10.1002/9783527824595.ch7.
12. Wernik, M.; Poechlauer, P.; Schmoelzer, C.; Dallinger, D.; Kappe, C. O. Design and Optimization of a Continuous Stirred Tank Reactor Cascade for Membrane-Based Diazomethane Production: Synthesis of α-Chloroketones. *Org. Process Res. Dev.* **2019**, *23* (7), 1359–1368. https://doi.org/10.1021/acs.oprd.9b00115.
13. Pinho, V. D.; Gutmann, B.; Miranda, L. S. M.; de Souza, R. O. M. A.; Kappe, C. O. Continuous Flow Synthesis of α-Halo Ketones: Essential Building Blocks of Antiretroviral Agents. *J. Org. Chem.* **2014,** *79* (4), 1555–1562. https://doi.org/10.1021/jo402849z.
14. DIAZOMETHANE. *Org. Synth.* **1935**, *15*, 3. https://doi.org/10.15227/orgsyn.015.0003.

Information about the authors:
Viacheslav V. Pendiukh (*corresponding author*), Ph.D. Student, Institute of Organic Chemistry of the National Academy of Sciences of Ukraine; Laboratory Head, Enamine Ltd.; https://orcid.org/0009-0003-7623-6028; e-mail for correspondence: p2v.chem@gmail.com.
Alexander B. Rozhenko, Dr.Sci. in Chemistry, Head of the Physicochemical Investigations Department, Institute of Organic Chemistry of the National Academy of Sciences of Ukraine; https://orcid.org/0000-0003-4022-7851.

Пам'яті Васильєвої Тетяни Анатоліївни (03.01.1987 – 20.12.2024)

З глибоким сумом і болем у серці повідомляємо, що 20 грудня 2024 року передчасно обірвалося життя старшого наукового співробітника науково-організаційного відділу Інституту органічної хімії НАН України, відповідального секретаря «Журналу органічної та фармацевтичної хімії», кандидата біологічних наук Тетяни Анатоліївни Васильєвої.

Колектив інституту знав Тетяну Анатоліївну як світлу, надзвичайно енергійну, працелюбну та творчу особистість, яка завжди сміливо зустрічала будь-які виклики. Для багатьох аспірантів вона була справжнім провідником на тернистому шляху науки. Її завжди пам'ятатимуть як життерадісну, оптимістичну та доброзичливу людину, до якої можна було звернутися за порадою та підтримкою, знаючи, що вас зустрінуть з щирою посмішкою та допоможуть у будь-якій ситуації.

Тетяна Анатоліївна народилась 3 січня 1987 року в м. Ямполі Вінницької області. 2009 року закінчила Вінницький державний аграрний університет, де здобула кваліфікацію еколога за спеціальністю «Екологія та охорона навколишнього природного середовища». Після закінчення аспірантури Інституту агроекології природокористування НАН України захистила дисертаційну роботу за темою «Еколого-ценотичні особливості Schoeneto-ferryginei L. в умовах трансформації карбонатних боліт України» за спеціальністю «Екологія» та отримала диплом кандидата біологічних наук. В Інституті органічної хімії НАН України Тетяна Анатоліївна працювала з 2016 року на посаді старшого наукового співробітника науково-організаційного відділу, вдало поєднуючи основну діяльність з виконанням обов'язків відповідального секретаря «Журналу органічної та фармацевтичної хімії».

Тетяна Анатоліївна була непересічною особистістю, талановитим науковцем, творчою та багатогранною людиною, залишаючись із цим інтелігентною та чуйною. Колектив Інституту органічної хімії НАН України глибоко сумує з приводу смерті Тетяни Анатоліївни, але водночас з вдячністю і великою повагою згадує її добрі справи та щиро поділяє горе з її рідними та близькими.

ISSN 2308-8303 (Print) / 2518-1548 (Online)

CONTENTS / ЗМІСТ

Original Research

ISSN 2308-8303 (Print) / 2518-1548 (Online)